DYNAMICS OF OLIGOTROPHIC PELAGIC ENVIRONMENTS:

NORTH WESTERN MEDITERRANEAN SEA AND SUBTROPICAL NORTH ATLANTIC

Nixon Bahamón Rivera

Barcelona, March 21st 2002

UNIVERSITAT POLITÈCNICA DE CATALUNYA

CENTRE D'ESTUDIS AVANÇATS DE BLANES (CSIC)

UNIVERSITAT DE BARCELONA

DYNAMICS OF OLIGOTROPHIC PELAGIC ENVIRONMENTS:

NORTH WESTERN MEDITERRANEAN SEA AND SUBTROPICAL NORTH ATLANTIC

by

NIXON BAHAMÓN RIVERA

Centre d'Estudis Avançats de Blanes (CSIC)

DISSERTATION

Directed by: Dr. Antonio Cruzado Alorda

Submitted toward a degree of

DOCTOR

by UNIVERSITAT POLITÈCNICA DE CATALUNYA

Barcelona, March 2002

Abstract

The response of phytoplankton to various ecological forcings was examined in the upper waters of the NW Mediterranean and the subtropical North Atlantic from field observations, analysis of historical data sets and numerical simulations. Particular emphasis was given to the role played by the water column structure in controlling the nitrogen diffusion and new production. Using numerical simulations, the effects of different levels of heating of surface waters and nutrient concentrations in waters below the euphotic zone were assessed.

Spring microplankton metabolism of surface mixed waters in a narrow-shelf area of the Mediterranean Sea was studied. An overall *heterotrophic* metabolism (-0.19 μmol O_2 m^{-2} d^{-1}) was found to prevail at the time of the study, explained by dark community respiration (DCR) rates always higher than gross primary production (GPP) rates. The GPP to DCR ratio was ~0.6, indicating that the system was far from balance between carbon production (photosynthesis) and consumption (respiration), probably caused by accumulation in the mixed layer of excess organic matter favouring respiration over production processes.

Summer primary production and nitrogen fluxes in stratified water layers in the subtropical North Atlantic were analysed. The nitrogen flux fuelling new primary production was closely linked to vertical turbulent diffusion at the nitracline rather than at the thermocline. Upward diffused nitrogen inducing new production was ~0.53 mmol N m^{-2} d^{-1} explaining 21% of total estimated primary production (~214 mg C m^{-2} d^{-1}) in agreement with previous observations. The vertical turbulent diffusion model used to estimate new production did not explain such a production in the Canary Current zone, where laterally advected nutrients from coastal upwelling areas altered the vertical nitrate gradients.

A numerical ecological model of the pelagic domain was developed to assess the plankton response to different environmental pressures. The model represents the vertical dimension of the upper and intermediate water layers of the open ocean. It includes time-variable irradiance and length of daylight in accordance with latitude of selected stations. N-Nitrate, N-nitrite, N-ammonium, N-phytoplankton and N-zooplankton are state variables of the model. Parameterisation of vertical turbulent diffusion from density (temperature, salinity) was functional for modelling the yearly ecological processes. The model structure and functioning makes it suitable for comparative ecological studies and it is expected to be applicable to other studies related to coastal and marine environmental issues.

A comparative study of the plankton functioning in NW Mediterranean and subtropical North Atlantic sites was carried out using the ecological model. The nitrate entering the euphotic zone through the lower boundary explained the low but continuous primary production in the two systems. The latitudinal variability of plankton scenarios implied a year round different solar heating of the upper waters, altering both phytoplankton photosynthesis and mixed layer processes in the water column, with the latter dominating over the former in controlling the phytoplankton biomass. The balance of light availability and nutrient concentration controlled the chlorophyll maximum depth, but the zooplankton grazing prevented this maximum to reach greater concentrations. The phytoplankton maximum was deeper in the subtropical NA than in the NW Mediterranean especially during summertime when the higher irradiance and daylight length made the euphotic layer thicker. Simulations of phytoplanktonic dark nitrate reduction and exudation were coincident with previous observations explaining the nitrite maximum.

Acknowledgements

A very particular inspiration many years ago aroused in me the interest for scientific research. I was finishing my high school in a year with a lot of ingenuity invading my mind - like many others before and afterward-, some far from rationality. I still remember such a day when, I believed, something like an angel came on me, touched me, and told me: “One of your future goals will be the biology”. Therefore, I became biologist. In the middle of my college I got into freshwater plankton ecology. Later, as a graduate student, I worked in coastal ecosystems plankton ecology. I had not finished assimilating the latter when marine plankton ecology came across my way. Thus, I moved from freshwater to marine ecology. Now I think, is not a bad time to go back across my career to try to visualise, a bit more rationally, how much of the acquired knowledge about aquatic ecology affected my ingenuity, or vice versa.

Meanwhile, I want to thank everybody contributing to this work. I feel indebted to my supervisor, Antonio Cruzado who, I think, trusted myself from the beginning of the doctorate more than I did. He entrusted me with responsibilities that improved my training on research, education and business around marine sciences. I am pretty grateful by his continuous support and friendship that he generously provided me.

I express my gratitude to Zoila Velásquez who stimulated me with continuous advice about work and life. I thank Hernán García, who transmitted me his certainties about science and everyday life. I would like to thank Tom S. Hopkins and Tarzan Legovic who encouraged me working on ecological modelling. I also thank Norma Grimaldo, Ljiljana Simic (*RIP*), Carlos Arias, Gitte Madse, Francesco Ridolfi, Maria del Carmen Pérez, Marlon Córdoba, Gloria Morán, Maria H. Angulo, Dorte Engels, Oscar Robledo, Michael Long and Ramon Coma, among others, by their invaluable friendship and affection.

I very much appreciate the support and love of my family, particularly my parents Ofelia and Vicente. My brother Hubert, with whom I shared most of my dreams, together with my sister Judith made possible that one day I took a plain to Barcelona to start this doctorate. Jairo and Cenon are not far from this context, as each one of my other brothers and sisters and their families: Iznardo, Jorge, Héctor, Alvaro, Alfonso and Aydé. My niece Alexandra, witness of the effort to make this work, also gave me her input to finish it. Finally, I feel deeply indebted with Bianka Anna Seils. She provided me a lot of support, understanding and love that made much easier to fulfil this dissertation. I think I never could pay back what they all did for me. I dedicate this work to they all.

I also thank several institutions that provided partial funding to develop this dissertation. Assistance from a fellowship from the Spanish Agency for International Co-operation and Universitat Politècnica de Catalunya (Spain) supported most of the staying in Spain. Support given by Antonio Cruzado at the Centre d'Estudis Avançats de Blanes (CEAB-CSIC), Spain, was fundamental. He allowed me to participate in European projects that widely contributed to complete my training in Marine Sciences. The projects were *Fluxes Across Narrow Shelves* (*FANS*), *YOYO 2001: Ocean Odyssey* and *Mediterranean Forecasting System, Pilot Project* (*MFSPP*). My attendance at two international courses on Modelling and on Mediterranean circulation at International Centre for Theoretical Physics (ICTP) in Trieste (Italy) in September 1998 and October 2000, was funded by the Kuwait Foundation for the Advancement of Sciences (KFAS), the International Atomic Energy Agency (IAFA), UNESCO, and ICTP. The Joint Global Ocean Fluxes Study (JGOFS) program and the Centre for Studies of Environmental and Resources at the University of Bergen, financed a presentation of partial results at *2nd JGOFS Open Science Conference* in Bergen (Norway) in April 2000. MSFPP also financed a presentation of partial results at *XXV General Assembly of the European Geophysical Society* in Nice, (France) in April 2000 and at a MFSPP workshop in Bologna (Italy) in October 2000. The present work was carried out at the Oceanography Lab., CEAB-CSIC in Blanes, Spain.

Contents

List of figures

List of Tables

Chapter 1

Introduction

1. Introduction

The upper waters of the open oligotrophic ocean sustain plankton communities whose structure and functioning depend on complex interactions between physical, geochemical and biological processes. Such a complexity is mainly motivated by convergence of atmosphere and ocean in the upper waters what controls internal mechanisms and interaction with adjacent environments. Plankton communities inhabiting the upper water layers of the ocean contribute to regulate the carbon fluxes between atmosphere and deeper waters at scales ranging from regional to global dimensions. Such a regulation is mainly carried out by phytoplankton photosynthesis that also requires sunlight and micronutrients to convert carbon dioxide into organic matter. Most of the organic matter thus produced is recycled by organisms within the euphotic zone but the remaining, highly variable, fraction (~30%) is exported down to the deep waters turning the deep ocean into a large carbon reservoir (Sarmiento, 1993). The present work deals with nutrient stocks and vertical fluxes in the upper and intermediate water layers of oligotrophic sites of the ocean that regulate phytoplankton primary production. This objective is tackled from analysis of field observations and historical data sets and from numerical ecological modelling of the plankton domain.

This dissertation fits well in the current challenge faced by marine biogeochemistry asked to provide suitable bases of the upper ocean functioning to make predictions of ocean response to climate change (Rasteter, 1996; Carril et al., 1997; Doney, 1999). This challenge together with the paucity of comparative ecological studies explaining the relatively wide variability of new production estimates in oligotrophic seas (e.g. Lewis et al., 1986; Jenkins, 1988; Jenkins and Wallace, 1992) were elements motivating the fulfillment of the present dissertation. Comparative ecological studies lead to identify key elements and processes regarding the plankton functioning that rather contribute to the required bases supporting realistic predictions of the upper ocean biogeochemistry. Nevertheless, various models of the upper water layers have been developed. Some of them highlight

plankton functioning dissimilarities in analogous trophic ecosystems, such as oligotrophic or mesotrophic areas in the ocean (e.g. Varela et al., 1994; Sharada and Yajnik, 2000; Hanhoh et al., 2001).

The role played by phytoplankton in the upper waters of the open ocean in removing the excess carbon dioxide accumulated in the atmosphere along the last 150 years, (after the beginning of the industrial revolution) is an issue still requiring to be better studied (Gruber and Sarmiento, 1997; Doney, 1999). In practice this lack of scientific knowledge affects everybody, from policy makers to environmental authorities requiring a clear research support to take their decisions about control measures on the anthropogenic carbon emissions and has been the main cause for the failure of the last world summits on the Kyoto Protocol (WMO-UNEP, 2001).

The global ocean distribution of phytoplankton allows distinguishing different trophic structures of water. The trophic structure is related to the organic matter production and is highly informative in comparing different ecosystems. As occurred in the late Triassic (~200 millon years ago), the emergency of diatom (bloom) led to exporting fixed carbon from the upper ocean to the interior (Falkowski et al., 1998). In contrast, these authors argue that coccolitophorids, another phytoplankton group widely represented in tropical and subtropical offshore waters (Smayda, 1958), known to use calcium carbonate to build their distinctive outer cover of small regular calcareous plates (coccoliths), allows the carbon to escape from the ocean to the atmosphere. At the global scale, phytoplankton biomass and production are highest near both poles and near the continents, especially where important fertilisation processes of the upper water layers take place, linked to freshwater discharges and coastal and open ocean upwellings (Figure 1.1). The biomass-rich areas are called mesotrophic or eutrophic, in contrast with oligotrophic areas in the centre of the north and south subtropical oceanic gyres (see Figure 1.1) where phytoplankton biomass and production are relatively low (Nixon, 1995; Morel et al., 1996). In oligotrophic oceans, the greatest part of the organic matter is recycled within the upper layers (~ 70%, Platt et al., 1989) but another part sinks into deeper waters before being remineralised (converted back to carbon dioxide) by bacteria

(Sarmiento, 1993). This is what is known as the "biological pump" that turns the phytoplankton production into a critical factor in the regulation of the global carbon cycle.

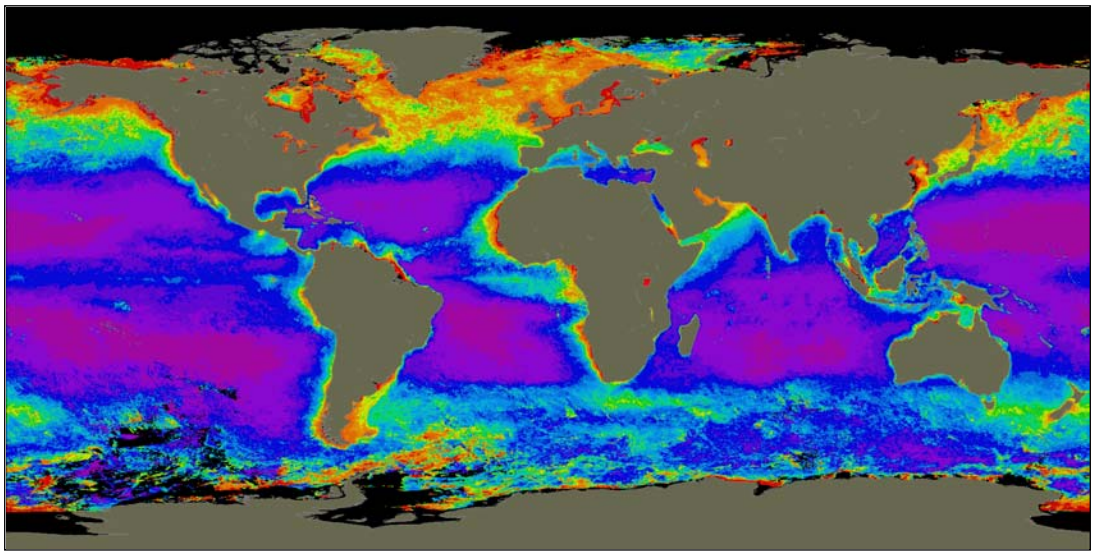

Figure 1.1. The map displays the composite of all Nimbus-7 Coastal Zone Colour Scanner (CZCS) chlorophyll *a* data acquired between November 1978 and June 1986. Approximately 66,000 individual 2 minute scenes were processed to produce this image. Orange regions represent higher phytoplankton chlorophyll a concentrations. Phytoplankton concentrations progressively decrease following yellow, green, blue and red areas. (Provided by the SeaWiFS Project, NASA/Goddard Space Flight Center and ORBIMAGE).

The complexity of phytoplankton primary production is due, among other, to the intracellular and external mechanisms regarding food-web interactions with zooplankton and bacteria, nutrients and light availability, and transport mechanisms of matter and energy. Figure 1.2 shows a conceptual nitrogen-based plankton model in which nitrogen is flowing as inorganic and organic components through the system. In order to be analysed and quantified, elements and processes of the plankton ecosystem must be represented by parameters and functions. In the present dissertation, key ecological external mechanisms governing biological production are evaluated, thus expected to contribute to a better understanding of key forcings constraining primary production in the water column of oligotrophic marine environments, leading to a standard parameterisation and modelling. For that, field observations of phytoplankton primary production and its connection with nitrogen

stocks and fluxes in the euphotic zone and below it are assessed. Then, using a pelagic model, a comparative study of the ecological processes regarding the plankton functioning in the NW Mediterranean and the subtropical North Atlantic is carried out.

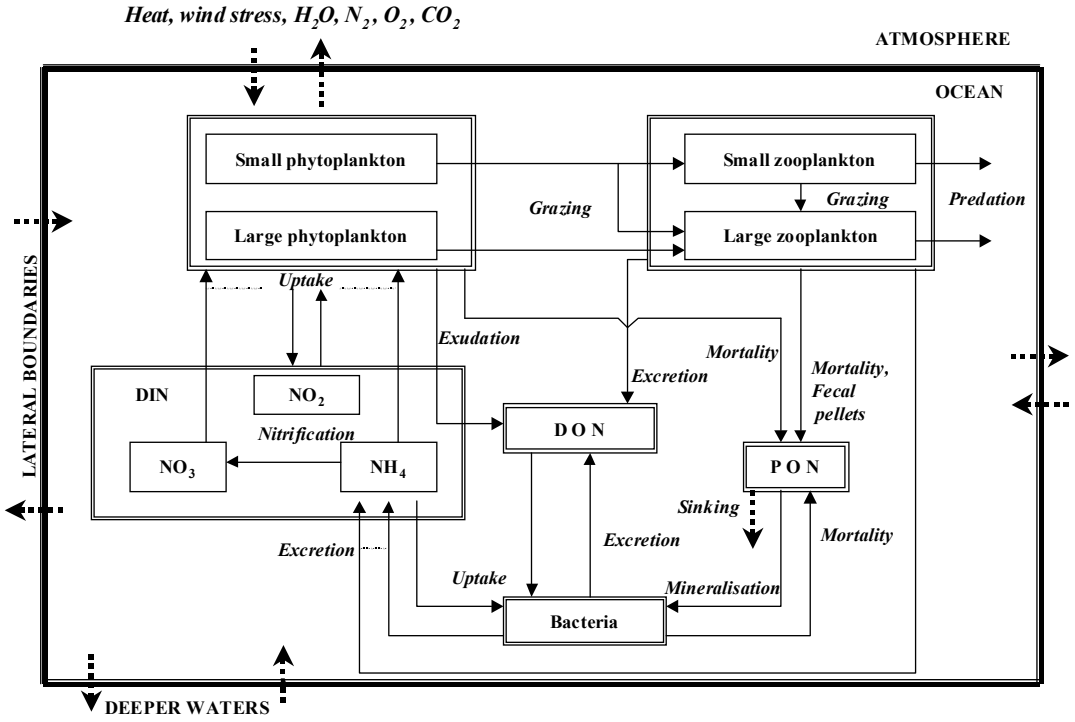

Figure 1.2. Scheme of a nitrogen-based plankton ecosystem in the upper water layers of the open ocean, standing out key elements and interactions among them (adapted and expanded from the Fasham et al., (1990) model).

The metabolic balance of plankton communities

Nitrogen stocks and fluxes in the upper waters of oligotrophic sites of the ocean are assessed in this work. The upward nitrogen flux compensation by downward sinking of matter is assumed. As described above, oligotrophic oceanic environments are characterised by a relatively high rate of recycled ammonium-based primary production ("regenerated" production) with a relatively small input of external nitrate inducing "new" production (Dugdale and Goering, 1967). Some regional and temporal metabolic imbalances between carbon production and consumption have been reported in oligotrophic environments tending to be net heterotrophic (Duarte and Agusti, 1988; Williams, 1988). Processes regarding

organic matter production and consumption in the upper waters can be assumed in a yearly cycle to be near the carbon balance (autotrophy) (carbon production approximately equal to carbon consumption) as commonly assumed for modelling purposes (e.g. Oguz et al., 1999; Bahamon and Cruzado, 2002). Unlike autotrophy in microplankton communities, occurring during summer and autumn, heterotrophy could take place in coastal waters particularly in periods with heavy storms and large depositions of continental runoff, making the carbon consumption to be dominating over biomass production (Serret et al., 1999). The mixed layer is often suggested to be the place where temporal pulses of high production such as those occurred during the spring bloom are stored (Blight et al., 1995; Serret et al., 1999). This would cause the oligotrophic ecosystems to be net heterotropic particularly in periods of thermal stratification, with oxidation processes dominating over biological production. Nevertheless, conflicting conclusions are given from regional and temporal studies regarding the plankton metabolism and, in general, about the role played by the biomass production and consumption balance in the upper water of the ocean (e.g. Williams, 1999; Duarte et al., 1999). In the present work, the metabolic balance of the plankton community is assessed during spring in a narrow shelf area of the NW Mediterranean, when accumulated nutrients and organic matter are expected to reduce the upward nitrogen fluxes. This also allows validating the turbulent diffusion parameterisation in a critical period with a thick mixed layer.

The effect of different surface irradiance on the pelagic system

The role played by the latitudinal variability of irradiance was also the objective of the present work. It is well known that irradiance changes with latitude, also affecting the phytoplankton photosynthesis requiring light to build biomass. The mixed-layer thickness is seasonally variable, mainly depending on changes in surface heating and wind stress. The study of irradiance affecting the light availability for photosynthesis in the water column and the thickness of the mixed layer, affecting the nutrient transport also altering the photosynthesis process, is an issue or great importance in primary production studies rather scarce in the literature. The mixed layer of the upper ocean is known to have relatively high diffusion rates contributing to homogenise the properties of water. During winter, when maximum thickness of

the mixed layer is often observed, mixing is responsible for bringing up nutrient to the surface from nutrient-rich deep waters. This flux favours phytoplankton biomass to increase in late winter or early spring (Bissett et al., 1994), a phenomenon known as "spring phytoplankton bloom". During summer, thermal stratification takes place with a mixed layer reduced to shallow nutrient-depleted water layers. Since relatively high nutrient concentrations are stored in deeper waters, most of phytoplankton growth takes place as deep as possible, also defining the lower limit for phytoplankton growth when there is no light limitation. The thickness of the mixed layer range from ~200 m in the western Mediterranean and 200 - 300 m in the Sargasso Sea in winter time (Hurtt and Armstrong, 1996; Levy et al., 1998). However, in summer time this thickness is reduced to about 10 - 20 m in the former and 40 m in the latter. The thickness of the mixed layer is also variable depending on various criteria to set up its lower boundary. Levy et al. (1998) assumed a mixed-layer thickness in western Mediterranean as that with turbulent diffusion higher than 10^{-5} m^{-2} s^{-1}. In the Sargasso Sea, Hurtt and Armstrong (1996) considered the lower boundary of the mixed layer as that with a temperature gradient higher than 0.5° C with respect to the surface temperature. Since the change of mixed layer thickness with latitude is crucial for the plankton functioning, it was a factor to be examined in the present study. In the present work, idealised density-dependent mixed layers were used for temperate and subtropical sites, assuming not only temperature but salinity as responsible for vertical stability of the water column and therefore, for turbulent diffusion.

Plankton scenarios at differing latitudes also allowed studying the role played by irradiance in controlling the phytoplankton biomass distribution in the water column. Figure 1.3 shows a scheme of seasonal phytoplankton chlorophyll evolution with changes in irradiance and mixed layer. Control of light availability in the water column on phytoplankton growth and structure has been widely studied. Light-saturated growth rates are often simulated to be between 1 d^{-1} and as high as 5 d^{-1} (Fasham et al., 1990; Hurtt and Amstrong, 1996), the higher rate being comparable with that of picoplankton (Bissett et al., 1994). Phytoplankton chlorophyll maximum in oligotrophic environments is often found at depths between 0.5 - 3.0 % of surface

irradiance (Estrada, 1985; Taguchi et al., 1988; Morel et al., 1993). The intensity of surface irradiance is variable according to latitude. Phytoplankton populations near North Pole are often non light saturated even in summer time (Sharples et al., 2001), in contrast to apparently light-saturated communities at lower latitudes (e.g. Williams and Robinson, 1991; Satta et al. 1996). At 20° N latitude in the Sargasso Sea, summer phytoplankton maximum has been observed at 120 m depth representing around 1% of surface irradiance (Bricaud et al., 1992; Jacques and Oriol, 1992), that is ~ 25 W m^{-2} average over the daylight period. At 50° N latitude in the North Sea, Sharples et al. (2001) reported summer chlorophyll maximum at 30 m depth with 1% of surface irradiance (~6 W m^{-2} over the daylight period). Adaptability of phytoplankton organisms to low irradiance levels and nutrient-limited conditions could explain these latitudinal differences of the amount of irradiance at the depth of

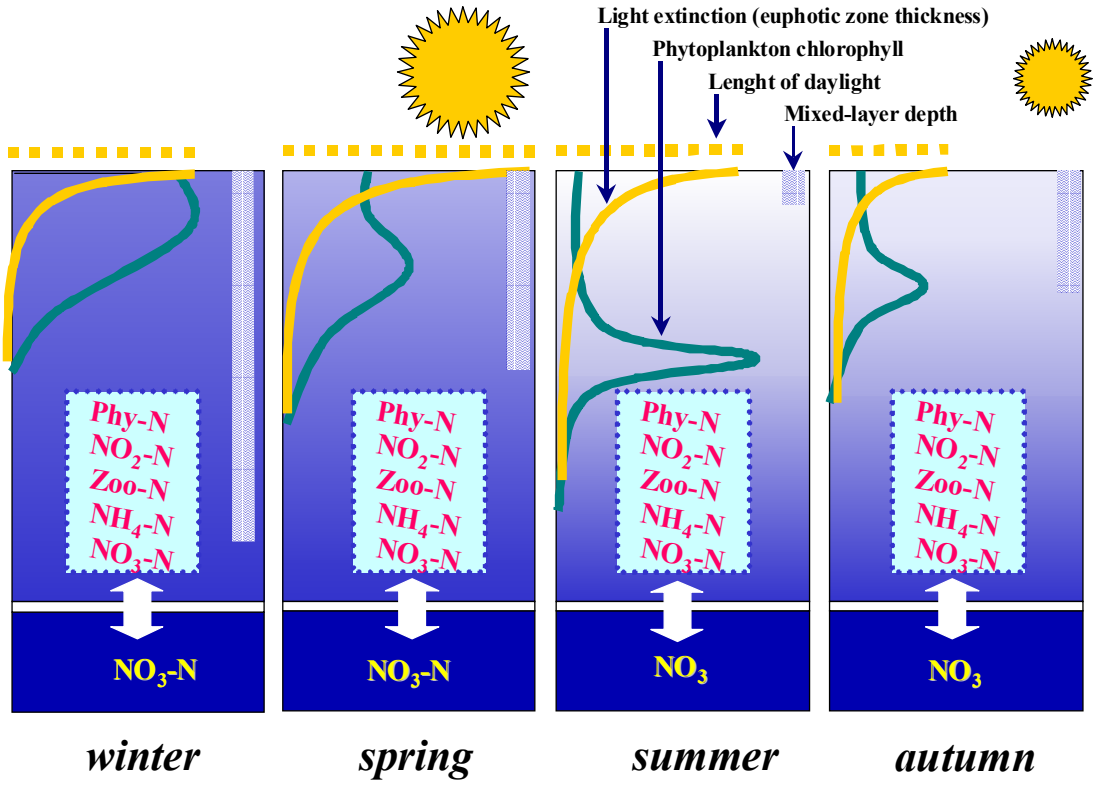

Figure 1.3. Scheme of seasonal phytoplankton chlorophyll evolution with light and mixed layer depth. The nitrogen stock is represented by bow containing the nitrogen forms in the plankton ecosystem, with nitrate (NO_3) input from nutrient-rich bottom waters.

chlorophyll maxima (Bisset et al., 1994; Taguchi et al., 1988). In the present work, two plankton scenarios where modelled and compared, one in temperate (NW Mediterranean) and another in subtropical (North Atlantic) sites of the open ocean, with light attenuation along the water column dependent on water and self-shading by particles. Limitation of phytoplankton growth was assumed driven by PAR or by nutrients following Liebig's law of the minimum in those simulations. This means that the first resource depleted at a given time and depth in the water column (PAR/nutrients) stops phytoplankton growth, following Varela et al. (1992) formulations. The phytoplankton biomass was analysed with regard to irradiance changes at different latitudes, affecting both the vertical stability of the water (mixing layer) and the structure of phytoplankton community.

Nitrogen flux assessment in the vertical dimension of the upper water layers

In this dissertation the role-played by nitrogen fluxes in the water column to control new phytoplankton production in oligotrophic places of the ocean was evaluated. This involved various interacting topics of plankton ecology and therefore, difficult to be treated separately. One of them is the role played by the vertical diffusion process in fuelling nitrogen from nutrient-rich deep waters to generate new production. Vertical fluxes of elements causing biological production have been assumed to be the main feature of the open ocean plankton ecosystem dynamics closely connected to turbulence and advection processes (Denman and Platt, 1977; Gargett, 1989; Catalan, 1991). Turbulence is often considered the most important factor for the vertical transport of matter in the ocean, from a quantitative point of view (Gargett, 1989). Its variability in the water column and complexity require simplifications in order to be used in numerical modelling with regard to ecological questions, such as the plankton functioning. Studies on seasonally alternating vertical mixing and stratification processes are crucial in the vertical flux studies, since they have a direct implication on the variability of microplankton structure, internal processes and interaction with adjacent environments. Seasonal transitions difficult the assessment of the intensity of mixing and the vertical transport process, therefore it is necessary to establish some restrictions to study turbulence in estimating the vertical transport. In this dissertation, a yearly stationary

carbon balance of oligotrophic ecosystems was assumed in the plankton ecosystem with regard to the downward exported matter and upward inputs of inorganic nutrients using the numerical ecological model of the plankton domain described in Chapter 4.

Several turbulent diffusion parameterisations are currently available in the ecological modelling context. Choosing among them depends on objectives and accuracy at which solutions are required. Good results in explaining the vertical distribution of chlorophyll concentration in the water column (*z*-system) of oligotrophic systems have been obtained using the density-dependant turbulent diffusion formulation of Osborn (1980) (Zakardjian and Prieur, 1994; 1998). Figure 1.4 shows a representation of the water column with parameters used to define the turbulent diffusion coefficient (K) as applied in western Mediterranean waters (Zakardjian and Prieur, 1998). In the present work, this formulation was used to assess ecological connections among vertical structure of water, nitrogen fluxes and plankton functioning. Other parameterisation approaches are those given by turbulent closure models computing finite mixing rates near the surface that increase with surface wind stress and variable surface buoyancy forcing (Mellor and Yamada, 1982; Gaspar et al., 1990).

The role played by the summer vertical structure of water (density) in controlling upward nitrogen fluxes from nutrient-rich deep waters to generate new production was assessed in a vast area of the open subtropical North Atlantic. This was very useful to quantitatively evaluate the role that nutrient flux plays in constraining new and total productions. In the oligotrophic open ocean, phytoplankton biomass has been described to be strongly controlled by the upward diffusive nitrogen flux across the thermocline making this vertical transport the main fuelling mechanism for phytoplankton production (Kiefir and Kremer, 1981; Lewis et al., 1986; Jenkins, 1988; Agusti and Duarte, 1999). In upwelling areas, upward

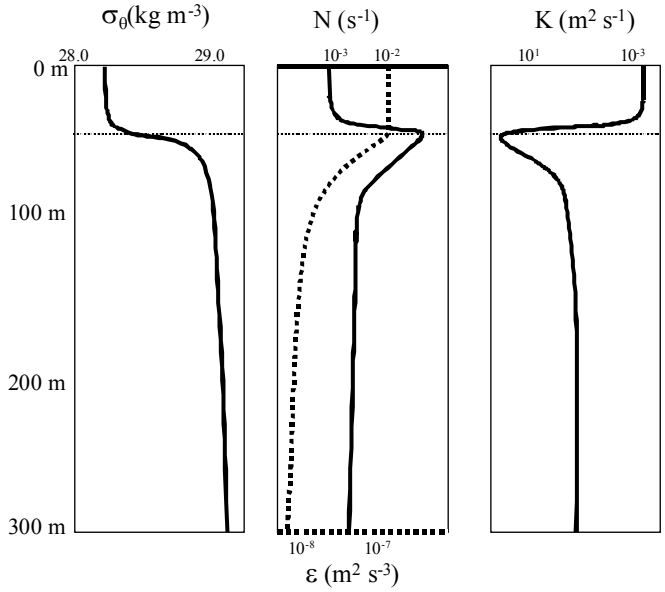

Figure 1.4. Reference scheme of a density profile (σ_θ(kg m^{-3}) (left) used to estimate the Brunt-Väisälä frequency (N) (centre, solid line) with imposed turbulent kinetic energy dissipation rate (ε) (centre, dashed line) that defined the turbulent diffusion coefficient (*K*) (left) (adapted from Zakardjian and Prieur, 1998).

advection of subsurface nutrients plays an important role in nutrient transport (McGillicuddy and Robinson, 1997). In the central subtropical north Atlantic gyre, the horizontal transport of nutrients may contribute to 40 - 80% of new production estimated in ~1 mol C m^{-2} yr^{-1} (Williams and Follows, 1998). Uncertainties regarding variations of phytoplankton new production with regard to nitrogen fluxes in the vertical dimension in oligotrophic oceans (e.g. Herbland and Voituriez, 1979; Cullen and Epply, 1981; Agusti and Duarte, 1999) suggest the need of refined observations in large areas of the open ocean. In the present work, the spatial variability of chlorophyll *a* in the summer thermally stratified tropical North Atlantic is examined under the assumption that upward diffusion of nutrients from waters below the euphotic zone support new production.

Zooplankton controls of phytoplankton biomass

Zooplankton grazing has been pointed out as an important factor controlling phytoplankton biomass by exerting pressure on phytoplankton populations (Alcaraz, 1988: Calbet et al., 1996). Controls of zooplankton on phytoplankton takes place at

different time scales, since the zooplankton growth rates range from days to weeks while phytoplankton growth rates are around one day. This makes, in optimal conditions for phytoplankton growth, a rapid increase of its populations with a lagged control by zooplankton. Temporal phytoplankton blooms taking place in late winter or early spring show this behaviour (Calbet et al., 1996). Zooplankton is fundamental in the food web, since it contributes not only to regulate the phytoplankton biomass but also to recycle material through ammonium excretion. Ammonium concentration influences uptake of nitrate and nitrite (MacIsaac and Dugdale, 1972), thus forcing the models to include a parameter for nitrate inhibition by ammonium uptake (e.g. Varela et al., 1994; Zakardjian and Prieur, 1994; Oguz et al., 1999). Ammonium represents the fraction of recycled material in oligotrophic systems. Such a recycled production has been observed to represent around 70% and more of total production (as pointed out above) in upper waters of the open ocean (Dugdale and Goering, 1967; Platt and Harrison, 1985; Selmer et al., 1993). The role of zooplankton grazing on phytoplankton and the ammonium excretions are factors well taking into account in the present work.

Presence of nitrite in upper water layers

Nitrite is a form of nitrogen contributing to the plankton growth. It appears in the upper waters of oligotrophic areas at concentrations with a maximum around 0.3 – 0.4 mmol m^{-3} (Kiefir et al., 1976; Alcaraz, 1989). Several experiments have been conducted in order to explain the nitrite concentrations due to excretions by specific phytoplankton population like diatoms (Blasco, 1971*a*; Waser et al., 1998) and dinoflagellates (Sciandra and Amara, 1994; Flynn and Flynn, 1998). Bacterial photoinhibition of nitrite and ammonia oxidising activity at intensities lower that 1% surface irradiance also has been pointed out as a responsible mechanism for production of the primary nitrite maximum (Olson, 1981). Zakardjian and Prieur (1994) used an ecological model to simulate a persistent nitrite maximum during summer time in the NW Mediterranean. In the present work, close association of nitrite maximum around but mainly below the chlorophyll maximum is assumed with the hypothesis that phytoplankton community exudation at low radiation and in darkness is responsible for such a peak of nitrite maximum.

The current context of numerical ecological model of the upper ocean waters

Coupling of physical and biological processes in plankton modelling, poorly developed in the beginning (e. g. Riley, 1942) was an issue that remained somewhat obscure until it was taken up again in order to solve diverse aspects of plankton ecology (e.g. Steele, 1977; Denman and Platt, 1977; Kiefer and Kremer, 1981; Cruzado, 1982). Most current numerical ecological simulations couple physical and biological aspects under specific schemes, some of them related to summer conditions with upper water layers vertically stratified (e. g. Varela et al., 1992; 1994; Zakardjian and Prieur, 1994). Other models have been developed to yield annual and even inter-annual variability of the plankton domain (e. g. Evans and Parslow, 1985; Varela et al., 1995; Doney et al., 1996; Oguz et al., 1996; Levy et al., 1998; Sharples et al., 2001).

Numerical ecological models of the plankton system have been developed along two lines. 1) Mixed-layer models assuming a homogeneous water column with vertical averages of ecological processes, representing the most simplified approach (e.g. Evans and Parslow, 1985; Fasham et al., 1990; Varela et al., 1995). 2) Vertically resolved models incorporating the *z*-dependence of biological processes in the water column giving rise to a more accurate approach to the plankton functioning (e.g. Varela et al., 1994; Oguz et al., 1996; Levy et al., 1998; Bahamon and Cruzado, 2002). In the discretised version of the latter models, *z*-variations are represented as a series of levels often ranging from one to five meters in thickness. Figure 1.5 schematises the *z*-level system (boxes) used to simulate the water column processes assumed in the present work. Use of *z*-level systems with simple parameterisations of the vertical turbulence (as described above) is of common use in ecological models. Some limitations of the *z*-level approach are pointed out in air-sea heat flux simulations of sea areas over irregular bottom and bottom sloping areas (Mellor et al., 1999). Sigma or *s*-level numerical systems are often used in general ocean circulation models obtaining good simulations with smoothed representation of the bottom topography as the main advantage (Mellor et al., 1999).

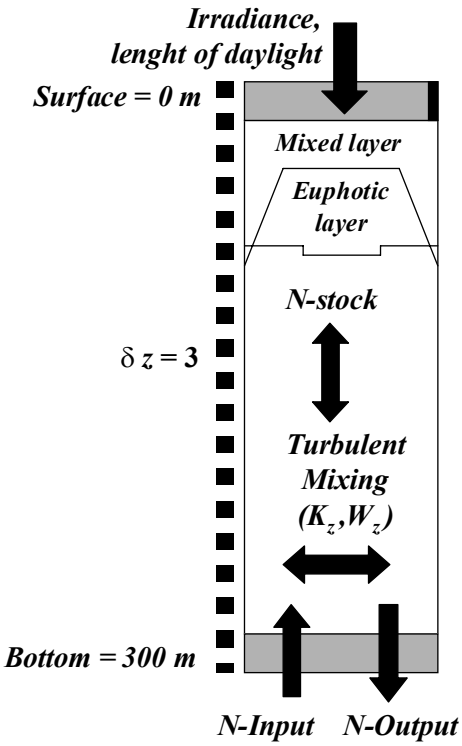

Figure 1.5. Diagram of the numerical grid used to simulate water column in and below the euphotic layer. *N* represents nitrogen, K_z and W_z are vertical turbulent diffusion and advection, respectively. Black block above to the right denotes lateral advection allowed compensating advection upward.

The response of phytoplankton biomass to variable nutrient-rich deep waters at two oligotrophic sites was assessed in this dissertation, using a vertically resolved numerical model. Surface phytoplankton biomass is commonly studied from satellite observations that point out evidence of latitudinal variability (e.g. Platt et al., 1991; Longhurst et al., 1995). Large amounts of satellite composite images (mainly CZCS and SeaWiFS) allow the global distribution of phytoplankton to be known, with higher phytoplankton concentrations at lower latitudes, near both poles, at the equator, near the continents and in the eastern boundary upwelling regions. Nevertheless, satellite viewing needs to be improved with regard to examining of subsurface waters allowing assessing the variability of the vertical water structure of plankton and nutrients. In this respect, numerical ecological models have been observed to make significant contributions to the understanding of the phytoplankton structure and functioning in the vertical dimension (as pointed out above).

With regard to modelling of biological processes regarding primary production, the Fasham et al. (1990) model (FDM) calibrated with oceanographic data from the Sargasso Sea has become a reference standard. It is a single mixed-layer and nitrogen dependent model whose original version used a large set of variables and parameters that subsequently has been revised and improved. More complex biogeochemical models like ERSEM, simulating biogeochemical seasonal cycles of carbon, nitrogen, phosphorous and silicon in the pelagic and benthic food webs of the North Sea have been built (Baretta et al., 1995; Varela et al., 1995). Sarmiento et al. (1993) coupled the FDM model to a hydrodynamic Princeton general circulation model (POM) finding, in general, not only a better fit of nitrate and ammonium dynamics but also inconsistencies in predicting the chlorophyll concentration as estimated by satellite data. Hurtt and Armstrong (1996) observed that the sinking rate of particulate organic nitrogen (PON) and the slope of photosynthesis-light curve were underestimated in the FDM. The application of POM-FDM in stations at latitudes over 30°N severely over-predicted the spring bloom and under-predicted the chlorophyll concentration along the rest of the year. The fit of this model and its constraining power of data were also studied in depth by Evans (1999). Coupled three-dimensional physical-biological models (v. gr. Skogen et al., 1995; Zavatarelli et al., 2000) have been developed to assess biological processes regarding the primary production.

In order to evaluate stocks and fluxes of nitrogen in oligotrophic ecosystems, a vertically resolved, one-dimensional turbulence driven ecological model simulating the intra-annual variability of the plankton ecological processes is proposed. Time-variable irradiance and length of daylight are in accordance with latitude of the selected stations. N-Nitrate, N-nitrite, N-ammonium, N-phytoplankton and N-zooplankton are state variables of the model. The nitrate entering the euphotic zone through the lower boundary is expected to explain the low but continuous primary production in the two oligotrophic systems. Intensity of irradiance, thickness of the mixing layer, nitrate gradients, and grazing pressure of zooplankton on phytoplankton are the main factors forcing the evolution of phytoplankton. The

numerical simulations carried out in the present work, even with limitations due to parameterisation and over simplification, provided a suitable response about the plankton functioning and estimates of annual budget of particulate and dissolved matter in the upper ocean waters.

Outline of the dissertation

Chapters 2 and 3 are dedicated to study cases regarding the phytoplankton biomass interactions with inorganic nutrients transported upward the euphotic layer in both mixed and stratified waters, based on field observations and historical data set analysis. Chapters 4 and 5 deal with a comparative study of the plankton dynamics in two oligotrophic marine environments, using a numerical ecological model with vertical resolution of the upper water layers, based on nitrogen fluxes across key state variables of the planktonic ecosystem.

Chapter 2 is about phytoplankton production and plankton community respiration measurements carried out in spring in a NW Mediterranean narrow shelf area. Relationship between the mixed layer functioning and the plankton metabolism was evaluated. Moreover, the sub-mesoscale variability of phytoplankton primary production was assessed with regard to the vertical nitrate flux inshore and offshore. In Chapter 3, summer mesoscale variability of phytoplankton primary production similarly to the former case was assessed, with regard to the nitrogen fluxes from nutrient-rich deep waters, using information of the WOCE A5 section carried out from NW Africa to Bahamas in the subtropical North Atlantic. Both case studies allowed the validation of parameterisation of the vertical turbulent diffusion in critical periods of mixed waters (springtime) and stratified waters (summertime). Chapter 3 has been submitted for publication (Bahamón et al., 2002).

An ecological numerical model with vertical resolution is proposed in Chapter 4, to study the plankton functioning in the upper water layers of the open ocean. Model description and calibration/validation exercises of the physical properties are presented. Finally, in Chapter 5, the coupled physical and biogeochemical model is calibrated/validated against two oceanographic stations in the eastern subtropical

North Atlantic and the Catalan Sea in NW Mediterranean. The model is intended to explain the response of the phytoplankton primary production to different ecological forcings at different latitudes. For that, similar state variables and parameters were used with different upper and lower boundaries, tuned for each oceanographic site. Key elements of the ecosystem and ecological processes that could alter the organic matter (carbon) fluxes in the upper water layers were examined. Chapters 4 and 5 were submitted for publication (Bahamón and Cruzado, 2002).

Objectives of this work were also used to fulfil the objectives of various European projects. First, the YOYO project was used to carry out parallel experiments of plankton metabolism and sub-mesoscale variability in the Blanes Canyon located in a narrow shelf of the NW Mediterranean, as presented in Chapter 2. The WOCE A5 (World Ocean Circulation Experiment, Section 5) served to develops Chapter 3 using unpublished data particularly of chlorophyll *a*. Finally, the *Mediterranean Forecasting System, Pilot Project* (MFSPP) at which the ecological model was initially addressed to was further modified as shown in Chapters 4 and 5.

Chapter 2

Late spring phytoplankton production and plankton metabolism in the Blanes Canyon, North Western Mediterranean Sea

Abstract

Spring mesoscale variability of primary production, chlorophyll and nutrients was assessed along the Blanes Canyon (NW Mediterranean) as a function of the vertical structure of water. There was a homogenous distribution of turbulent diffusion (~22 m^2 d^{-1}), nitrate gradient (~0.0132 mmol N m^{-4}) and a new production to total production ratio ~3%, the latter indicating the recycling processes prevailing over allochthonous nitrogen-dependent production. However, significant differences of chlorophyll concentration and primary production were found between inshore and offshore areas, with the former area typically mesotrophic and the latter, typically oligotrophic. This was probably due to a slower circulation pattern that in the canyon head could be favouring the accumulation of organic matter produced in the late winter, as observed in previous works. The plankton community metabolism was also assessed in the Blanes Canyon head. It was found to be net heterotrophic (- 0.19 ± 0.08 µmol O_2 m^{-2} d^{-1}) explained by high dark community respiration rates (DCR = 0.50 ± 0.27 µmol O_2 m^{-2} d^{-1}) dominating over gross primary production (GPP = 0.31 ± 0.17 µmol O_2 m^{-2} d^{-1}). Net community production decreased with the increasing of daily-integrated irradiance, suggesting a light-saturated phytoplankton community with irradiance favouring the community respiration over phytoplankton production. This, together with a relatively low vertical transport of matter from surface to deeper water layers could be favouring that GPP to DCR ratio (~0.6) was far from the metabolic balance (1.0).

2.1. Introduction

Oligotrophic oceanic environments are characterised by a relatively high rate of recycled ammonium based primary production ("regenerated" production) with a relatively small input of external nitrogen inducing "new" production (Dugdale and Goering, 1967). NW Mediterranean Sea shows a general cyclonic circulation that generates a moderate oligotrophy with longshore currents leaving the coast to the right giving rise to relatively poor nutrient supply due to the cross-sectional circulation that brings nutrient depleted surface water onto the shelf (Cruzado et al., 2002*a*). The cyclonic circulation generates persistent thermohaline fronts, with "new" primary production associated to turbulent transport of nitrate from deeper waters (Lohrenz et al., 1988; Salat, 1995; Zakardjian and Prieur, 1994; 1998, Estrada et al., 1999). This circulation pattern has been also observed in canyons located in narrow shelf areas of the NW Mediterranean (Granata et al., 1999). Besides nitrate supply from deep waters to the upper water layers, biological fixation of molecular nitrogen by planktonic cyanobacteria and benthic macroalgae (Gasol et al., 1997) and the deposition of airborne N-containing particles (Alarcon et al., 1990; Béthoux and Copin-Montégut, 1986) have also been pointed out as nutrient sources for primary production in coastal and open sea areas. Nevertheless, nutrient-rich deep waters are the most often considered nutrient store supporting the low but continuous new production in most oligotrophic areas (Eppley and Peterson, 1979; Campbell and Aarup, 1992; McGillicuddy and Robinson, 1997).

Primary production in coastal temperate areas has time and space variability strongly influenced by local seasonal and hydrodynamic regimes and atmospheric fallout (Hoch and Kirchman, 1993; Serret et al., 1999). In the NW Mediterranean, rainfall and continental runoff have been observed to increase the phytoplankton biomass and primary productivity particularly near shore (Estrada et al., 1996; Estrada, 1999). Wide-shelf coastal environments show internal fluxes of inorganic material controlled by biological regeneration, mostly in surface sediments (Cruzado et al.,

2002*a*). Contrarily, narrow-shelf coastal environments show relatively strong longshore currents with density fronts controlling internal fluxes of organic and inorganic materials mainly by interaction of marine currents with bottom topography (Granata et al., 1999). Processes regarding the organic matter production and consumption in upper waters of oligotrophic seas, appear to be in a year round state near the carbon balance (autotrophy) with carbon production rates close to those of carbon consumption (Duarte and Agusti, 1988; Williams, 1988). Heterotrophy has been observed taking place near shore in periods with heavy storms and large contribution from continental runoff, that make the organic matter oxidation (consumption) to prevail over biomass production (Serret et al., 1999).

The Blanes canyon, an oligotrophic ecosystem located in a narrow shelf area in the NW Mediterranean shows an annual carbon budget near equilibrium with a weak net heterotrophy (Satta et al., 1996; Granata et al., 1999). This is supported by observations of downward flux of particulate organic matter mainly derived from allochthonous material and minor portions of in situ produced biomass. Such a reduced contribution of biological production to downward fluxes appears to be favoured by a slow cycling pool during the spring bloom accumulating material in the upper mixed layer to be later consumed by microplankton, as observed in other coastal temperate areas (Blight et al., 1995). In agreement with the last hypothesis, an annual time series study of surface plankton metabolism in coastal waters near the Blanes canyon, suggested the system to be near equilibrium (with a weak trend to be heterotrophic) in absence of heavy storms supplying external materials (Satta et al., 1996). Spring observations of the vertical structure of water in the Blanes canyon suggest that this area is comparable with oligotrophic ecosystems in the open ocean with relatively small variability offshore (Cruzado et al., 2002*b*) (Figure 2.1). Nevertheless, plankton communities in the Blanes Canyon head could be subject to different regimes of local circulation with respect to those located offshore thus altering the mesoscale carbon balance estimates (Granata et al., 1999).

The change in heat supplied to the surface waters along the year makes them to be continuously modifying the vertical structure (density) altering the micro-

communities structure and functioning. Particularly, during the transient period from spring to summer in NW Mediterranean, the upper water layers modify the vertical structure from well-mixed waters induced by winter convection processes, to a thermally stratified state (Schott et al., 1996). Winter convection forces a rapid homogenisation of surface waters making that new denser water sink to reach equilibrium with deeper waters. Sinking of surface waters dilutes the relatively abundant phytoplankton cells in deeper waters. At the same time, this mixing process that reaches depths below the euphotic layer (see diagram in Figure 1.3) brings up nutrients to the surface from nutrient-rich deep waters. Microplankton communities metabolism is modified according to new environmental changes that favour the increase of both respiration rates (oxygen consumption) and oxygen production (photosynthesis) (Masó et al., 1998). Since nutrients are in excess in the euphotic zone, a rapid phytoplankton biomass increase takes place generating an organic matter surplus. This organic matter is being simultaneously oxidised at rates often lower than those of oxygen production, thus generating a net heterotrophy (organic matter consumption exceeding production) in the system (Serret et al., 1999). Part of the organic matter excess can remain accumulated in the mixing layer to be later

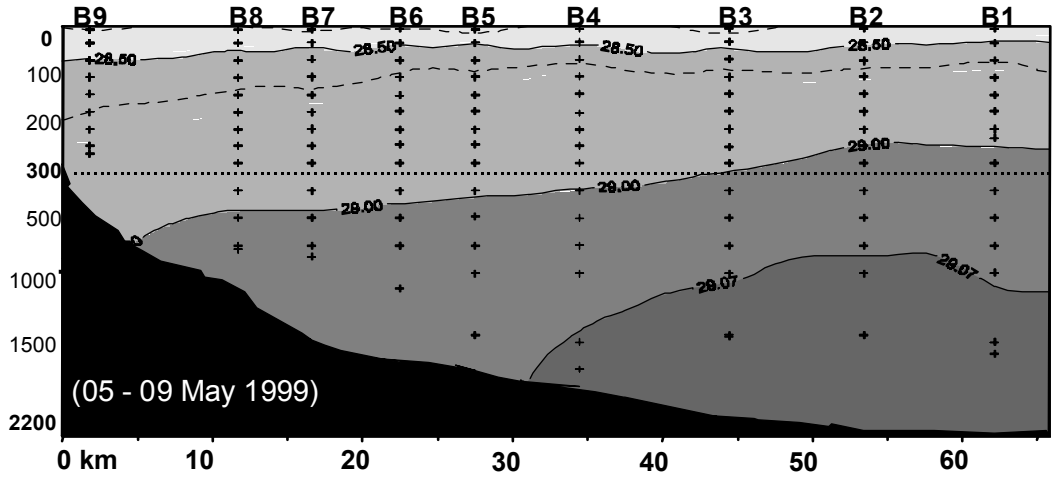

Figure 2.1. Vertical distribution of σ_θ(kg m^{-3}) along the Blanes Canyon as measured in section B of the YOYO I cruise carried out in May 1999 (Cruzado et al., 2002). Note a relatively little sub-mesoscale variability from the head of the canyon (left) to the offshore area (right). X-axis represents the offshore distance from the Canyon head.

consumed during springtime while another part is exported toward adjacent ecosystems as organic aggregates and detritus. With the increase of surface nutrient concentration, phytoplankton and bacterial biomass tends to increase followed by a lagged increase of zooplankton biomass (Calbet et al., 1996). Nevertheless, the in situ produced organic matter in NW Mediterranean appears to be irrelevant over the year as downward exported organic material pool (Miquel et al., 1994; Granata et al., 1999).

Microplankton metabolism is relevant to understand the organic matter production and consumption in upper water layers. Nevertheless, discussions still remain about concepts and methods of plankton metabolism measurements that historically have generated gaps preventing a suitable interpretation of related process (Duarte and Agusti, 1998; Serret et al., 1999; 2001). The common related procedure is based on oxygen or carbon evolution experiments in water contained in dark and clear bottles that, after a given incubation period under certain light conditions, allow to estimate respiration rates in dark bottles and both photosynthesis and respiration rates in the clear ones. Handling of data sets (e. g. Duarte et al., 1999; Williams et al., 1999), interpretation of analytical methods used to determine gross and net productions (Williams, 1993), and relative shortage of net carbon production measurements (Serret et al., 2001), have been pointed out as main responsible for gaps in the plankton metabolism understanding.

In the present work, the submesoscale variability of phytoplankton chlorophyll and primary production and the short-term microplanktonic metabolism is assessed in late spring in the Blanes Canyon. Sub-mesoscale variability is tackled from the viewpoint of total primary production as deduced from a chlorophyll-irradiance model. Examination of the short-term variability of gross primary production and dark community respiration (plankton metabolims), have also been included. Assuming nitrate as limiting factor for primary production in western Mediterranean (Béthoux and Copin-Montégut, 1988) the upward nitrogen fluxes are estimated from the density field and nitrate gradients in the water column. This nitrogen is expected to generate new production required to compensate eventual losses of organic matter removed from the mixed layer.

2.2. Methods

Sub-mesoscale variability measurements

A section along the main channel of the Blanes Canyon was carried out on board *R/V García del Cid* during 5 – 6 May 1999. This section (B) was part of the YOYO I Cruise carried out to validate nutrient measurements taken from a moored instrument in the Blanes Canyon. Co-ordinates of the section are along 2.86°W between 41.09° - 41.65° N (Figure 2.2). 3 m depth averaged CTD data were analysed from surface to 300 m depth. 10 L Niskin bottles were used to take water samples for chlorophyll, nutrients and dissolved oxygen measurements.

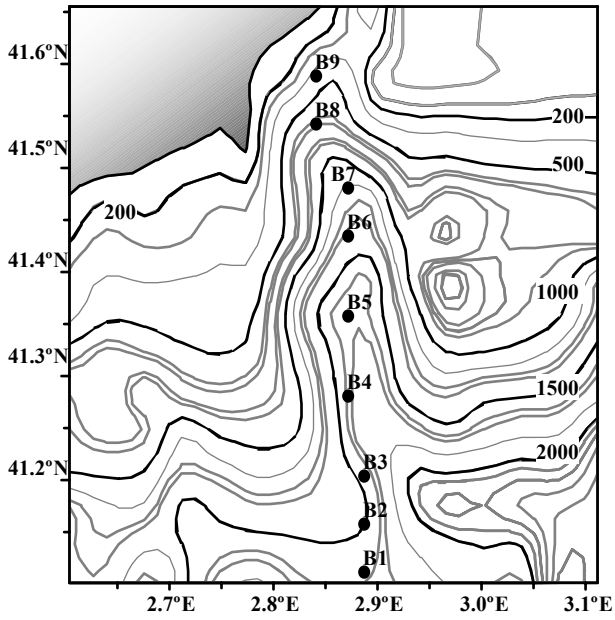

Figure 2.2. Station locations along the Blanes Canyon. All the stations were visited once for the sub-mesoscale measurement. Station B9 was visited weekly four times to assess the short-term variability.

Parameterisation of vertical turbulence

In order to estimate upward diffused nitrogen, parameterisation of the turbulent diffusion in the water column was carried out following Osborn (1980). This method

allows computing turbulent diffusion values from vertical density gradients. Thus, a large increase in density gradient promotes a high stability of the water layers with lower turbulent diffusion rates, and vice versa. The model has been previously used in ecological models of the plankton domain, particularly during summertime (e.g. Zakardjian and Prieur, 1994; 1988). Such a turbulent diffusion multiplied by nitrate gradients in the water column allowed estimating upward nitrogen fluxes fuelling new production in the euphotic zone.

The vertical diffusion term (K_z) was estimated as follows:

$$K_{(z)} = \frac{0.25\ \varepsilon_{(z)}}{N^2{}_{(Z)}} \tag{2.1}$$

where, $$N^2{}_{(Z)} = -\frac{g}{\rho_w} \bullet \frac{\partial \rho}{\partial_Z} \tag{2.2}$$

$\varepsilon_{(z)}$ is the turbulent kinetic energy (TKE) dissipation rate at a given depth. N^2 (s^{-2}) is the Brunt Väisälä, computed according to Millard et al. (1990). g represents gravity acceleration (9.82 m s^{-2}), ρ_w is density anomaly (kg m^{-3}), and $\partial\rho/\partial z$ is the vertical density gradient. Density anomaly (σ_θ, T, S, 0) was calculated following Millero and Poisson (1981).

TKE links the turbulent regime and the stratification of the water column being assumed 4E-07 m^2 s^{-3} in the mixing layer but decreasing exponentially downward until reaching a background value of 4E-08 m^2 s^{-3}. Various ecological models have successfully applied this range and distribution pattern of TKE in order to simulate the vertical distribution pattern of chlorophyll in oligotrophic ecosystems in western Mediterranean and subtropical north Atlantic (Zakardjian and Prieur, 1994, 1998). Above the pycnocline, the surface wind stress is assumed to be the source of energy for turbulent mixing. Below the pycnocline, turbulent diffusion (K_z) would be the result of decreasing Brunt-Väisälä frequency (buoyancy frequency) and internal waves breaking (Gaspar et al., 1990). Similar K_z parameterisations involving direct measurements of turbulent dissipation rates has been reported (Sharples, 2001). In the present work, N^2

and K_z profiles were smoothed using the Nearest Neighbour gridding method assigning the value of the nearest datum point to each grid node. In this chapter, the Osborn model parameterisation of the turbulent diffusion is used to estimate nitrogen fluxes under non-stratified conditions of the upper water layers. In Chapter 3, similar parameterisation will be used for the same purpose under thermally stratified waters. Both experiences serve as preliminary validations allowing a later application of the Osborn model to yearly simulations of the upper waters in hypothetical oceanographic stations as described in Chapters 4 and 5.

Following Archimedes principle, N^2 assumes a water mass to be stable when it is imagined as a solid body embedded in surrounding water that remains floating at rest if the weight of the water displaced by the water body equals the weight of the body. In other words, the water remains floating if the density of the embedded water mass equals the density of the surrounding water. This is why N^2 is also called buoyancy frequency also serving as a pathway to estimate turbulent diffusion (K_z). High N^2 values indicates relatively high stability of the water layers as occur at the maximum density gradient layer depth (pycnocline) separating the mixed layer from deeper waters. On the contrary, low values of N^2 indicated lower water stability, as occurs in the surface mixed layer and deep waters with small density gradients. As a result of this parameterisation, K_z is expected to be inversely proportional to the Brunt Väisälä frequency (Gaspar et al., 1990) with maximum values in the mixed layer and minimum within pycnocline.

Dissolved Oxygen

Samples were collected for dissolved oxygen analysis as soon as the CTD/rosette sampler was brought on board. Gravimetrically calibrated 140 cm^3 flasks were rinsed carefully with minimal agitation, then filled via a drawing flexible tube, and allowed to overflow for at least 2 flask volumes. Reagents were added to fix the oxygen dissolved in the seawater samples before stoppering. The flasks were shaken twice immediately after reagent addition, and after 30 min, to assure thorough dispersion of the precipitate (Aminot, 1983). The samples were analysed within 8-24 hours after sample collection. Dissolved oxygen samples were titrated following the technique of

Carpenter (1965). The overall precision of the data is estimated to be comparable to WOCE specifications for oxygen data (0.5 %). The oxygen data, expressed in volumetric units, were converted after post-cruise calibration and processing, to units of μmol kg^{-1} using the molar volume of oxygen as a real gas. A density corresponding to the measured salinity and measured sample temperature at the time of collecting the sample from the Niskin bottles was used.

Dissolved Inorganic Nutrients

Unfiltered samples were drawn from the Niskin bottles following sampling for dissolved inorganic nutrients. Samples were frozen in ~100 cm^3 high-density polyethylene, narrow mouth, screw-capped bottles after adding one drop of $HgCl_2$. The samples were kept frozen on board for the duration of the cruise and were analysed, after thawing, for nitrate + nitrite, nitrite, orthophosphate, and orthosilicic acid (silicate) immediately upon arrival to the laboratory. Standardisation ran at various nutrient concentrations performed to monitor the reproducibility of the results and for data quality assurance procedures was carried out at the CEAB. Replicate samples were taken from selected Niskin bottles closed at the same depth for monitoring short-term precision.

Chlorophyll a

Chlorophyll *a* was estimated from non-fractionated particulate matter. Water samples of 0.5 to 3 litres taken at several depths with Niskin bottles were filtered through 4.7 cm Whatman GF/F filters that were kept frozen until they were processed in the laboratory. The phytoplanktonic pigments were determined by the spectrophotometric technique described by Jeffrey and Humphrey (1975) after extraction for more than 24 hours with 5 ml acetone (90 %). The resulting suspension was centrifuged at 3000 rpm for 30 minutes. The absorbances were read in the supernatant at 750, 664, 647 and 630 nm. In spite of chlorophyll B and C are deduced from this equation, solely chlorophyll *a* was used here to be examined, given its major accuracy as estimator of phytoplankton biomass (Jeffrey and Welschmeyer, 1997).

Estimates of primary production

A photosynthesis-irradiance relationship (*P-I*) (units in mgC [mgChl a]$^{-1}$ h $^{-1}$) was used to estimate primary production. An idealised *P-I* curve is shown in Figure 2.3, where the carbon fixation rate is normalised with respect to the phytoplankton chlorophyll mass P^B. This primary production estimating method was that described by Herman and Platt (1986):

$$(P-I) = P_m^B \, tanh\left(\frac{\alpha^B I}{P_m^B}\right) - R \tag{2.3}$$

where P_m^B is the assimilation number, this is, the rate of photosynthetic available radiation (PAR) saturation; *tanh* is the hyperbolic tangent function of the light saturation curve; α^B is the initial slope of the curve (mg C [(Chl a) W^{-1} m^2 h^{-1}]); *I* is the PAR fraction (W m^{-2}) of surface irradiance; *R* is respiration in a dark bottle (mg C [mg Chl a]$^{-1}$ h^{-1}). α^B and P_m^B are strongly dependent on the season of the year, therefore they where chosen as those deduced from spring time studies in coastal and open ocean areas at similar latitudes than those in the present study (Kyewalyanga et al., 1998). Thus, P_m^B values were assumed to be 6.64 and 8.23, and α^B values were assumed as 0.069 and 0.078 in near shore and offshore areas, respectively. *R* was assumed to be negligible relative to gross production as typically assumed in production models (Herman and Platt, 1986). *I* (PAR) was assumed 46% of surface solar irradiance (Baker and Frouin, 1987). Surface irradiance was 600 W m^{-2} at noon, resulting from averaged measurements carried out in the short-term variability experiment described below in the text.

In order to estimate absolute primary production profiles, PAR extinction in the water column was assumed to be declining exponentially due to water absorption (K_w) and phytoplankton self-shading (K_c):

$$PAR_{(z,t)} = PAR(0,t)\, exp^{-Z(k_w + k_c \bullet [PHY])} \tag{2.4}$$

where K_w = 0.06 m^{-1} and K_c = 0.01 (mg Chl $m^{-2})^{-1}$ according to previous ecological modelling in the same area (Bahamon and Cruzado, 2002).

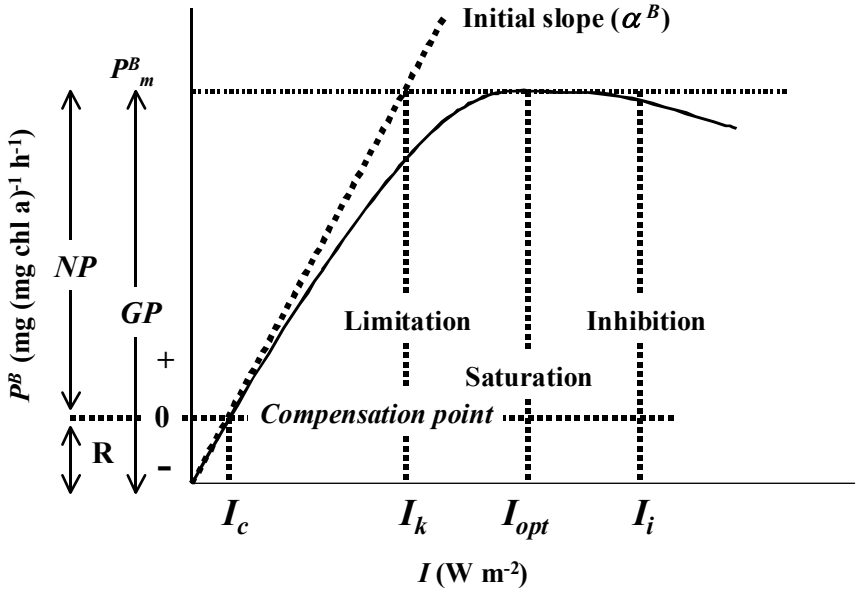

Figure 2.3 A schematic diagram of photosynthesis-irradiance relationship. P^B is the phytoplankton chlorophyll mass (PHY), I is the PAR fraction, R is respiration; NP and GP represent net and gross productions, respectively. Note that $GP - R = NP$. I_C is the compensation point. The light intensity at the intersection of α^B is I_k. I_{opt} indicates the onset of irradiance-saturated regime at the PHY maximum (P^B_m). From I_{opt}, the increasing irradiance promotes photosynthesis inhibition (I_i).

Primary production per unit mass was calculated from absolute production profiles (P_v) obtained multiplying $P\text{-}I_{(z)}$ by chlorophyll *a* biomass $P^B_{(z)}$ (mg m^{-3}):

$$P_v\,(z) = P\text{-}I_{(z)} * P^B_{(z)} \tag{2.5}$$

Then, volumetric daily primary production ($Cd_{(z)}$, units in mg C m^{-3} d^{-1}) was computed by integrating the previous equation over time *t:*

$$Cd_{(z)} = \int_0^{24} Pv(z,t)dt \tag{2.6}$$

Finally, depth-integrated primary production (C_a, units in mg C m^{-2} d^{-1}) was obtained by integrating Equation 2.6 from surface to the depth where PAR curve became asymptotically zero:

$$C_a = \int_0^{Zf} \int_0^{24} Pv(z,t)dtdz \tag{2.7}$$

Short-term variability experiment

The short-term variability experiment was carried out in a fixed station in the Blanes Canyon head (Station B9) at 41° 39' N, 2° 51'E. The station was visited four times weekly from 20 May to 11 June 1999 on board *R/V Itxasbide*. As in the mesoscale experiment, chlorophyll *a*, nutrients, and CTD data were measured. However, this experiment is focused on the microplankton metabolism based on the oxygen evolution in dark and clear bottles with simulated incubation depths as described below. In each of surveys, 5-6 discrete samples were taken in the euphotic zone using 10 L Niskin bottles. Approximately half of the water volume was used to assess production and respiration rates (as described below) and the rest of the water was used for chlorophyll and nutrient determinations. In both cases, water was filtered over a 200 µm mesh size to avoid eventual large plankton in the samples altering the expected results. Nutrients and photosynthesis-irradiance primary production were estimated following the methods described in sub-mesoscale experiment.

Size-fractionated chlorophyll

Size fractionated and total chlorophyll *a* was measured from 250 ml water. 5 µm policarbonate membrane filters were used to separate chlorophyll fractions over and under 5µm diameter. Further extraction in 90% of acetone was carried out and lectures made in a Turner Designs Fluorometer. Calculations were made following Jeffrey and Welshmeyer (1997). These measurements were calibrated against spectrophotometric lectures, the latter procedure as described above. Strong correlation was found between total chlorophyll *a* measured by both methods (Figure 2.4).

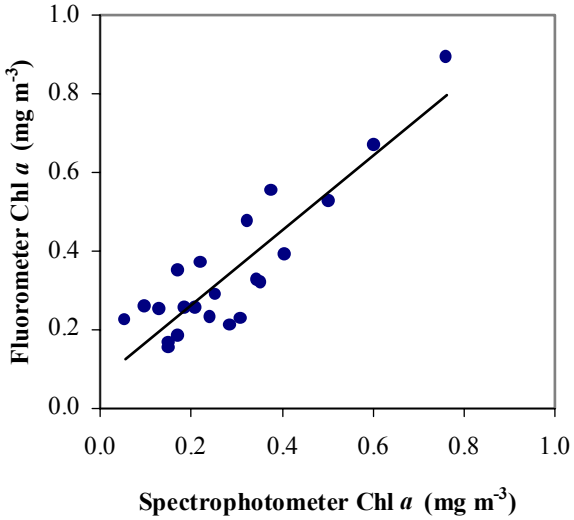

Figure 2.4 Fluorometic (F) versus spectrophotometric (S) measurements of chlorophyll *a*. The solid line is the linear regression F = 0.9497 (S) + 0.0727 (n = 22, r^2 = 0.79, $P < 0.001$), and the dashed line is the 1:1 line.

Community metabolism

Gross primary production (GPP), dark community respiration (DCR), and net community production (NCP) were estimated from 24 hours oxygen evolution in dark and light bottles. This incubation time was necessary to obtain reliable estimates of oxygen changes in the plankton community, as used for relatively oligotrophic ecosystems (Williams and Jenkinson, 1982). Previous profiles of sunlight penetrating the water column were carried out using a Li-Cor quantometer SPQA 2550 in order to determine depths for sampling at subsurface, 75, 50, 12, and 1 % of total surface sunlight irradiance. About 5 litres of water were drawn in a dark plastic bottle placed on deck with surface water flowing around in order to homogenise temperature. On land, not more than one hour later, water was drawn into 150-ml glass bottles avoiding air bubble formation. From each depth, five replicate bottles were filled to measure initial oxygen (O_i). Five dark bottles and five light bottles were incubated outside the lab under natural irradiance conditions to obtain final oxygen concentrations. These two bottle sets were kept with water flowing around to avoid overheating and covered with shaded films according to desirable surface irradiance percentages. Irradiance was measured hourly using the Li-Cor quantometer and the total daily-integrated irradiance was determined. Simulation of percentage irradiances at each depth was made covering each set of bottles water-immersed with PPC transparency films previously laser

printed with grid points making desirable shadings. Shadings were accurately calibrated by using an UV-160 visible recording spectrophotometer measuring transmittance of visible light across the films. After the incubation period, dissolved oxygen concentration was measured in dark (O_d) and light (O_l) bottle sets and production and respiration rates were determined as follows: NCP = O_l - O_i; DCR = O_i - O_d; GPP = NCP + DCR. Dissolved oxygen was measured by the high precision Winkler titration method as described in the mesoscale method description.

2.3. Results

Sub-mesoscale variability

The upper waters along the main channel in the Blanes Canyon showed relatively little variability in temperature, salinity and density (Figure 2.5). Surface temperature ranged between 15.0 ºC and 16.5 ºC and surface salinity ranged from 37.5 to 37.9 with lower salinity inshore. The 37.8 salinity isoline (located ~24 km offshore) suggests an empirical division of the upper waters in inshore and offshore areas, the former grouping stations B9 to B6 and the later stations B5 to B1. A subsurface temperature minimum layer (<12.9 ºC) appears to be a remnant of Winter Intermediate Water (WIW), evident in most stations with a sloping in the isopleths of density anomaly (σ_θ) consistent with a south-westerly flow of the Catalan current, as described by Cruzado et al. (2002*b*).

Along the water column, chlorophyll *a* showed important difference from inshore to offshore (Figure 2.6). Inshore, the surface values were above 0.4 mg m^{-3} with a sub-surface maximum of 1.8 mg m^{-3} between 25-50 m. Offshore, surface chlorophyll was under 0.4 mg m^{-3} without the presence of a subsurface chlorophyll *a* maximum. This distribution pattern is consistent with the salinity distribution, evidencing the influence of remnant WIW retained in the canyon head. Along the whole section, a relatively homogenous bottom isoline of chlorophyll *a* concentration around 0.1 mg m^{-3} was found at 110-130 m depth (Figure 2.6), independent of the isopycnal distribution

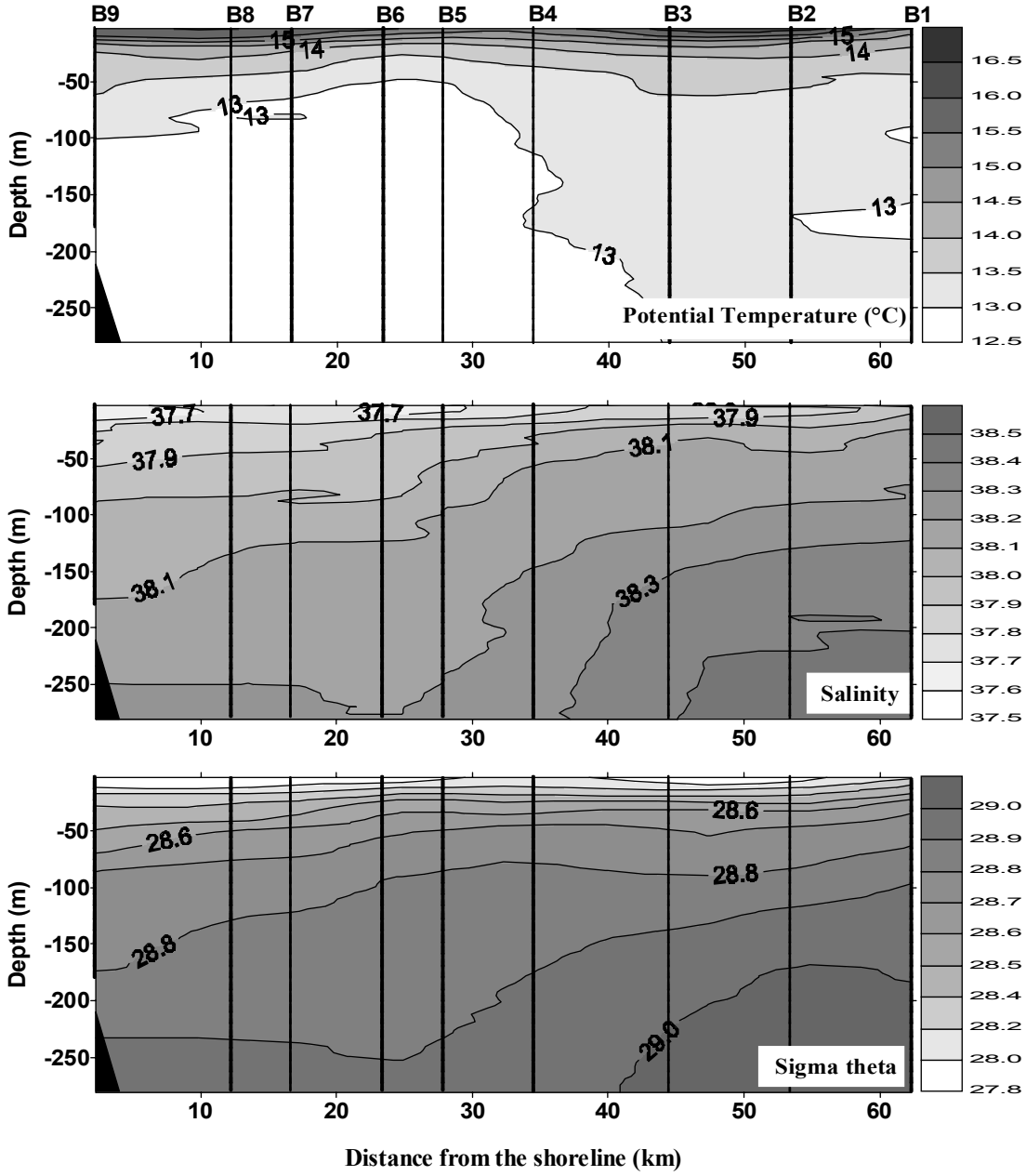

Figure 2.5. Vertical distribution of temperature (°C), salinity and σ_θ (sigma theta) (kg m^{-3}) in the upper waters of the Blanes Canyon.

(Figure 2.5, down) but suggesting an apparent light limitation of the phytoplankton photosynthesis at such a depth.

The nutrient concentrations were relatively low in surface waters. Surface nitrate was around 0.5 µmol kg^{-1} reaching values between 3.0 and 4.0 µmol kg^{-1} at 200 m depth,

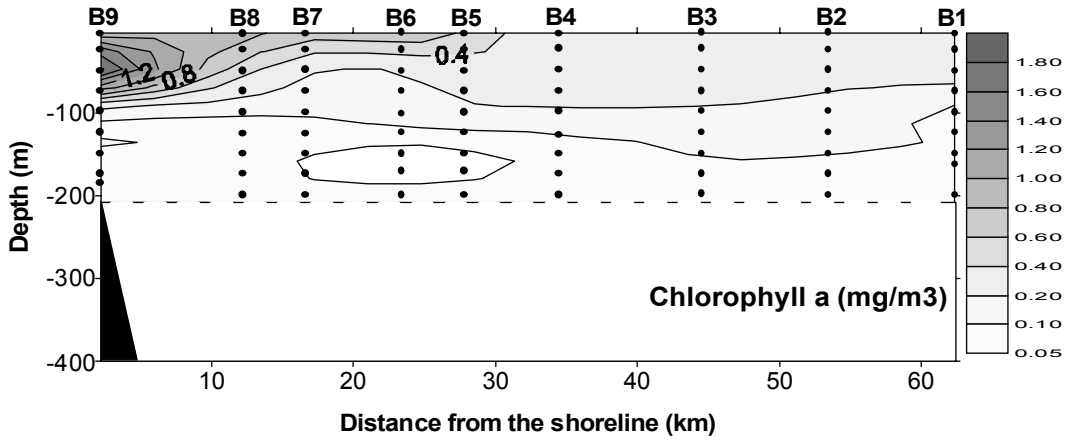

Figure 2.6 Chlorophyll *a* concentrations (mg m^{-3}) along the Blanes canyon. Points indicate sampling depths.

the lower value being inshore and the higher value offshore (Figure 2.7, above). The nitrate isoline of 1.0 μmol kg^{-1} followed approximately the 37.8 salinity isoline inshore reinforcing the boundary with the offshore area. Offshore, such a nitrate isoline sank to about 60 m deeper. Nitrite peaks were remarkable at all stations with maximum concentrations around 0.4 μmol Kg^{-1} between 50 and 100 m depth in the head of the canyon (Figure 2.7, centre). This nitrite distribution pattern appears to be driven by the phytoplankton distribution, since the nitrite maximum is found below phytoplankton maximum and in general around 0.2 mg m^{-3} of chlorophyll *a*. At such depths, light is rather scarce as a consequence of the phytoplankton self shading in the layers above. At 110 – 130 m depth, a nitrite layer of 0.30 – 0.35 coincided with chlorophyll concentrations lower than 0.5 mg m^{-3} and irradiance around 0.5 and 0.1% of surface irradiance, as deduced from the photosynthesis-irradiance model scheme. Nitrite maximum has been observed and modelled in oligotrophic environments as the result of phytoplanktonic dark nitrate reduction and exudation (v. gr. Carlucci et al., 1970; Blasco, 1971*a*; Raimbault, P., 1986; Bahamon and Cruzado, 2002). A similar hypothesis is here assumed to explain the observed nitrite maximum in the Blanes Canyon. It will also be examined through numerical simulations of phytoplankton

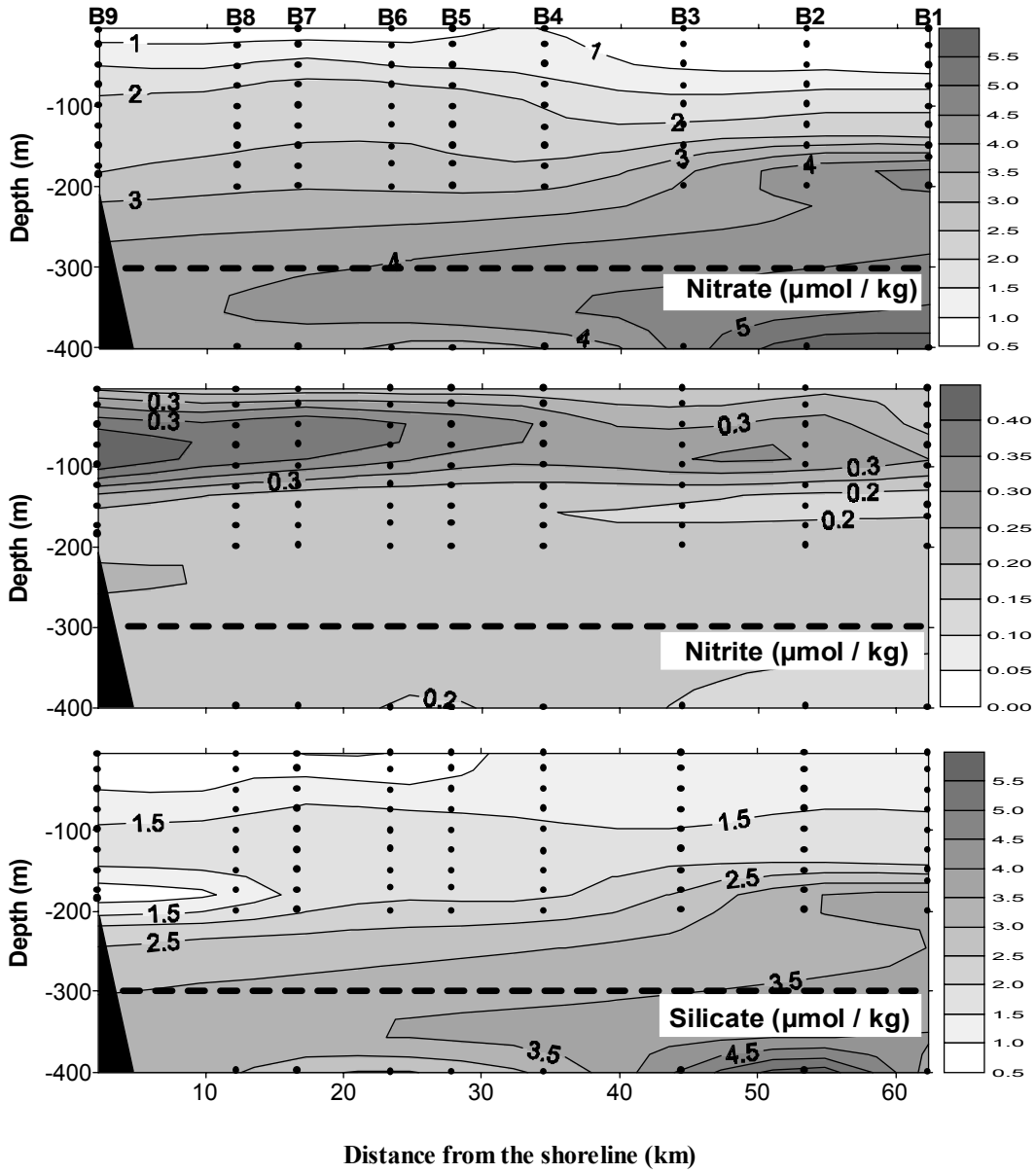

Figure 2.7. Nitrate, nitrite, and silicate (µmol kg^{-1}) concentrations along the Blanes canyon with black points indicating sampling depths.

exudation in a numerical model as described in Chapter 4 and validated in Chapter 5. Finally, Figure 2.7 shows the silicate distribution with lower values in surface waters inshore, suggesting that diatoms and silicoflagellates could be dominating the phytoplankton population. Diatoms often dominate in coastal waters with strong influence of continental runoff and coastal upwelling (Riley et al., 1942; Goldman, 1993) but the temperature, salinity and density measurements in the present study do not allow validating these assumptions. Diatoms are known to be responsible for large

part of nitrate reduction to nitrite in oligotrophic waters (Raimbault, 1986). Moreover, there were no apparent reasons explaining low silicate concentrations at waters around 180 m depth in stations B9 and B8. In general, silicate showed surface values somewhat higher than nitrate being ~1.5 µmol kg^{-1} up to a depth near 100 m depth, close to the 0.2 mg m^{-3} chlorophyll isoline. Following the general nutrient distribution pattern, chlorophyll *a* appears to depend primarily on the nitrate followed by the silicate concentrations.

Surface waters along the section were oxygen over-saturated from 75-50 m depth (>100%), except in the two far stations (B2 and B1) with oxygen-saturated waters (Figure 2.8, above). This distribution pattern is consistent with that of apparent oxygen utilisation (AOU) with negative values in the over-saturated surface waters and positive values (~25 - 60 µmol kg^{-1}) at 200 m depth (Figure 2.8, below). AOU reflected the along-section nutrient concentration variability, particularly nitrate, with deep waters

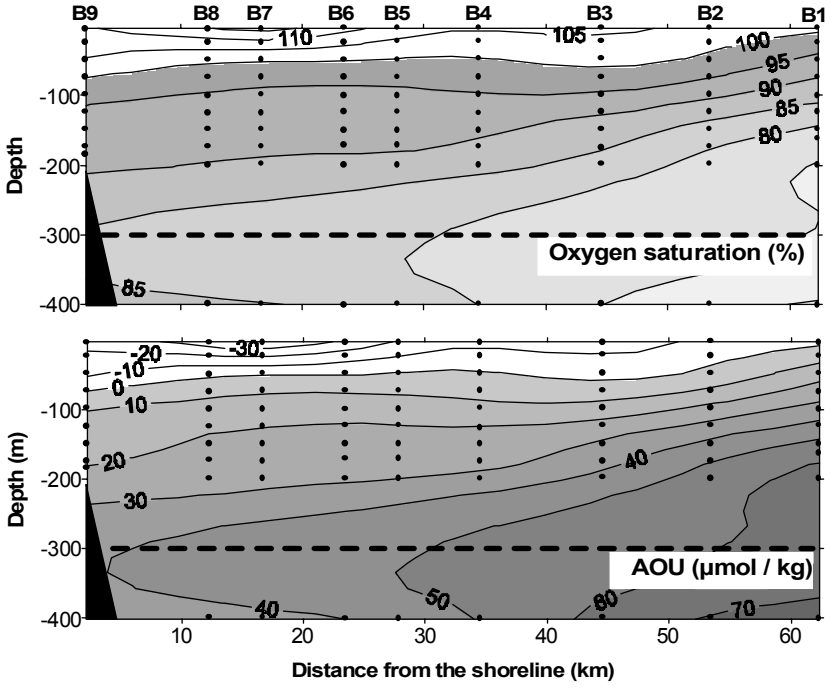

Figure 2.8. Oxygen saturation (%) and apparent oxygen utilisation (AOU) (µmol kg^{-1}) in the upper waters along the Blanes Canyon. Points indicate sampling depths.

nearshore showing lower AOU and nutrient concentrations than offshore stations. Density anomalies are also consistent with dissolved oxygen concentrations. The surface or subsurface dissolved oxygen maximum layer was always close to 250 μmol kg^{-1} and an oxygen minimum was found at 400 m depth (<200 μmol kg^{-1}). In the cold, less saline WIW in the canyon head, dissolved oxygen showed higher concentrations (>220 μmol/kg).

Short-term variability

Evolution of physical properties

The first survey carried out in May 20 evidenced a relatively homogenous water column as observed during the YOYO I Cruise at the beginning of May, described above. A weak signal of summer thermal stratification observed in the first survey was becoming stronger with time (Figure 2.9). A WIW remnant inshore was continuously

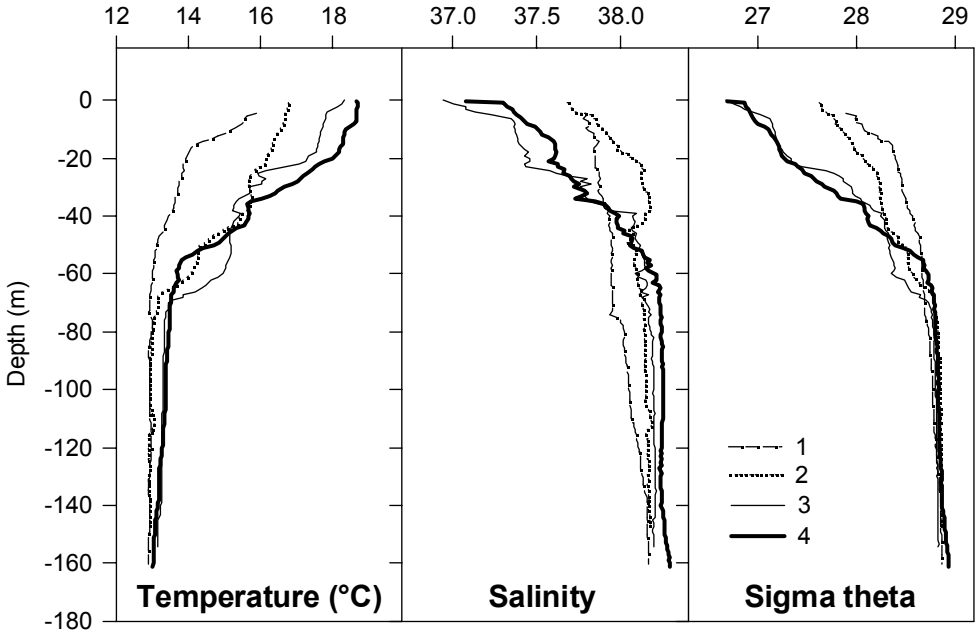

Figure 2.9. Weekly progression of temperature (°C), salinity and density anomaly (sigma theta) (kg m^{-3}) in the Blanes Canyon head. Note trend of surface temperature and density to increases as salinity decreases with time above 60-70 m depth, indicating the early formation of the seasonal thermocline. Numbers (1 to 4) indicate the survey sequences.

displaced by surface warmer waters limited at thebottom by the lower limit of the thermocline observed at ~60 m depth (Figure 2.9, left). The thermocline was nearly coincident with the 0.6 – 1.0 % surface irradiance (lower boundary of the euphotic zone). Salinity decreased with increasing temperature at the surface (Figure 2.9, centre). Stronger density gradients were observed at about 20-30 m depth in the last two cruises, evidencing the increasing of surface heat with proximity of summer (Figure 2.9, right).

Evolution of the plankton metabolism

Vertical profiles of NCR and DCR did not show strong variability in the short-term, suggesting that at least for this period of the year, measurements taken in surface waters (above ~15 m) approximately reflect the whole euphotic water layer functioning. However, a single strong variation in vertical production profiles was observed in the first survey. Positive NCP values (1.2 mmol O_2 m^{-3} d^{-1}) at 50% of surface irradiance (~15 m depth), favoured by a low DCR were found (3.9 mmol O_2 m^{-3} d^{-1}) (Figure 2.10).

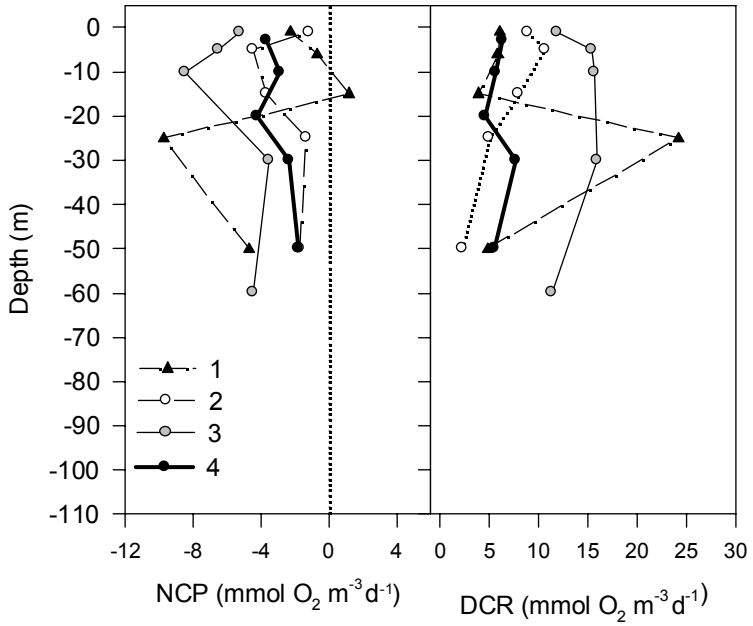

Figure 2.10. Vertical profiles of NCP (left) and DCR (right) (mmol 0_2 m^{-3} d^{-1}) in the euphotic layer at the Blanes canyon head station in the spring. Numbers (1 to 4) indicate the surveys sequence. Standard errors associated to the oxygen measurements were 0.8, 0.6, 0.5, and 0.2% for surveys from 1 to 4, respectively.

The opposite happened in the sample at 12% of surface irradiance (~25 m depth), with a relatively strong increase of respiration (24.1 mmol O_2 m^{-3} d^{-1}) inducing the lowest NCP value (-9.5 mmol O_2 m^{-3} d^{-1}). Vertically integrated DCR, GPP and NCP, suggested in general, a non-linear trend with time (Figure 2.11). In this figure, the negative NCP rates are found to be consequence of the respiration rates (DCR) always exceeding the gross production (GPP) measurements.

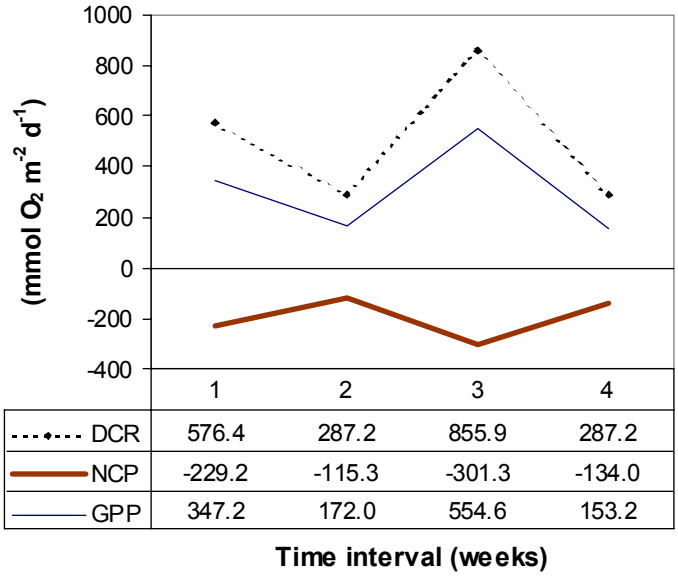

Figure 2.11. Euphotic zone integrated DCR, NCP and GPP (mmol O_2 m^{-2} d^{-1}) during the late spring in the head of the Blanes canyon.

Evolution of chlorophyll a

In the first survey, the chlorophyll *a* profile (Figure 2.12) was consistent with the variation of both oxygen production and oxygen consumption in the water column (see Figure 2.10). Subsurface chlorophyll maximum coincided with a respiration rate maximum suggesting that, at least for this single case, the phytoplankton biomass is relevant among the plankton populations (heterotrophs included) to determine the system metabolic state. The trend of chlorophyll maximum to be deeper with time was also evident, coinciding with the increase of vertical thermal gradient.

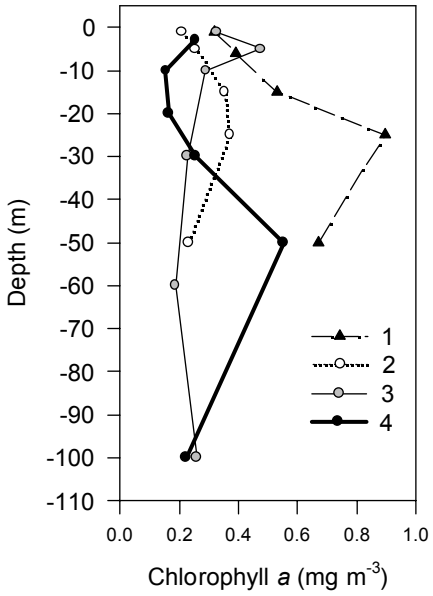

Figure 2.12. Vertical profiles of chlorophyll *a* concentrations (mg m^{-3}). Numbers (1 to 4) indicate the surveys sequence.

Evolution of inorganic nutrients

As observed in the mesoscale measurements, nutrients were found scarce in surface waters with nitrate and silicate around 0.7 µmol kg^{-1}, nitrite around 0.12 µmol kg^{-1} and phosphate under the detection limit (Figure 2.13). Nutrient concentrations in

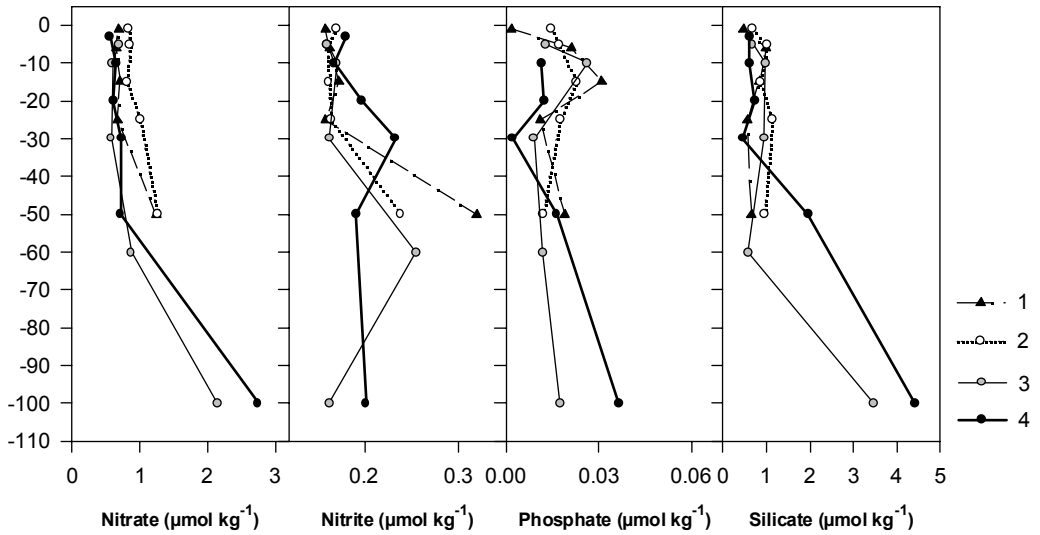

Figure 2.13. Late spring nutrient concentrations (µmol kg^{-1}) at the Blanes canyon head. Numbers (1 to 4) indicate the surveys sequence.

the water column did not reflect eventual horizontal inputs of inorganic matter from coastal runoffs modifying the general pattern of the vertical nutrient profiles. Even though climatological data are not reported, there were no observations of meteorological alterations related to heavy storms or strong riverine inputs influencing the study area during the sampling time. The vertical distribution of nutrients are therefore, assumed to be result of internal mechanisms rather than allochthonous inputs.

2.4 Remarks and discussion

Sub-mesoscale variability along the Blanes Canyon

Observations of physical and biochemical properties of upper waters allowed distinguishing two transient areas in late spring, mainly differentiated by chlorophyll and primary production estimates. The inshore area was set at ~24 km off the shoreline with higher chlorophyll concentrations and primary production rates (mesotrophic) than the offshore area (oligotrophic). A weak variability of surface salinity also differentiated inshore from offshore with less saline waters in the former, separated by a 37.8 salinity isoline from somewhat more saline offshore surface waters. Nitrate and silicate appear to be tracers contributing to such space differentiation along the canyon, with silicate depleted inshore. Colder and less saline inshore waters (Figure 2.14) suggested a higher residence time of the WIW remnant (Cruzado et al., 2002*b*), probably as a response to a reduced horizontal advection in the head and centre of the canyon, (Granata et al., 1999). During summer time, oligotrophy has been observed along the main channel of the Blanes Canyon (inshore and offshore) (Cruzado et al., 2002*b*), thus the observed variability in phytoplankton chlorophyll *a* and PP in the late spring is expected to disappear with time.

The starting of seasonal thermal stratification was conspicuous as deduced from the relatively strong vertical temperature gradient (Figure 2.15, left) and density gradients (Figure 2.15, right) above ~50 m depth, contrasting with smaller gradients for the same variables in the lower water layers. Smaller density gradients below 0.7 kg m^{-4}

indicated relatively homogeneous water layers, particularly in the WIW remnant inshore. This promoted a less stable water column (Figure 2.16, above) thus increasing the turbulent diffusion estimates (Figure 2.16, below). The upper water layers, above

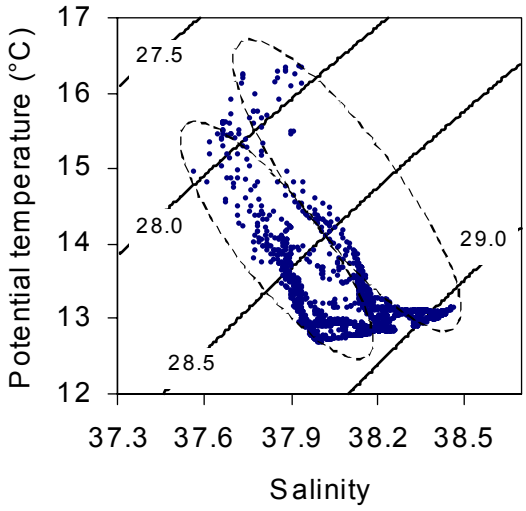

Figure 2.14. T-S diagram of the upper 300 m depth along the Blanes Canyon, showing a WIW remnant near shore (ellipse down) less evident offshore (ellipse up).

~50 m depth, were found well stratified with a maximum in the Brunt-Väisälä frequencies and lower turbulent diffusion rates. Below this layer, the Brunt-Väisälä frequency decreased toward the bottom and K_z increased. The general vertical distribution pattern of K_z was that expected from the model diffusion application (Osborn, 1980; Zakardkian and Prieur, 1998) making it suitable for a transitional period from spring to summer. The relatively high K_z values observed near the continental

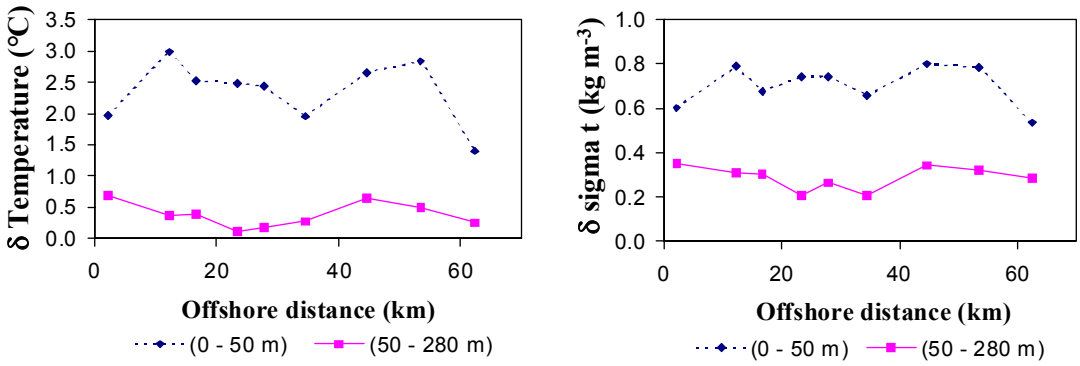

Figure 2.15. Along-section temperature (left) and sigma-t (right) differences in the upper and lower water layers.

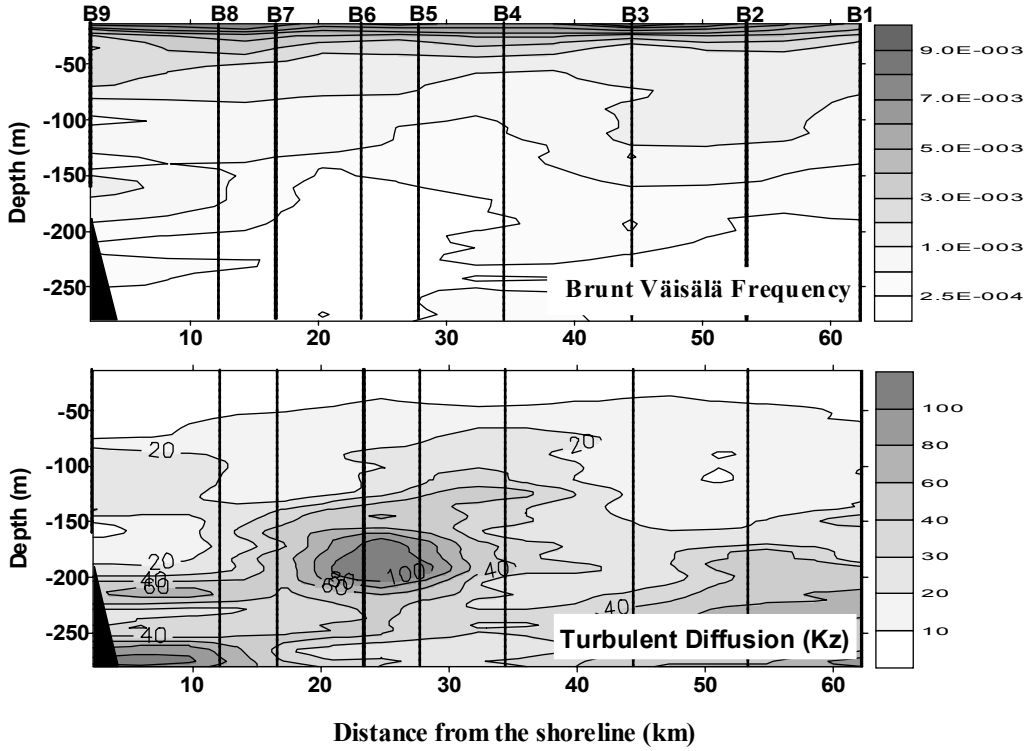

Figure 2.16. Above, the stability frequency (Brunt Väisälä frequency) (s^{-2}) used to estimate the vertical turbulent diffusion coefficient (K_z, m^{-2} d^{-1}) showed below.

slope (Station B9) are not caused by the vertical structure of water, but by a boundary problem derived from the grid interpolation making K_z to be overestimated.

Vertically integrated primary production estimates were higher with a chlorophyll *a* maximum close to the surface. This is the case observed at stations B6, B7, and B8 as shown in Figure 2.17. The highest vertically integrated chlorophyll showed the chlorophyll maximum not close to the surface but in the subsurface (25 - 50 m depth) thus making the primary production estimation not to increase proportionally (see Station B9, Figure 2.17). This was due to the rapidly downward extinguishing (exponentially) of surface irradiance used to estimate primary production, with low values limiting the production estimates in subsurface water layers. Offshore stations showed chlorophyll *a* concentrations decreasing homogeneously with depth. This homogeneous distribution made the primary production estimates show a linear trend in

respect of chlorophyll concentrations (Stations B1-B5, Figure 2.17). The general distribution pattern of chlorophyll and primary production is consistent with previous measurements of primary production in NW Mediterranean (Estrada, 1985; Estrada et al., 1999).

Average vertically integrated chlorophyll *a* and primary production values were found significantly different ($P<0.001$) between inshore and offshore areas in the Blanes Canyon. Inshore, average (±SE) chlorophyll *a* and primary production were 0.11 ± 0.04 mg m^{-2} and 1.38 ± 0.2 mg C m^{-2} d^{-1}, respectively. Offshore, mean values for the same variables were 0.06 ± 0.01 mg m^{-2} and 0.62 ± 0.06 mg C m^{-2} d^{-1}, respectively. This suggests that upper water layers along the canyon are subject to different fertilisation processes induced by space variability. Granata et al. (1999) suggested that plankton communities near the Blanes Canyon are subject to different regimes of local circulation with respect to those located offshore, the former with slow cycling pool making negligible the downward flow of in situ produced organic matter. This latter assumption is consistent with observations of inshore WIW remnant in the present study, explain the phytoplankton biomass (chlorophyll) and primary production differentiation along the Blanes Canyon.

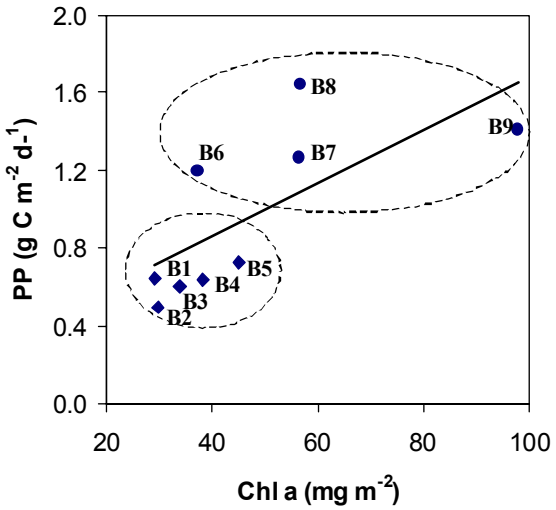

Figure 2.17. Primary production rates (PP) as a function of chlorophyll *a* concentrations along the Blanes Canyon. Ovals up and down indicate inshore and offshore stations, respectively. Line illustrates a non-significant trend between variables ($P<0.05$).

Using the nitrate gradients from the surface up to 150 m depth and the average turbulent diffusion entering the mixed layer (between 150-200 m depth), the upward diffused nitrogen and new primary production was estimated (Table 2.1). Unlike chlorophyll *a* and primary production, turbulent diffusion, nitrate gradients and new production estimates in Table 2.1 were found relatively homogenous along the section. As expected for springtime, most of the primary production (93 – 99 %) was regenerated production, as deduced from low estimates (1 – 7 %) of new production to

Table 2.1. Mean estimates of upward diffused nitrogen generating new primary production (NPP) into the euphotic zone along the Blanes Canyon during springtime. Note the very low values of NPP regarding total chlorophyll-irradiance primary production (TP). Primary production values were estimated assuming a C:N Redfield ratio of 6.625.

(Station) Distance from the shoreline (km)	K_z ($m^2\ d^{-1}$)	N+N gradient (mmol N m^{-4})	N+N flux (mmol N $m^{-2}\ d^{-1}$)	NPP (mg C $m^{-2}\ d^{-1}$)	NPP/TP (%)
(B9) 2.2	14.89	0.0134	0.20	15.9	1.1
(B8) 12.3	15.82	0.0107	0.17	13.5	0.8
(B7) 16.7	20.24	0.0204	0.41	32.8	2.7
(B6) 23.4	38.93	0.0136	0.53	42.0	3.3
(B5) 27.9	28.83	0.0157	0.45	36.0	7.3
(B4) 34.5	28.21	0.0067	0.19	15.0	2.4
(B3) 44.5	13.64	0.0131	0.18	14.2	2.0
(B2) 53.5	17.34	0.0118	0.20	16.3	2.7
(B1) 62.4	19.03	0.0131	0.25	19.8	3.1
Mean	21.8	0.0132	0.28	22.8	2.8
±SE	*8.4*	*0.035*	*0.14*	*10.9*	*1.88*
Inshore area*					
(B9-B6) *Mean*	22.4	0.0145	0.33	26.1	2.0
±SE	*5.6*	*0.0021*	*0.09*	*6.8*	*0.6*
Offshore area*					
(B5-B1) *Mean*	21.4	0.0122	0.25	20.3	3.5
±SE	*3.0*	*0.0015*	*0.05*	*4.5*	*1.0*

* Means are not significantly different as deduced from ANOVA with a Tukey honest significant difference test (95% confidence level).

total production rations. This means that near 93 to 99% of primary production is due to organic matter regeneration process, in good agreement with expected estimates. Selmer et al. (1993) pointed out that during spring in the NW Mediterranean,

ammonium uptake rates (derived from regenerate material) prevail over nitrate uptake that is often negligible, resulting in a dominance of regenerated production (98 to 100% of total production). Negligible ratios of in situ-produced organic matter to total downward exported material have been reported in other coastal areas of NW Mediterranean Sea (Miquel et al., 1994), support this observation. The percentage of new production was lower than that reported by Fowler et al. (1991) in the Ligurian Sea, NW Mediterranean (~25%) probably due to differences in the estimate methods, since the later authors used indirect calculations and sediment traps. The external input from coastal freshwater runoff affecting the estimates inshore is an issue that could contribute to explain such differences, but this hypothesis is not validated here.

Short-term variability in the Blanes Canyon head

Phytoplankton chlorophyll and primary production

Short-term variability of biogeochemical properties in the Blanes Canyon head is assumed to be as a continuity of the inshore observations in the mesoscale experiment. The relatively high nutrient concentrations, primary production rates and chlorophyll *a* concentrations observed in the canyon head were found to be indicating a transient mesotrophy. The first survey carried out 14 days after the mesoscale study, still showed a transient event of high productivity probably induced by a remaining spring phytoplankton bloom tending to disappear with the sampling time. The first survey showed the highest productivity (1.8 g C m^{-2} d^{-1}) coinciding with the highest value of depth integrated chlorophyll *a* concentration (46.7 mg Chl *a* m^{-2}). The production rate is over three times the yearly average production reported for NW Mediterranean around 157 g C m^{-2} y^{-1} (equivalent to 0.5 g C m^{-2} d^{-1}) (see compilation by Estrada, 1996). This single primary production value was comparable with values in the Canary Current area with water nutrient enriched by coastal upwelling (mesotrophic environment) (Morel et al., 1996). However, the integrated chlorophyll *a* value was similar to those found inshore in the mesoscale experiment, being in the upper rank of the measurements reported in both coastal and open NW Mediterranean waters during summer time (Velásquez, 1997; Pedrós-Alió et al., 1999). In the other three surveys, primary production and chlorophyll *a* values were less than a half of those in the former survey indicating the progressive surface nutrient depletion with the early signals of thermal

stratification. Mean primary production and chlorophyll *a* values (±SE) were 0.7 ± 0.2 g C m^{-2} d^{-1} and 21.2 ± 0.6 mg m^2, respectively, closer to the other estimates given for the same area.

New nitrogen from the nutrient-rich deep waters flowing up to the euphotic water layers was estimated and compared against values found inshore in the mesoscale experiment. The upward diffused nitrogen (nitrate + nitrite) was estimated using the nitrogen gradient from the surface to 100 m depth (due to the proximity of the continental slope) with diffusion values compared at the baseline. In absence of nitrogen values for the bottom in the first two cruises, a realistic value of 2.5 µmol kg m^{-3} was imposed at 100 m depth, similar to those observed in the last two surveys. Integrating all observations, the average upward diffused nitrogen entering the euphotic zone was 2.44 mmol N m^{-2} d^{-1}. Assuming a C:N Redfield ratio of 6.625, this nitrogen represented 18% (0.19 g C m^{-2} d^{-1}) of total chlorophyll-irradiance primary production (1.07 g C m^{-2} d^{-1}). This new production is higher than that estimated in the mesoscale experiment (between 1 to 7%), but is still in the range (up to 25%) deduced for NW Mediterranean from indirect calculations and sediment traps by Fowler et al. (1991). These results are also comparable with estimates in the open NW Mediterranean (Bahamon and Cruzado, 2002) and with estimates given for the Sargasso Sea in late winter (Platt and Harrison, 1985).

Phytoplankton chlorophyll size structure has been pointed out as a factor that selectively alters the plankton food web and therefore, the plankton metabolism (Maloney et al., 1991). In the present work, the size - chlorophyll *a* fractions (greater and smaller than 5 µm) were very similar (Figure 2.18). In the fist survey, with the highest chlorophyll value, the smaller fraction represented 35%. In the following surveys, with lower values of chlorophyll *a* this fraction increased to 55% in the rest of the period suggesting a trend to higher size chlorophyll fractions to dominate toward summer (Figure 2.18). In the open oligotrophic sea, size fractionated phytoplankton is often found mainly represented by picoplankton (<2 µm) (70 – 80%) during spring, with a picoplankton fraction tending to increase with highly productive waters (Jochem and Zeitzschel 1993; Serret et al., 2001). Picoplankton in the Blanes Bay has been

reported to represent about 10% of total phytoplankton biomass showing low variability along the year (Mura et al., 1996). Picoplankton have also been observed dominating the ammonium uptake inducing a relatively low new production to total production ratio during springtime in NW Mediterranean (Selmer et al., 1993) supporting the

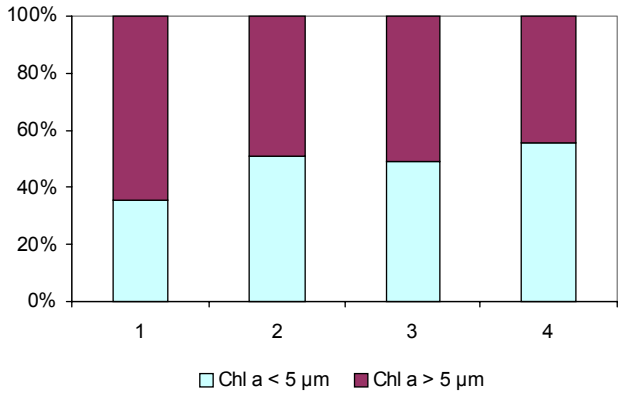

Figure 2.18. Phytoplankton chlorophyll fractions at every sampling time (survey sequence indicated with numbers 1 to 4).

observations in this work. Comparing oligotrophic with eutrophic waters in the eastern Atlantic, Serret et al. (2001) found an inverse relationship between carbon picoplankton (<2µm) assimilation and phytoplankton production. In the present work, even with chlorophyll fraction greater and smaller than 5 µm, small-size picoplankton chlorophyll was better represented in the higher productive period (first survey) similarly to observations of the expected picoplankton trend.

Microplankton metabolism in the Blanes Canyon head

Mean net community production (NCP) in the Blanes Canyon head was -195 mmol O_2 m^{-2} d^{-1} indicating a transient net heterotrophy. Plankton communities were stressed by a relatively rapid increase in density in the mixed layer (up to –1.3 kg m^{-3} in surface during 22 days) (Figure 2.19, left). Net heterotrophy during springtime has been reported in NW Mediterranean coastal waters (Satta et al., 1996) and open ocean (Williams and Robinson, 1991) along the year. In the present case study, dark community respiration (DCR) prevailed over gross primary production (GPP) from 20 May to 11 June. Surface thermocline in the canyon head showed general features of

salinity increasing with decreasing temperature in the range observed inshore and offshore (Figure 2.19, right).

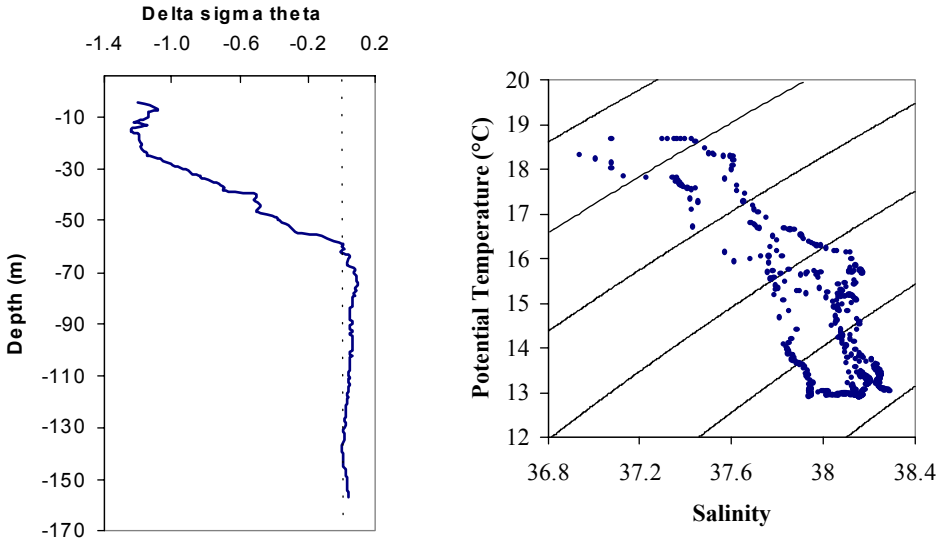

Figure 2.19. On the left is shown the term variation of the density gradient (sigma theta, kg m^{-3}) in the head of the Blanes canyon during 22 days from May 20 to June 11, 1999. T-S diagram (right) shows the gradual salinity increasing with temperature decreasing, as characteristics for Mediterranean waters.

Volumetric measurements of phytoplankton chlorophyll *a* were not correlated with DCR rates ($P > 0.005$) suggesting the phytoplankton respiration to be negligible in comparison with that of microheterotrophs (bacteria, ciliates) (Satta et al., 1996). On the contrary, the phytoplankton chlorophyll in the present study contributed significantly to GPP (Figure 2.20). A similar pattern has been observed in coastal and open ocean waters of NW Mediterranean (Williams and Robinson, 1991; Pedrós-Alió et al., 1999).

Volumetric NCP measurements in the water column during the whole period of sampling were 69% explained by the DCR variability (Figure 2.21). Along the euphotic layer, net production was predominantly negative (heterotrophic), with a single exception at 50% depth of surface irradiance in the first survey, where NCP reached 1.2 mmol O_2 m^{-3} d^{-1} (autotrophy) induced by a low respiration rate (3.9 mmol O_2 m^{-3} d^{-1}). Variability of DCR in this study (from 2.2 to 24.1 mmol O_2 m^{-3} d^{-1}), falls in the range

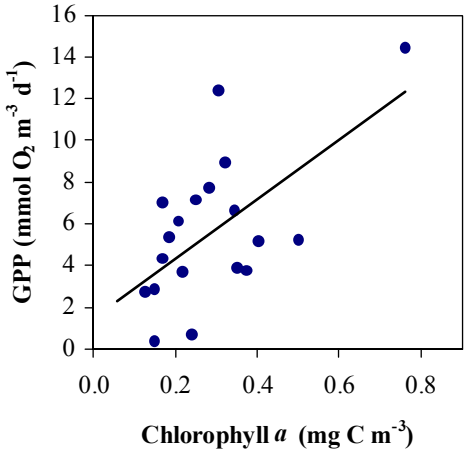

Figure 2.20. Relationship between GPP (mmol O_2 m^{-3} d^{-1}) and chlorophyll *a* concentration (mg m^{-3}) with solid line indicating a lineal tend (GPP=14.225 (Chl *a*) + 1.494; n=19; r^2=0.374 $P < 0.001$).

reported for surface NW Mediterranean water measurements suggesting once more that heterotrophs organisms are responsible for most of the community respiration (Satta et al., 1996). Coinciding with the peak of DCR, a chlorophyll *a* maximum was observed in the same period (0.76 mg m^{-3}), showing a single positive correlation between phytoplankton biomass and oxygen consumption.

Net community production decreased with increasing daily-integrated irradiance at the time that community respiration and gross production increased (Figure 2.22),

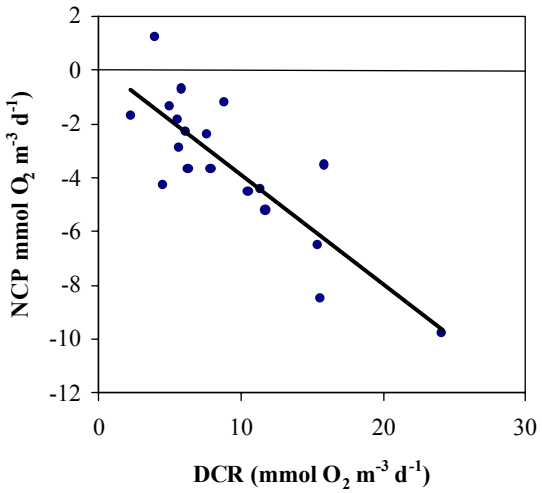

Figure 2.21. Relationship between NCP with DCR in the euphotic zone of Blanes canyon head. Solid line represents a linear regression NCP= - 0.409 (DCR) + 0.2213 (n = 18; r^2 = 0.69; $P < 0.001$).

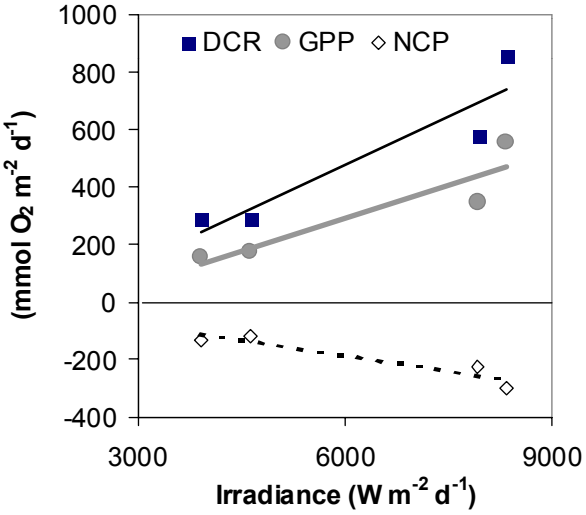

Figure 2.22. Trends of DCR, GPP and NCP (mmol O_2 m^{-2} d^{-1}) with irradiance (W m^{-2} d^{-1}) in the time sampling. Note the DCR and GPP to decrease while NCP increases with total daily irradiance.

suggesting a light saturated phytoplankton community with irradiance favouring DCR over NCP. This is consistent with previous observations of phytoplankton communities in NW Mediterranean during spring (Williams and Robinson, 1991; Satta et al., 1996). In the present study, DCR rates are constant over two orders of magnitude (Figure 2.23) in ranges given for open ocean mesotrophic ecosystems in the eastern Atlantic (Duarte et al., 1999). These values are also comparable to those measurements in productive provinces in the eastern Atlantic (Benguela Current, Canary Current and North Atlantic Drift province), following a similar methodology than that in the present experiment (Serret et al., 2001).

In the Blanes Canyon head, daily and vertically integrated gross primary production to dark community respiration (GPP : DCR) was quite constant at the time of the study (mean ± SE = 0.60 ± 0.02) indicating that the plankton metabolism was far from the equilibrium between consumption and production (1:1). Preliminary time series observations in coastal NW Mediterranean suggest a trend of the ecosystem towards net heterotrophy with a GPP : DCR ratio similar to that found here, only when high external inputs of material by heavy storms are added to the system, being the

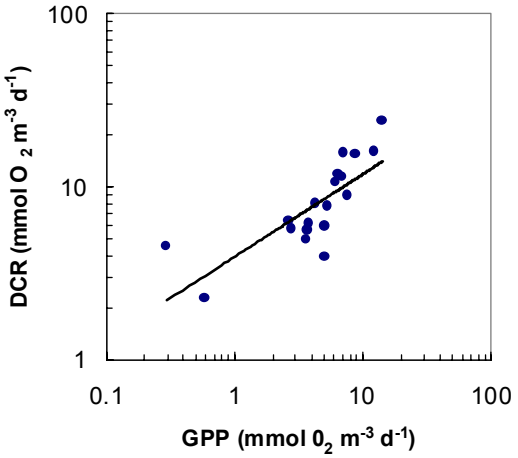

Figure 2.23. Relationship between volumetric GPP and DCR rates in the late spring in the Blanes canyon head. Solid line is the reduced axis with DCR=3.9359 $(GPP)^{0.4765}$ ($n = 19$, $r^2 = 0.599$, $P < 0.001$). Dashed line is the ratio 1:1.

system near the equilibrium in absence of such events (Satta et al., 1996). The transitional spring to summer period suggests a relatively recent fertilisation event that is attributable to the winter vertical convection that could force an important increase of the organic matter (phytoplankton bloom) stored in the upper mixed layer. Often, when this accumulated material is consumed in the late summer and no substantial external input takes place, a period of net autotrophy occurs (Serret et al., 1999). A similar trend has been observed in various productive and unproductive areas in the eastern Atlantic (Serret et al., 2001). Observations in the present study contrast with those in the open ocean with a GPP : CDR ratio close to equilibrium (Williams, 1998). Explanation for heterotrophy in the present study is the same given to explain the mesotrophic conditions of the system. The reduced downward flux of organic material favoured by winter convective mixing and the slow cycling pool make the organic matter excess produced during the late winter phytoplankton bloom is accumulated in the mixed layer, thus increasing the respiration rates over production rates. This coincides with observations by Blight et al. (1995) and Granata et al. (1999) in temperate waters and appears to be the more suitable explanation for both mesotrophy and heterotrophy in the Blanes Canyon head. The offshore microplankton metabolism -not measured here-, is expected to differ of in the Blanes Canyon, with a probably GPP : DCR ratio tending to be closer to 1:1. William and Robinson (1991) found in surface waters off the Golf of Lions during springtime a net production around 5 mmol O_2 m^{-3} d^{-1} (autotrophy)

using similar methodology than in this study. However, they found negative values of net production (-0.77 mmol O_2 m^{-3} d^{-1} = heterotrophy) in waters below 30 m depth. The Blanes canyon head is expected to show more homogeneous features along its main channel with time, as suggested by Cruzado et al. (2002) who observed a summer trend of chlorophyll and nutrient values to be typically oligotrophic and close to the metabolic balance.

Chapter 3

Summer phytoplankton primary production and diffusive nitrogen fluxes in the subtropical North Atlantic

Abstract

Estimates of new primary production along 24° 30'N latitude in the subtropical North Atlantic are given from upward diffused nitrogen across the top depth of nitracline. The nitracline was found at ~136 m depth west of 23°W, and ~80 m depth east of this longitude. The thermocline was located at depths between 28 – 44 m along the whole area showing less variability. The upward diffused nitrate, deduced from density fields and nitrate gradients reasonably explained "new production" in most part of the studied area. The average upward diffused nitrogen in the Western Sargasso (WS), Central Sargasso (CS) and Western Atlantic (WA) areas was ~0.53 mmol N m^{-2} d^{-1} equivalent to ~43 mg C m^{-2} d^{-1}, i.e. 21% of total primary production (~ 214 mg C m^{-2} d^{-1}) coinciding with previous observations. In the Canary Current (CC) zone, the estimates of upward diffused nitrogen did not explain the new production that appear to depend on laterally advected nutrients from coastal upwelling. The depth of the 26.0 isopycnal was always greater than that of the thermocline and was closely related to nitracline depths in the CS, WA and CC areas. In WS, the depth of the 26.0 isopycnal was highly variable responding to local subthermocline oscillations while the nitracline depth remained relatively constant, thus suggesting factors other than density (probably light) as responsible for the top depth of nitracline. Typical depth-integrated phytoplankton chlorophyll *a* concentrations (around 24 mg m^{-2}) showed an average maximum of 0.27 mg m^{-3} at ~119 m depth in the subtropical NA, except in the CC area. In the latter zone, influenced by coastal upwelling, the average of integrated chlorophyll *a* concentration was 32 mg m^{-2} with an average maximum concentration around 0.39 mg m^{-3} at ~80 m depth. New primary production appeared to be controlled by the diffusive nitrate fluxes taking place at the top of the nitracline depth, far below the nutrient depleted seasonal thermocline waters.

3. 1 Introduction

In upper waters of the open ocean, new phytoplankton primary production is closely linked to the transport of inorganic nutrients from nutrient-rich deeper waters influenced by the vertical structure (thermal gradients) of the water column (Eppley and Peterson, 1979; McGillicuddy and Robinson, 1997). An important feature of the water column in temperate seas is the seasonal thermocline formed in summer time that represents a physical barrier separating the surface mixed layer from deeper waters. In summer, surface waters are often nutrient depleted but in winter, the convection processes homogenise the water column particularly at high latitudes, breaking the seasonal thermocline. Convection brings nutrients from nutrient-rich bottom waters and initially dilutes phytoplankton accumulated in the surface in late autumn, inducing a phytoplankton production higher than that found at lower latitudes (Lohrenz et al., 1992; Goericke and Welschmeyer, 1998). In permanent stratified environments, such as the tropics, winter convection does not take place thus making the vertical diffusion term crucial in maintaining new production along the whole year.

Besides the upward nitrogen flux to the euphotic zone where photosynthesis takes place, other mechanisms have been suggested to explain part o new production in the open ocean. In eddy-induced areas in the Sargasso Sea, the upward advection of subsurface nutrients takes an important role in the nutrient transport to generate new production (McGillicuddy and Robinson, 1997). In the central subtropical north Atlantic gyre, the horizontal transport of nutrients could contribute to fuel about 40 - 80% of new production estimated to be near 1 mol C m^{-2} yr^{-1} (Williams and Follows, 1998). The supply of nutrients deposited from the atmosphere can also play an important role in generating new primary production in subtropical areas (Planas et al., 1999; Romero et al., 1999) but such an input could not alter the subsurface phytoplankton biomass maximum (Varela et al., 1994). However, it is widely accepted that vertical diffusion of nutrients from deep waters to the euphotic zone is the most important way to restricting new production and phytoplankton biomass

maximum in permanent stratified waters (Menzel and Ryther, 1960; 1961; Denman and Gargett, 1983).

Subsurface phytoplankton chlorophyll maximum in stratified water columns has been reported to be associated with density discontinuities at depths with 0.5 – 5% surface light intensity (Cullen and Epply, 1981; Longhurst and Harrison, 1989; Goericke and Welshmeyer, 1998). In the Sargasso Sea, during summer, the low surface chlorophyll concentration increases with depth reaching maximum values of ~0.5 mg m^{-3} at 100 - 140 m depths, receiving ~1-3% of the surface photosynthetically active radiation (PAR), as deduced from direct measurements by Bricaud et al. (1992). In the subtropical North Atlantic, widely variable isotherm oscillations are closely connected to the phytoplankton chlorophyll distribution. The depths of 17-19° C isotherms near the surface in the Guinea Dome in the Atlantic Ocean are linked to the upwelling off northwestern Africa coast (Meyer et al., 1998). They appear somewhat deeper near 10° N due to the divergence of water masses and sink at depths between 150 - 250 at latitudes between 20° - 30° north and south, being deeper in the southern than in the northern hemisphere. These isotherm oscillations has been observed closely linked to the position of the phytoplankton chlorophyll maximum, located below the depth of maximum stability receiving on average 3% surface irradiance (Agusti and Duarte, 1999).

Although the subsurface phytoplankton chlorophyll maximum in stratified waters is generally linked to maximum thermal and density gradients, a higher correlation has been observed with the maximum nitrate gradient (nitracline) than with the thermocline (Herbland and Voituriez, 1979; Cullen and Epply, 1981; Varela et al., 1994; Helguen et al., 2002). However, no single mechanism is responsible for the formation of subsurface chlorophyll maximum. The differential plankton sinking rates, physiological changes in the carbon to chlorophyll *a* ratio and differential grazing by zooplankton, among others, have been suggested as potential mechanisms controlling the chlorophyll maximum (Longhurst and Harrison, 1989). At present, ecological processes connecting phytoplankton primary production in stratified waters still require more studies providing robust support to the understanding of

such processes (Furuya, 1990; Varela et al., 1994; Agusti and Duarte, 1999; Helguen et al., 2002).

As a contribution to the enlargement of the physical and biogeochemical structure and circulation knowledge on ocean, the World Ocean Circulation Experiment (WOCE) evaluated components of the ocean variability and its fluxes on scales of thousands of kilometres. Statistics on smaller scales were also addressed in this program, in order to develop models predicting regional and global changes. In the present chapter, interactions between the vertical structure of water and phytoplankton primary production in upper waters of the subtropical transatlantic section WOCE A5 carried out from NW Africa to Bahamas were evaluated.

Previous works have been conducted along the same latitude related to the WOCE A5 Section, but they have been focussed mainly on deeper waters. Evaluation of time variability of physical features and of tracer distributions in this section were made by Parrilla et al. (1994) and by Garcia et al. (1998), who compared observations made on the same latitude several times during the twentieth century. In the present work, the spatial variability of chlorophyll *a* in summer thermally stratified subtropical North Atlantic is examined on the basis of density and estimates of upward diffusion of nutrients supporting new production. The nitrate flowing across the nitracline is assumed to control new production. Basic information from the WOCE A5 section (temperature, salinity) was obtained while measurements of nitrate, phosphate, silicate, dissolved oxygen and chlorophyll *a* data were made by A. Cruzado and Z. Velásquez on board the *BIO Hespérides* during the 1992 WOCE cruise.

3.2 Methods

Study area and sampling

The present work was carried out based on oceanographic information taken in the WOCE A5 cruise along 24° 30’ N in the North Atlantic between the North West African coast (16° W) and the Bahamas (75° W). This area is, in general,

governed by a hydrographic regime driving the southern part of the subtropical anticyclonic gyre. In the western basin, near Bahamas, large oscillations of currents take place induced by intense frontal structures in the North Equatorial Current. In the eastern basin, the Canary current that flow southward, merges with the North Equatorial Current off Africa, appearing relatively weak and diffuse and generating coastal upwelling of intermediate waters (Schmitz and McCartney, 1993).

The WOCE A5 transatlantic section was conducted on board the *BIO Hespérides* from July 12th to August 15th, 1992 as part of the WOCE Program (Figure 3.1). Oceanographic data used in this work were compiled by the CEAB/CSIC Chemical Oceanography Group and submitted to the WOCE Program Office, a component of the World Climate Research Program. Data are also available at http://www.ceab.csic.es/~oceanlab/. A total of 101 full-depth oceanographic stations were occupied. The average distance between stations was 59 km with small variation in the entire section. CTD data were 3 m depth averaged from surface to bottom, however only the upper 500 m were used in this work. Typically, 12 L

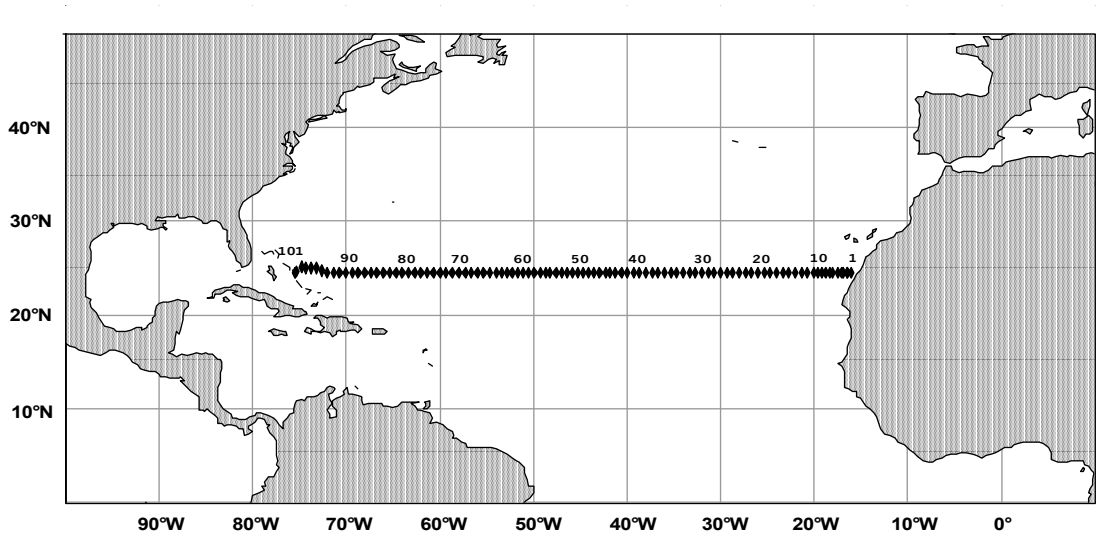

Figure 3.1. Location of the 101 oceanographic stations in the WOCE-A5 transatlantic section along 24.5°N latitude. Distance between stations was 59 km average with small variations in the entire section.

Niskin bottles samples were taken. Bottles triggered above 500 m depth were used for chlorophyll and nutrient analysis in the present work.

Dissolved inorganic nutrients

Nitrite + nitrate (hereafter called as nitrate), phosphate and silicate (μmol kg^{-1}) were measured following analytical processes according to Whitledge et al. (1981). Precision of data (described in García et al., 1998) were 0.2 and 0.3 μmol kg^{1} (±1 SD) for nitrate plus nitrite and 1.9 and 0.9 μmol kg^{-1} for silicate in the eastern and western Atlantic, respectively. Precision of phosphate was 0.08 μmol kg^{-1} in both eastern and western basins. Precision data were used as reference to make contours of vertical distributions.

Dissolved Oxygen

Oxygen was measured in samples replicates taken at different depths. The Winkler procedure following Culberson (1991) using reagents following Carpenter (1965) was used to measure dissolved oxygen (μmol kg^{-1}). Methodology is similar to that used in the NW Mediterranean case study with details described in the WOCE (1991) Operation Manual. The average precision of measurements was 1.5 μmol Kg^{-1} (García et al., 1998). The oxygen saturation was calculated using García and Gordon (1992) equations.

Chlorophyll a *and primary production*

Procedure to determine non-fractionated chlorophyll *a* concentration is similar to that described in Chapter 2. A similar scheme of primary production (*P-I*) estimations is also used, but modifying the physiological parameters in Equation 2.3. The P_m^B and α^B parameters in the equation were the regional, summer mean values estimated by Sathyendranath et al. (1995) in the North Atlantic. Thus, P_m^B was 3.6 for stations in the Canary current and 1.7 for the rest of the section. α^B was taken as 0.06 and 0.14, respectively. *R* was assumed to be negligible relative to gross production as typically assumed in production models (Herman and Platt, 1986). Units of *P-I* are given in mgC $[mgChl\ a]^{-1}\ h^{-1}$. Along the entire section, the "open ocean" stations

were those located between 75°W and 23.3°W (stations 18 – 101) and the "Canary Current" stations those located between 23.3°W and 16°W (stations 1 – 17). Surface solar irradiance was taken as 800 W m^{-2} at noon (Bricaud et al., 1992) with 46% of such irradiance assumed to be PAR (Baker and Frouin, 1987). Coefficients for PAR extinction in the water column were those used in the NW Mediterranean Sea case.

Phytoplankton

In order to determine prevailing phytoplankton taxonomical groups, 200 ml water samples were taken from Niskin bottles. Samples were immediately fixed with lugol's iodine and stored in plastic bottles in the darkness for further counting under inverted microscope following Uttermöhl technique (Hasle, 1978). Stations at west central Sargasso and eastern Atlantic 21, 22, 59, 60, 61, 67-74, 76-78, 90-92, 94, and 95 (see approximate locations in Map 3.1) were selected for illustration purposes. Representative taxa were identified to genus following Sournia (1986), Hasle and Syvertsen (1997), Steidinger and Tangen (1997) guides and also with the assistance of phytoplanktologist Z. Velásquez.

3. 3 Results

Distribution of physical properties

Contours of temperature, salinity and density in the upper 500 m depth are shown in (Figure 3.2). Surface temperature increased ~10 degrees from east to west the warmer waters being near Bahamas (~29° C) and the colder waters near Africa (~19° C). Typically, the base of the seasonal thermocline was found at depths between 23 and 69 m along the whole section, except near Africa, because of colder, nutrient-rich, oxygen poor coastal upwelling induced by the Canary Current outcropped thermocline between 16.6 and 17° W (Figure 3.2, left). A large surface lens of salty water with values over 37.0 reaching 37.6 close to the surface was observed in the eastern and central parts of the section (Figure 3.2, centre). The upper part of the lens was located between 25° - 58 °W. It is attributed to the injection of salty surface waters of the subtropical gyre (Kawase and Sarmiento, 1985). A

deepening of the 26.0 isopycnal from surface to the east to ~200 m depth on the west side of the section, evidenced the differing hydrographic pattern governing eastern and western basins (Figure 3.2, below). Subthermocline isopycnal oscillations

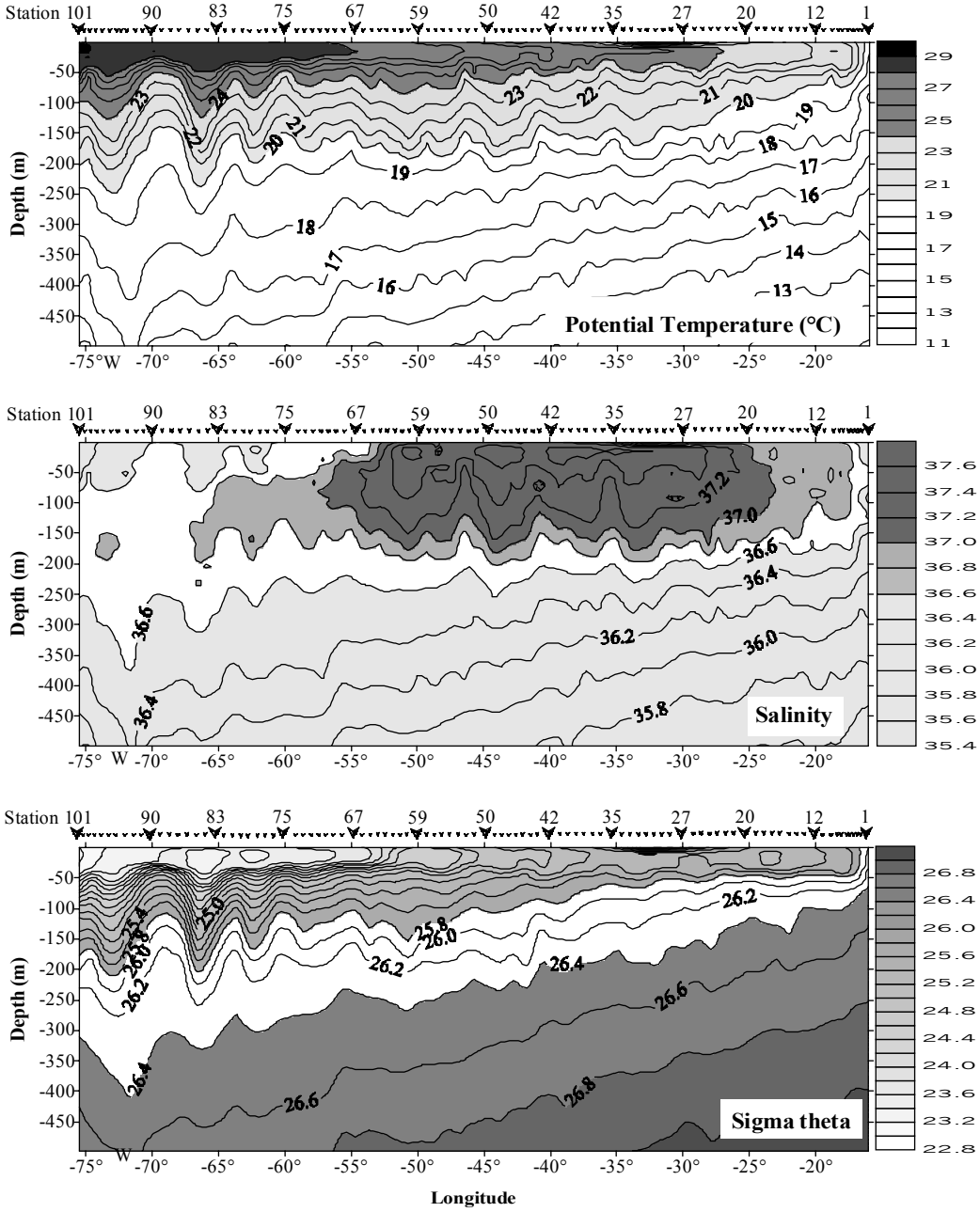

Figure 3.2. Longitudinal distribution of temperature (°C), salinity and σ_θ (kg m^{-3}) in the subtropical north Atlantic. 16,766 data points were use to built contours (101 stations with 166 depth-averaged data each one).

reflected the existence of eddies particularly in the western basin. A relatively strong surface horizontal density gradient (isopycnal front) is observed around the middle of the section between 51 - 54° W longitude.

Distribution of dissolved inorganic nutrients and oxygen

Nutrients were in general depleted in the surface to depths greater than the seasonal thermocline. The 0.5 μmol kg^{-1} nitrate isoline was found between 120 and 160 m depth in most of the section, except near Africa where it was found between 70 – 90 m depth (Figure 3.3). Nutrients in the water layers below the euphotic zone (depth of 1% surface irradiance) showed important longitudinal variability since their concentrations near Africa were approximately twice those near Bahamas. Subsurface wedges of nitrate, phosphate and silicate were observed at the Canary Current area extending westward from the African side (16.6° W) up to about 25° W evidencing the enrichment of nutrient due to the upwelling of nutrient-richer coastal waters (Figure 3.3, above and centre). Unlike nitrate and phosphate, 1.0 μmol kg^{-1} silicate isoline showed a relatively homogeneous longitudinal distribution in the surface layers (between 150-200 m) (Figure 3.3, below).

The subtropical north Atlantic was oxygen supersaturated in surface. West of 26° W, the lower limit of oxygen super-saturation layer was located at around 125 m while east of this longitude, oxygen saturation was found quite shallower (around 25 m). This variability followed the phytoplankton vertical distribution and concentration patterns, with deeper and lower concentrations in most of the section, except in the east boundary with shallower and higher oxygen biological production (Figure 3.4, above). Apparent oxygen utilisation (AOU), taken as the difference between oxygen saturation at a potential temperature of a given water parcel and observed measurements, confirmed these patterns. In the Canary Current area, AOU clearly reflects the interaction between oxygen concentrations and distribution of nutrients. There, AOU is under 5 μmol kg^{-1} in the subsurface following the nutrient wedges coming from the upwelled waters in the NW African coast (Figure 3.4, below). Nevertheless, the lower compensation depth, i. e. the isoline with AOU equal

to zero, is clearly constant along the whole section, no matter longitudinal variability of chlorophyll *a* and nutrients. Below the layer of biological production, AOU

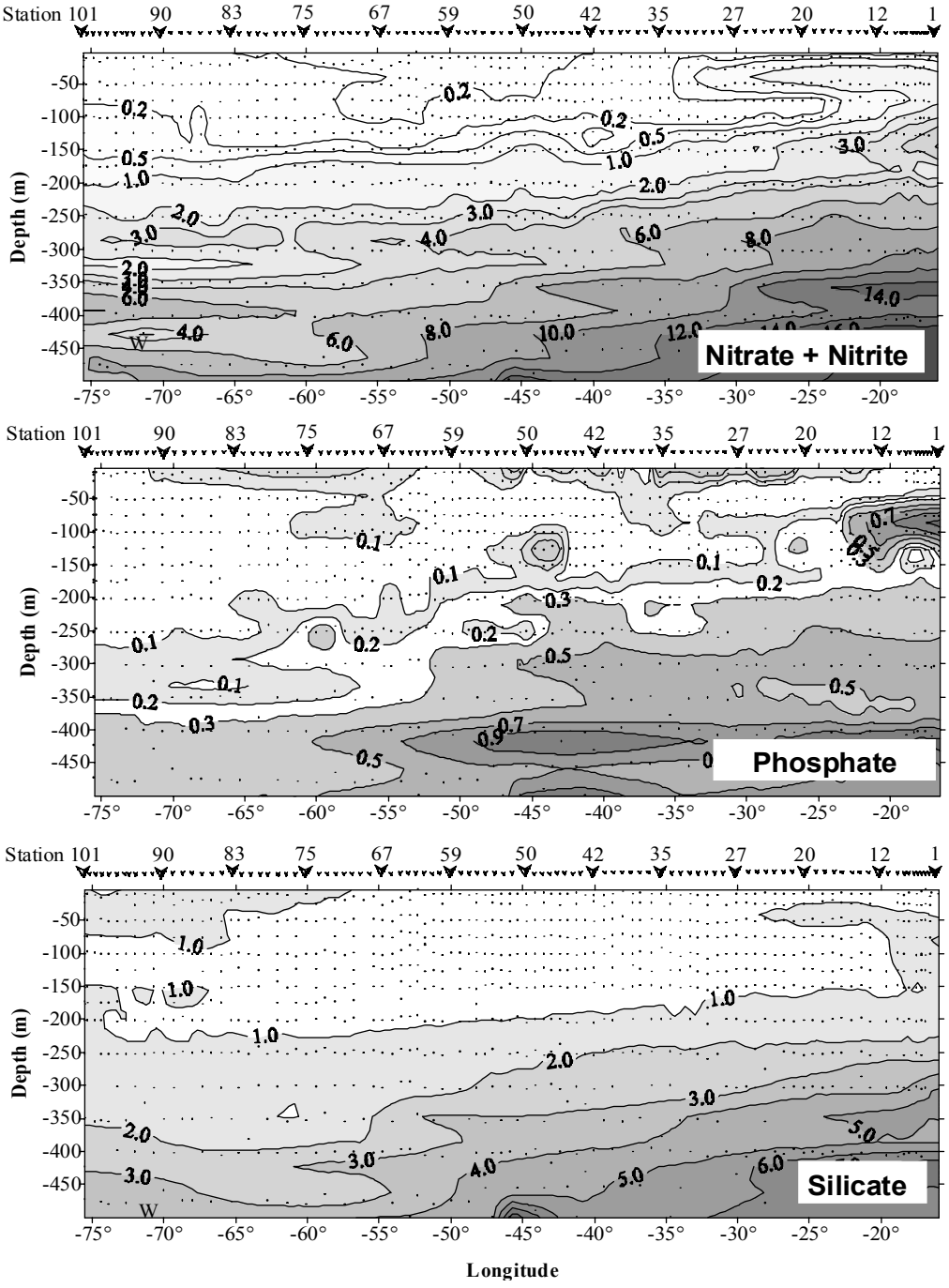

Figure 3.3. Longitudinal distribution of nutrients: nitrate + nitrite, phosphate and silicate (μmol kg^{-1}). Points indicate sampling depths.

showing higher values in the eastern basin (around 50 µmol kg^{-1}) that in the western basin (around 40 µmol kg^{-1}) reflects the nutrients trend to be more concentrated in the eastern basin than in the western basin (Figure 3.3).

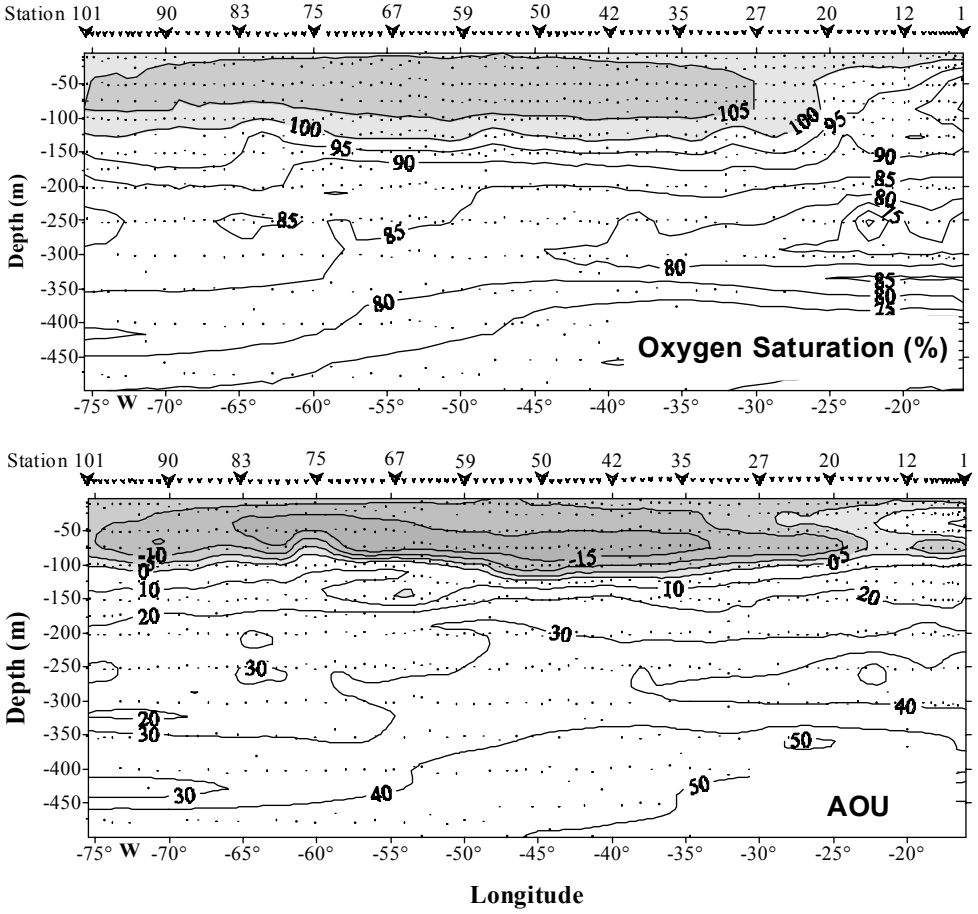

Figure 3.4. Longitudinal distribution of oxygen saturation (%) (above) and apparent oxygen utilisation (AOU, µmol kg^{-1}) (below). Points indicate sampling depths.

Distribution of phytoplankton biomass and primary production

The depth of maximum chlorophyll was found around 130 m, except at stations east of 24° W where such a maximum was at 80 m depth (Figure 3.5). A continuous chlorophyll *a* maximum layer (> 0.15 mg Chl *a* m^{-3}) is found over the whole section. The upper boundary of the maximum surface chlorophyll *a* layer was close to the surface east of 25°W, but deepened to 98 m depth west of 35°W. The lower depth boundary was found at 95 - 155 m at the same longitudes, respectively.

Chlorophyll *a* was scattered in various layers of the density field, but chlorophyll *a* was not higher than 0.15 mg Chl *a* m^{-3} below the 24.3 σ_θ, corresponding to surface waters in the Sargasso Sea (west 58° W). Various patches of chlorophyll *a* were observed inside the continuous chlorophyll *a* maximum layer, being more frequent at both east and west extremes of the section. In stations other than near Africa, chlorophyll *a* concentration was negligible above the thermocline (located at ~36 m depth). Surface chlorophyll *a* was lower than 0.02 mg m^{-3} west of 40°W, lower than 0.05 mg m^{-3} between 40°W and 27°W and around 0.1 mg m^{-3} east of 27°W, in the Canary Current area.

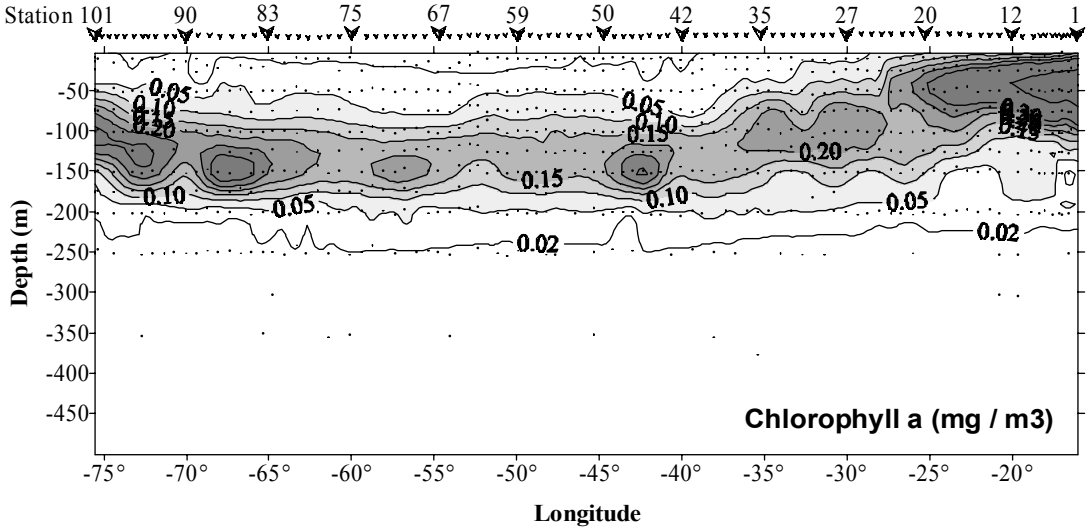

Figure 3.5. Longitudinal distribution of chlorophyll *a* concentrations (mg m^{-3}) in the water column. Points indicate sampling depths.

In most of the stations, depth-integrated chlorophyll *a* (Figure 3.6, above) ranged between 15 and 35 mg m^{-2}. Chlorophyll *a* overpasses this range in stations located at the eastern and western boundaries (west 71°W and east 24°W) and at the centre of the section (between 41°W and 49°W). From depth-integrated chlorophyll *a*, primary production was estimated (Figure 3.6, below) using the Equations 2.3 to 2.7. A different distribution pattern than that of chlorophyll *a* was found for depth-integrated computed primary production. Primary production ranged approximately from 100 to 300 mg C m^{-2} d^{-1} in almost all the stations, showing an increasing trend east of 35°W up to 820 mg C m^{-2} d^{-1} near Africa. The chlorophyll *a* maximum explained 42% of the total primary production variance (n = 81, r^2 = 0.4241, P <

0.001) (Figure 3.7). The remaining primary production is attributable to photosynthesis taking place in water layers above the chlorophyll maximum. In those

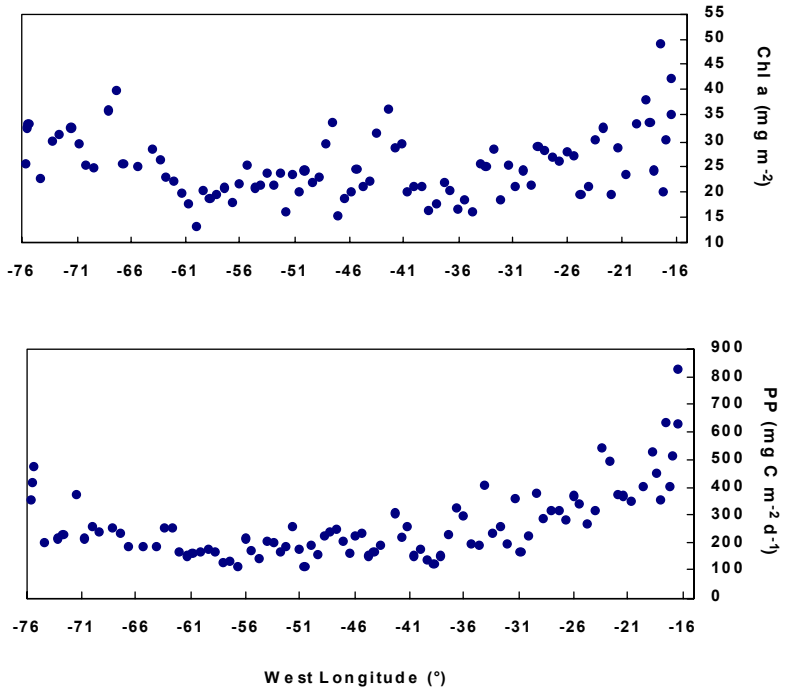

Figure 3.6. Depth integrated chlorophyll *a* (mg m^{-2}) (above) and primary production (mg C m^{-2} d^{-1}) (below), the latter estimated from a photosynthesis-irradiance model (Herman and Platt, 1986).

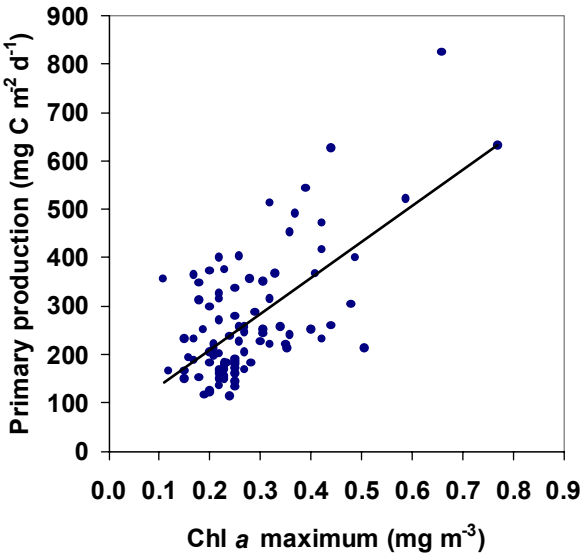

Figure 3.7. Relationship between chlorophyll *a* concentration at the maximum (*chlomax*) (mg m^{-3}) and integrated primary production (mg C m^{-2} d^{-1}) with solid line indicating a lineal tend: PP = 744.38 (*chlomax*) + 60.198 (n = 81; r^2 = 0.4241; $p < 0.001$).

water layers (above ~ 40 m, west of 32º W), the chlorophyll *a* values were rather homogenous (< 0.5mg m^{-3}) what is assumed to be the factor forcing a relatively homogenous depth-integrated primary production.

In the Sargasso Sea, dinoflagellates and non-identified coccoid cells were the best-represented phytoplankton (54% and 36%, respectively). 5% of the remaining cells were diatoms and another 5% corresponded to silicoflagellates, unicells and chains of cyanophyceae, and other non-identified taxa. Observations made in scanning electron microscopy contributed to better identification (Figure 3.8). The greatest diversity was shown in dinoflagellates, with cells between 10 – 22 μm length being dominant. The genus better represented were *Gyrodinium*, *Gynmodinium*, *Gonyaulax*, *Dinophysis*, *Katodinium*, *Torodiniumn*, *Protoperidinium*, *Oxytoxum* and *Podolampas*. The greatest frequency was found in *Gyrodinium* spp. and *Gymnodinium* spp. appearing in 46% and 40% of total samples, respectively. *Ceratium* spp., *Podolampas* spp. and *Oxytosum* spp. where the rare species (less than

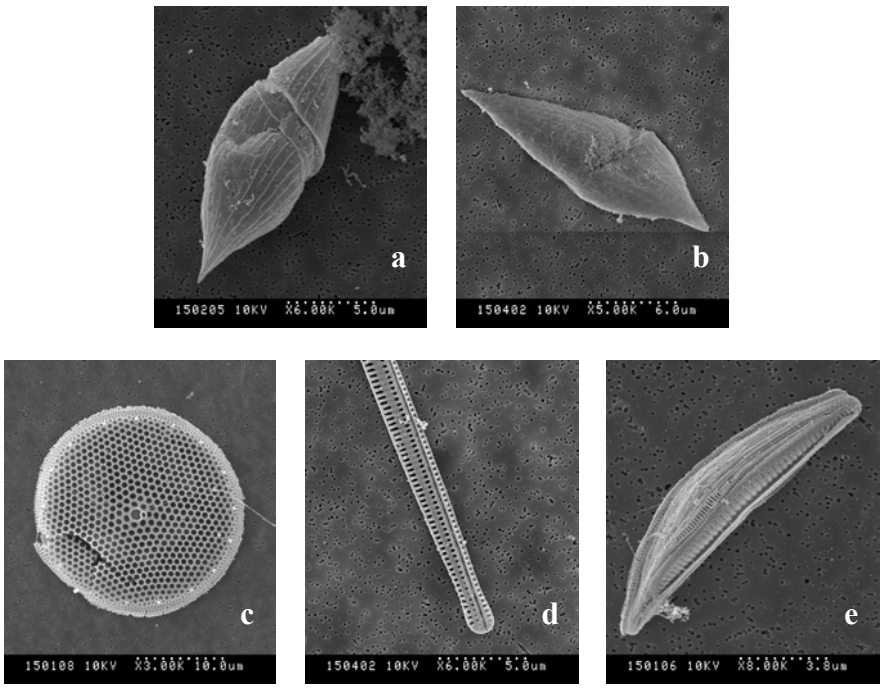

Figure 3.8. Scanning electron micrographs of some phytoplankton taxa in the Sargasso Sea. a) and b) *Gyrodinium* spp., c) *Thalassiosira* sp., d) *Nitzschia* sp. e) *Amphora* sp.

5 cells by 100 ml) more frequent (between 7 - 10 %). Spherical and subspherical non-identified cells were 10-14 μm along the longer axis. They were counted with magnification of 600, while the remaining cells were counted with magnification of 300. Diatoms were not particularly abundant.

3. 4 Remarks and discussion

On the vertical distribution of physical properties

The depth of the thermocline in the subtropical north Atlantic was quite stable around 38 m, being somewhat shallower in the central Sargasso Sea (~30 m depth) and deeper in both extremes. The shallower thermocline in the central Sargasso Sea is probably due to increase of surface elevation, leading to a thickening of the mixed surface layer (Mayer et al., 1998). Contrary to the relatively homogeneous thermocline depth, the temperature gradient in the thermocline was more variable with an eastward decreasing trend (Table 3.1). Thermocline water was clearly

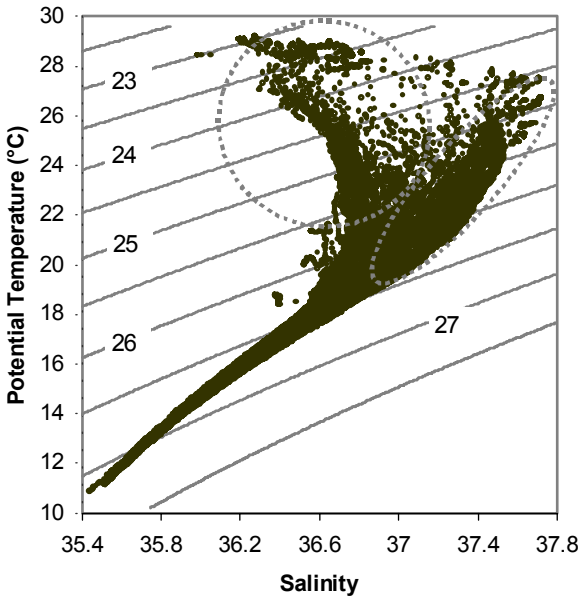

Figure 3.9. T-S diagram of the upper 500 m depth along the transatlantic 24.5°N section, with thermocline waters from eastern (ellipse) and western (circle) North Atlantic basins. Note the salinity increasing with temperature, in opposite to the observations in the NW Mediterranean case study (Figures 2.14 and 2.19).

Table 3.1. Basic statistics of summer physical and biogeochemical features of subtropical north Atlantic areas. Boundaries of the areas are: Western Sargasso (WS) (75.5°W - 58.0°W), Central Sargasso (CS) (57.3°W - 47.6°W), Eastern Atlantic (EA) (47.0°W - 24.0 °W), and Canary Current (CC) (23.3°W - 16.0 °W) [a].

	WS (N=23)		CS (N=17)		EA (N=37)		WS + CS + EA (N=77)		CC (N=13)	
	Mean	*SE*	*Mean*	*SE*	*Mean*	*SE*	*Mean*	*SE*	*Mean*	*SE*
Thermocline gradient (°C m^{-1})	0.331	*0.031*	0.273	*0.015*	0.246	*0.011*	0.281	*0.024*	0.194	*0.021*
Depth of thermocline (m)	41	*3*	30	*2*	37	*2*	36	*2*	40	*3*
Density gradient at pycnocline (kg m^{-4})	0.104	*0.010*	0.086	*0.005*	0.062	*0.003*	0.083	*0.003*	0.055	*0.0046*
Depth of pycnocline (m)	43	*3*	30	*2*	37	*1*	36	*2*	38	*3*
Buoyance frequency maximum (s^{-1})	0.028	*0.001*	0.026	*0.001*	0.022	*0.001*	0.025	*0.001*	0.021	*0.001*
Depth of buoyance frequency maximum (m)	49	*3*	35	*2*	42	*2*	42	*2*	44	*2*
K_z at the nitracline depth (m^2 d^{-1})	16.54	*0.50*	22.02	*0.78*	27.36	*1.86*	21.98	*0.80*	18.14	*1.78*
Nitrate gradient at nitracline depth (mmol N m^{-4})	0.013	*0.002*	0.022	*0.003*	0.033	*0.004*	0.023	*0.003*	0.045	*0.011*
Depth of the top of nitracline (m)	132	*6*	149	*8*	130	*6*	136	*3*	80	*4*
Integrated chlorophyll a (mg m^{-2})	25.8	*1.3*	22.7	*1.0*	22.9	*0.8*	23.9	*0.5*	31.6	*2.4*
Chlorophyll a maximum (mg m^{-3})	0.30	*0.02*	0.24	*0.01*	0.25	*0.01*	0.27	*0.01*	0.39	*0.05*
Depth of chlorophyll a maximum (m)	127	*6*	141	*5*	118	*5*	129	*3*	79	*6*
Nitrate flux at nitracline (mmol N m^{-2} d^{-1})	0.223	*0.026*	0.504	*0.040*	0.913	*0.073*	0.526	*0.039*	0.866	*0.101*
New primary production (NP, mg C m^{-2} d^{-1})	18.5	*2.0*	40.7	*3.2*	72.9	*5.7*	42.7	*3.1*	70.1	*7.8*
P-I based primary production (TP, mg C m^{-2} d^{-1})	233.0	*18.5*	183.8	*10.9*	243.2	*12.6*	213.9	*9.5*	488.4	*39.2*
NP / TP x 100	10.1	*2.0*	23.7	*3.0*	31.5	*4.1*	20.8	*1.8*	15.2	*2.9*

[a] The WOCE A5 oceanographic stations were numbered westward from 1 to 101 following the cruise direction as shown in Figure 3.1. Station numbers in each section are: [WS] 72 - 101; [CS] 55 - 71; [EA] 18 - 54; [WS+CS+EA] 18 - 101; [CC] 1 - 17. The following stations were excluded of the analysis due to the lack or unreliability of data: 1, 2, 10, 12, 82, 84, 88, 93, 96, 98, and 101.

differentiated from the deeper North Atlantic Central Water (NACW), with the former spreading above ~26.0 pycnocline in the eastern north Atlantic basin and above ~26.5 pycnocline in the western basin (Figure 3.9). Basic statistics of physical (and biogeochemical properties as well) in the subtropical north Atlantic are summarised in Table 3.1. For a better distinction of longitudinal differences, the whole section was divided in four areas or provinces as is further described in the text.

The vertical density profiles allowed estimating the vertical stability of the water column (N^2) (Figure 3.10, above) used to estimate the turbulent diffusion coefficient (K_z) (Figure 3.10, below) applying Equations 2.1 and 2.2. The vertical

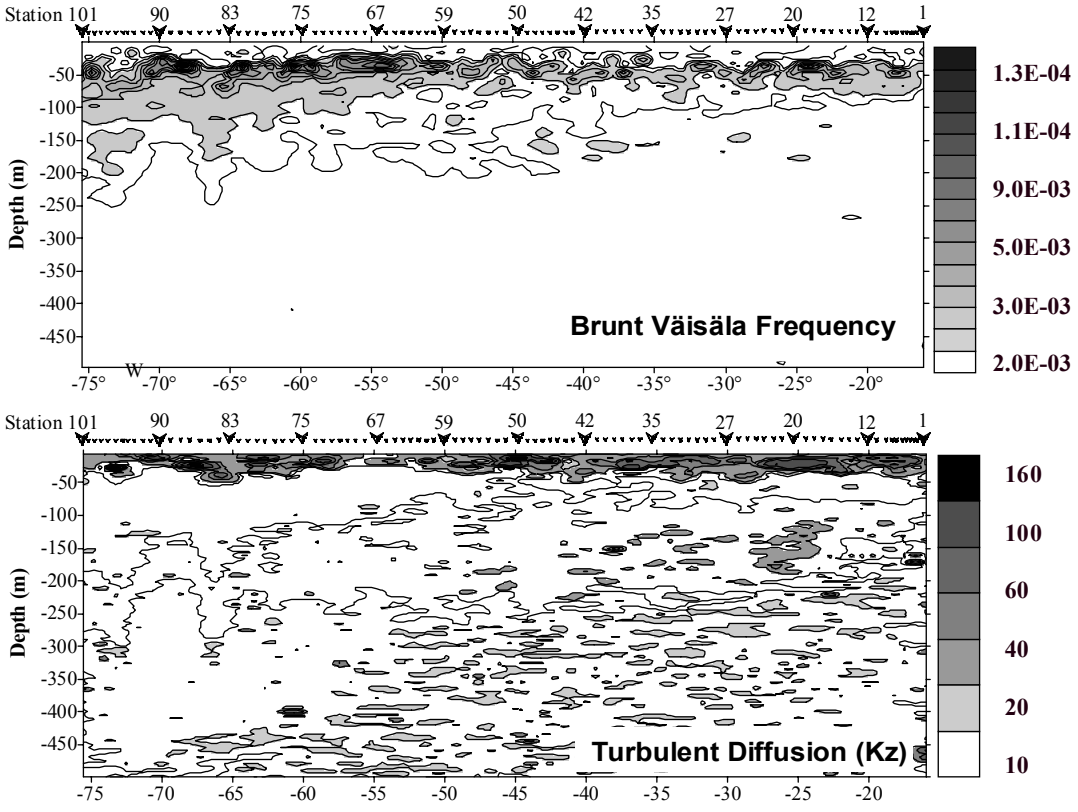

Figure 3.10. Above, longitudinal distribution of the Brunt-Väisälä (BV) frequency (N^2, s^{-2}). Below, BV was used to estimate the vertical turbulent diffusion coefficient (K_z, $m^2\ d^{-1}$) following the Osborn (1980) formulation.

distribution of N^2 highlighted subthermocline instabilities (oscillations) near Bahamas as observed by physical properties shown in Figure 3.2. N^2 values appeared scattered below the thermocline in the western basin, smaller in the inter-oscillation boundaries. The vertical distribution pattern of the turbulent diffusion coefficient (K_z) (Figure 3.10, below) was found as expected, opposite to that of N^2. In general, large values of N^2 around the thermocline forced small diffusion rates. Thus, K_z is higher in the subthermocline oscillations while it increases in the inter-oscillation boundaries. Larger values of K_z are found above the thermocline in the mixed layer, increasing toward the bottom boundary, reaching near three times the values in the thermocline. This is the result of decreasing buoyancy and internal waves breaking (Gaspar et al., 1990).

On the dissolved oxygen distribution

In the present work, AOU is assumed to be an indicator of the trend in remineralisation rates (organic matter conversion to inorganic minerals) with higher AOU values indicating higher remineralisation rates (Anderson and Sarmiento, 1995). Thus, it is deduced from the WOCE section, that remineralisation rates are higher in the eastern than in the western basin, resulting in higher nutrient concentrations in the former than in the latter. Since remineralised nutrients (such as nitrate) are higher eastward, the nitrate dependent production (new production) is also expected to also be increasing eastward, as long as the upward transport mechanisms (advection and diffusion) are not strongly variable with longitude. In the Canary current, AOU ranges were between –5 and 4 μmol kg^{-1} contrasting with the values found in the open ocean domain, where AOU was negative corresponding to the surface depletion of chlorophyll *a* and nutrients. In the CC, the surface temperature ranged between 19 and 24° C while the oxygen saturation was around 10 μmol kg^{-1} lower than values in remaining section, with 24 – 29 °C temperature. This can be attributable to the relatively low temperatures of upwelled waters that increase the oxygen solubility but mainly to the oxygen generated by the local relatively high biological production. In the subtropical Pacific gyre at 28°N, the summer biological production contributes about 72% to the oxygen supersaturation (Craig and Hayward, 1987). Taking into account the physical processes altering the oxygen

concentrations, Jenkins and Wallace (1992) suggest that the summer subsurface oxygen supersaturation in subtropics is attributable to the dominance of photosynthesis over respiration, this is a net autotrophy.

On interactions among phytoplankton, nitrogen and primary production

Phytoplankton chlorophyll *a* and nutrients at the isopycnal front located between 51 – 54° W longitudes were not apparently altered. At the Canary Current zone, relatively high concentrations of chlorophyll *a* are found spread from subsurface to about 100 m depth as response to horizontal nutrient wedges coming all the way from the coast up to about 800 km offshore. Nitrate concentrations increased with density with the higher gradient (nitracline) being close to the 26.0 isopycnal (Figure 3.11). Near Bahamas, the 26.0 isopycnal was quite variable with depth, often crossing down the bottom boundary of the euphotic zone at ~125 m depth, as a response to subthermocline oscillations. These oscillations did not alter the nitracline depth that remained relatively constant, what suggests light limitation of phytoplankton growth at such a boundary. Subthermocline oscillations were correlated with moderate increases of nitrate concentrations (~ 0.2 μmol kg^{-1}) close to the surface west of 64° W. This appears to be responsible for peaks of integrated chlorophyll *a* at 64, 69 and 75° W (see Figure 3.6, above). Similar subthermocline oscillations have been described at higher and lower latitudes as potential mechanisms for upward pumping of nitrate (Arhan et al., 1998; McGillicudy and Robinson, 1997). In the Canary Current area, the upwelling of deeper waters close to the coast was found responsible for fertilising the offshore subsurface by horizontal transport of nutrients (nitrate concentrations > 0.5 μmol kg^{-1}) that favoured the increasing of integrated chlorophyll, as shown in Figure 3.5.

A comparison of estimated total production (TP) with expected new production (NP) deduced from the upward nitrogen flux was made assuming 6.625 N:C Redfield ratio (see TP and NP mean values in Table 3.1). The mean value of TP along the subtropical north Atlantic was 214 mg C m^{-2} d^{-1}. This value is in reasonable agreement with previous ^{14}C field estimates of primary production. Lohrenz et al. (1992) gave estimates of primary production at higher latitudes in the

Sargasso Sea between 302 and 394 mg C m^{-2} d^{-1}. In the eastern subtropical gyre, crossing the 24° 30' N parallel, Marañon et al. (2000) found large inter-annual variability of summer primary production. In 1995, they measured PP between 50-125 mg C m^{-2} d^{-1} but in 1996, they found a PP between 250 – 500 mg C m^{-2} d^{-1}. This difference was attributed to changes other than chlorophyll *a* concentrations. In the Sargasso Sea, Malon et al. (1993) estimated primary production to be between 69 and 291 mg C m^{-2} d^{-1} in August. As previous observations of primary production, sea satellite estimates (~ 220 - 300 mg C m^{-2} d^{-1}) fit well with the estimates in this work (214 mg C m^{-2} d^{-1}).

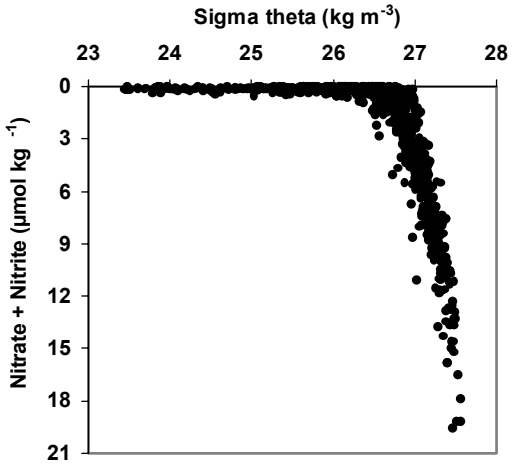

Figure 3.11. Nitrate + Nitrite (µmol kg^{-1}) distribution as a function of σ_θ (kg m^{-3}) (*n* = 965). Note the nitrogen trend to increase from ~26.0 σ_θ.

Phytoplankton cells in this study (larger than 5 µm) are expected to represent less than 50% of the phytoplankton chlorophyll, since most part of phytoplankton cells could correspond to smaller sizes, as characteristic for oligotrophic systems (Agawin et al., 2000). Thus, the accounted phytoplankton fraction in this work allows an approach to the phytoplankton composition of communities other than picoplankton. Noticeable was the phytoplankton biodiversity that increased with number of cells found in each sample (Figure 3.12). For example, the relatively high diversity (14 - 20 species/100 ml water sample) in stations 71 and 72 were made up of dinoflagellate species. The cells were very scarce (< 10 cells / 100 ml) at the time that coccoid unicellular organisms were the most abundant. A diffuse relationship

has been pointed out between a relatively high dinoflagellates diversity and stratified waters, away from thermohaline fronts where nannoplankton dominate (Estrada and

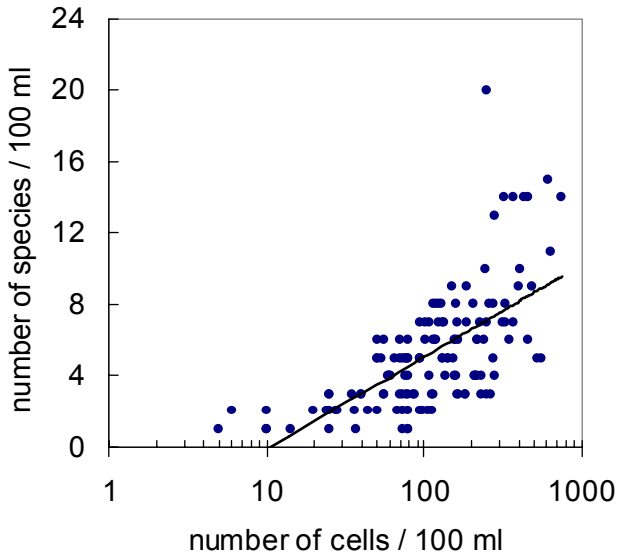

Figure 3.12. Relationship between number of cells and number of species in the phytoplankton community. Solid line is the reduced axis with Number of species = 2.242 *Ln* (Number of cells) - 5.2712 (n = 138, r^2 = 0.4197, P < 0.0001).

Margalef, 1988). In the western and central Sargasso Sea, total phytoplankton cells increased with depth up to the chlorophyll *a* maximum depth at 110 – 130 m, Figure 3.13, left). Variation of the total phytoplankton cells was mostly driven by coccoid unicells with a similar distribution pattern (Figure 3.13, centre) while dinoflagellates were continuously decreasing with depth, from below 60 m depth (Figure 3.13, right). This vertical distribution pattern of phytoplankton is different from that reported by Claustre and Marty (1995) in the tropical Atlantic, with small phytoplankton populations dominating upper water layers. They found that in summer, cyanobacteria dominate the subsurface waters, prochlorophytes prefer the intermediate waters, and flagellates prevail below the euphotic zone. This spatial distribution allowed concluding that the light availability mainly regulates the two former phytoplankton populations and nutrient availability regulated the latter one. The present work does not provide evidence of this distribution pattern, since the

study was restricted to phytoplankton larger than 5 µm, thus excluding cyanobacteria and prochlorophytes populations.

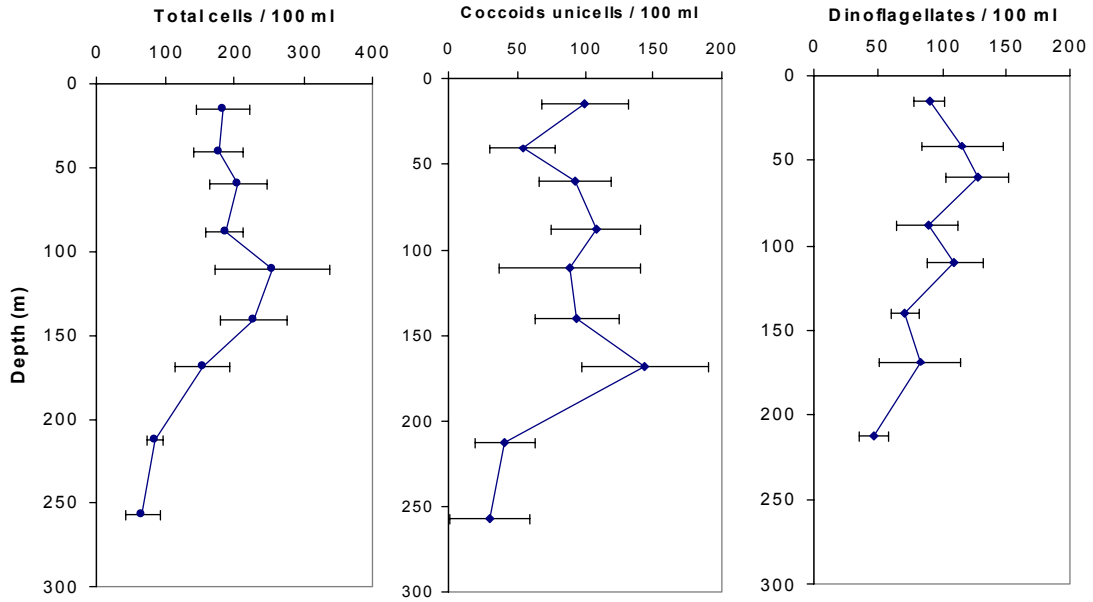

Figure 3.13. Phytoplankton abundance (± SE) in the Sargasso Sea (in 100 ml water). *Left*, total cells (left). Most representative groups: *Centre*, coccoid unicells; *right*, dinoflagellates.

On regional differences along the subtropical north Atlantic

Physical characteristics assumed to control phytoplankton ecology, are the base to suggest division of the upper ocean in bio-goechemical provinces (Longhurst et al., 1995; Sathyendranath et al., 1995). Integrating surface satellite observations with field data, these authors have given estimates of primary production highlighting regional differences of surface waters in the Atlantic Ocean. Based on yearly observations, these authors distinguish three zones along the subtropical north Atlantic fitting with the WOCE A5 section: West Gyre, East Gyre and Canary Current provinces. The west-gyre province includes the poleward part of the anticyclonic gyre from the western current to the Mid-Atlantic Ridge (at about 50°W). The east-gyre province is formed as a continuity of the western province from the Mid-Atlantic Ridge to the Canary Current boundary at east. The Canary Current province includes the eastern boundary current from Galicia (Spain) to Cape

Verde in North West Africa, characterised by coastal upwelling. In the present study, following empirical observations of the vertical structure of water (Figure 3.14),

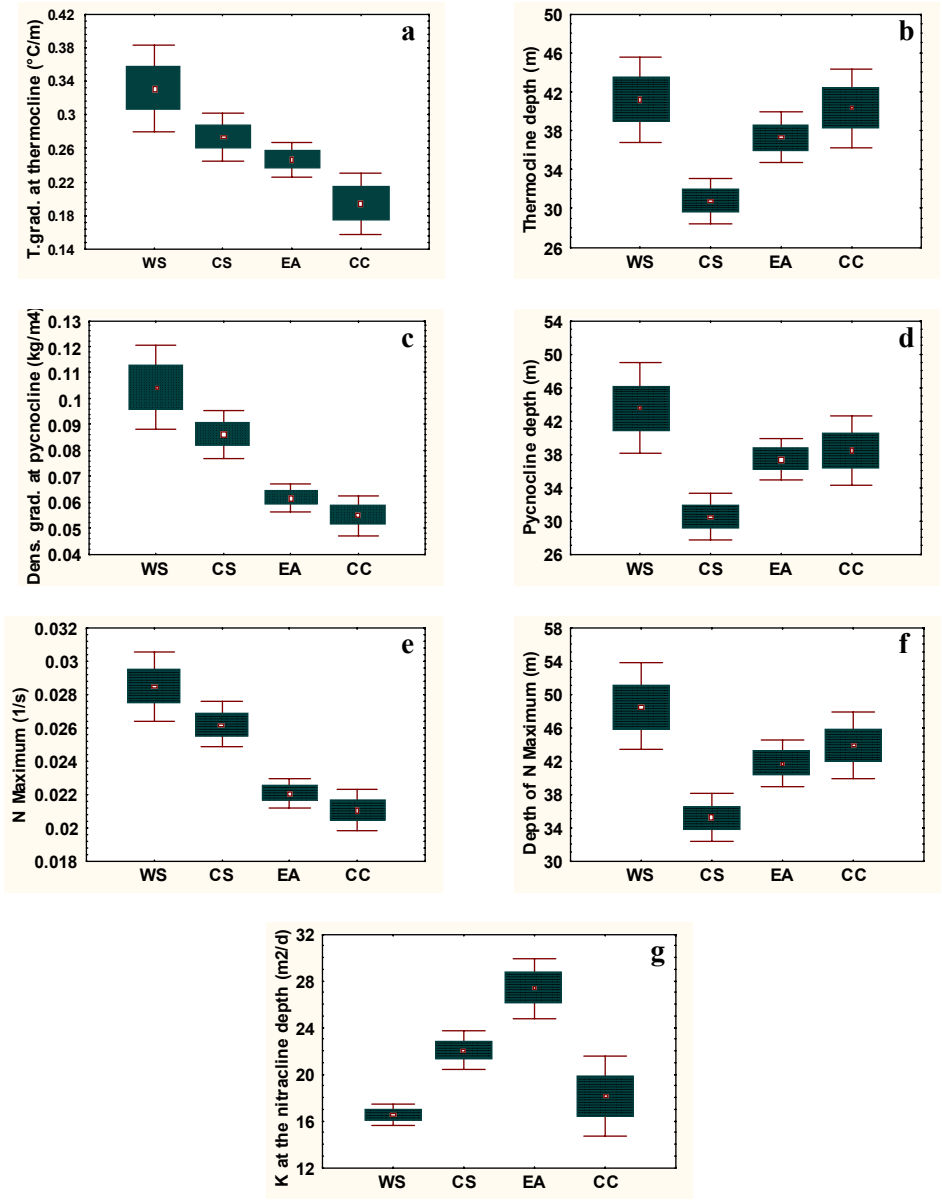

Figure 3.14. Mean values (boxes indicating ± 1 SE and whiskers ± 1.96 SE) of physical properties in the water column at Western Sargasso (WS), Central Sargasso (CS), Eastern Atlantic (EA) and Canary Current (CC) provinces. Note similarities in the space distribution of temperature at the thermocline depth (a), density at the pycnocline depth (c) and Brunt-Väisälä maximum (e). The depths at which these variables were found are also very similar among them: thermocline (b), pycnocline (d) and Brunt-Väisälä maximum (f).

nitrate (Figure 3.15) and phytoplankton chlorophyll *a* and primary production (Figure 3.16), not three but four biogeochemical areas (provinces) in the subtropical NA were considered attempting to explain the longitudinal variability along the whole section. The new areas are Western Sargasso WS (75.5°W - 58.0°W), Central Sargasso CS (57-3°W – 47.6°W), Eastern North Atlantic EA (47.0°W - 24°W) and the Canary Current CC (23.3°W - 16.0°W). Stations in WS, CS and EA will be further referred to as the "open ocean" domain in contrast with the CC domain.

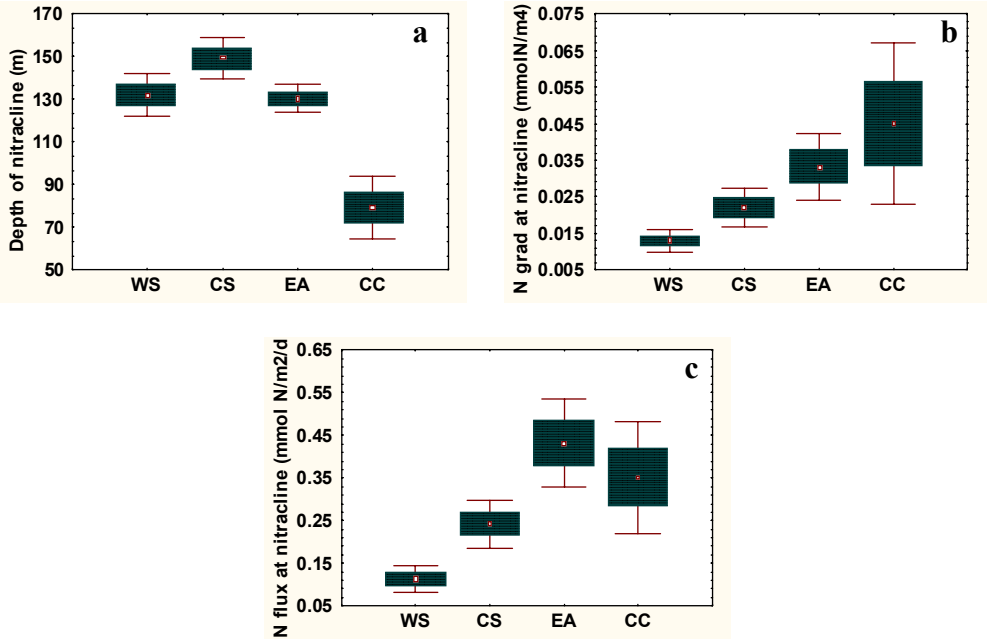

Figure 3.15. Mean values of nitrogen features (boxes indicating ± 1 SE and whiskers ± 1.96 SE) in the water column at Western Sargasso (WS), Central Sargasso (CS), Eastern Atlantic (EA) and Canary Current (CC) provinces. Depth of nitracline (a) does not appear to affect the nitracline gradient (b). The latter, together with turbulent diffusion (Figure 3.14, g) were used to estimate the nitrogen flux at the nitracline depth (c).

Analysis of variance of physical and biogeochemical features among provinces (Figure 3.17) showed that they partially differ, being the CC, the area with more differences with respect to the rest of the provinces. Such variability is not observed in the physical properties (Figure 3.14), but in biogeochemical features (Figures 3.15 and 3.16). Depth of the top of nitracline (3.15, a), depth-integrated chlorophyll *a*, depth-integrated primary production and chlorophyll *a* maximum (Figure 3.16, a b, c) were the features that significantly ($P < 0.001$) distinguished the

open ocean provinces (WS, CS, EA) from the CC province. Differences among open ocean provinces are found, particularly in physical characteristics. In the CS, the pycnocline was shallower (Figure 3.14, d) than in the rest of the provinces. The maximum vertical stability of water (N^2) was similar in the eastern basin provinces (EA and CC) but significantly smaller than in the west provinces (WS and CS)

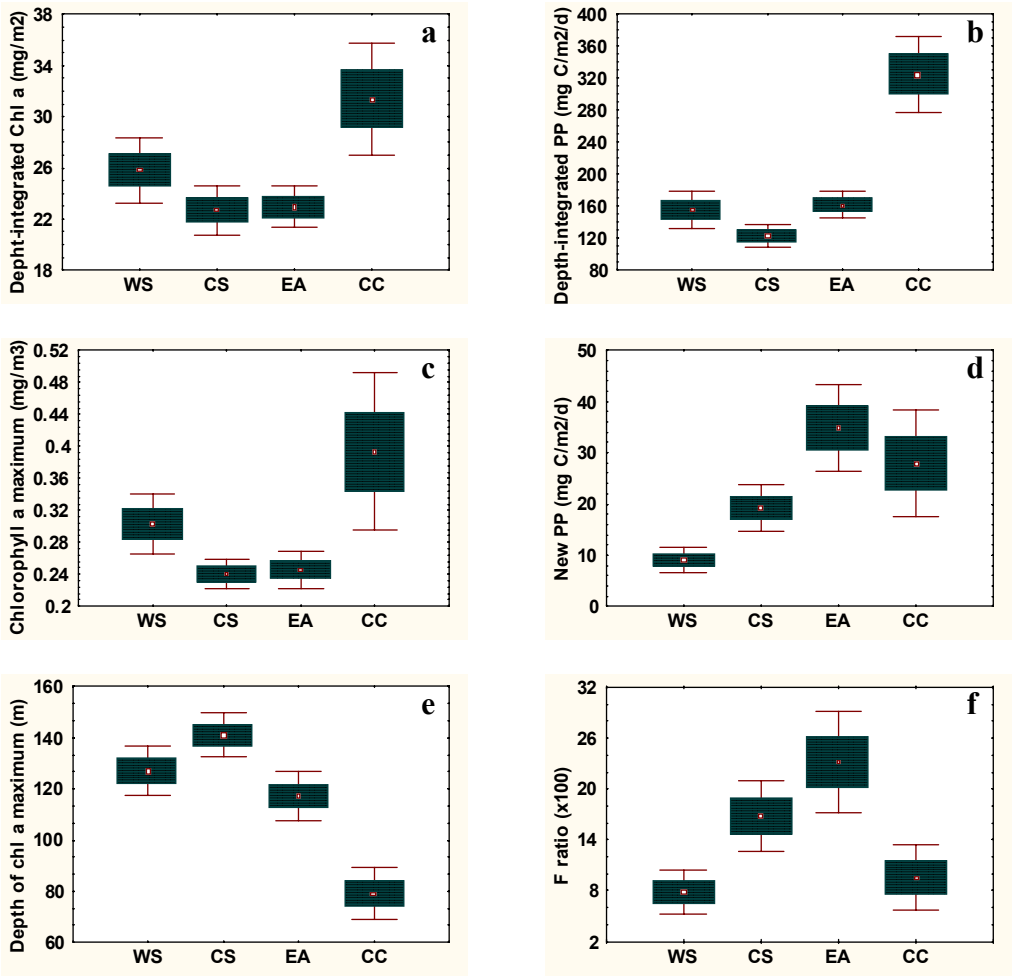

Figure 3.16. Mean values (boxes indicating ± 1 SE and whiskers ± 1.96 SE) of phytoplankton chlorophyll and primary production in the water column at Western Sargasso (WS), Central Sargasso (CS), Eastern Atlantic (EA) and Canary Current (CC) provinces. The depth integrated chlorophyll *a* (a) was strongly correlated with the chlorophyll *a* maximum (c) (see text), the latter found at variable depths along the section (e). Depth-integrated primary production (b) was not driven by estimates of new production (d), the latter with different space distribution with respect to the former. New production to total production ratio (*f*-ratio) (f) evidenced a lack of the new production model to estimate *f*-ratio in the CC site, where higher values were expected.

(Figure 3.14, e), driven by the stronger westward trend of the density gradient (Figure 3.14, c). K_z at the nitracline depth was similar in the middle of the section (CS and EA) being significantly higher in EA (Figure 3.14, g). K_z increased eastward in the thermocline, while the nitrate gradient decreased, preventing the upward diffused nitrogen to follow the same pattern of the turbulent diffusion. The pycnocline depth (Figure 3.14, d), controlling the depth of Brunt-Väisälä maximum (Figure 3.14, f) did not show particular space variability in the entire section. Since the vertical water column properties in the CC did not reflect the biogeochemical variability, it is suggested that the CC respond to physical factors other than those

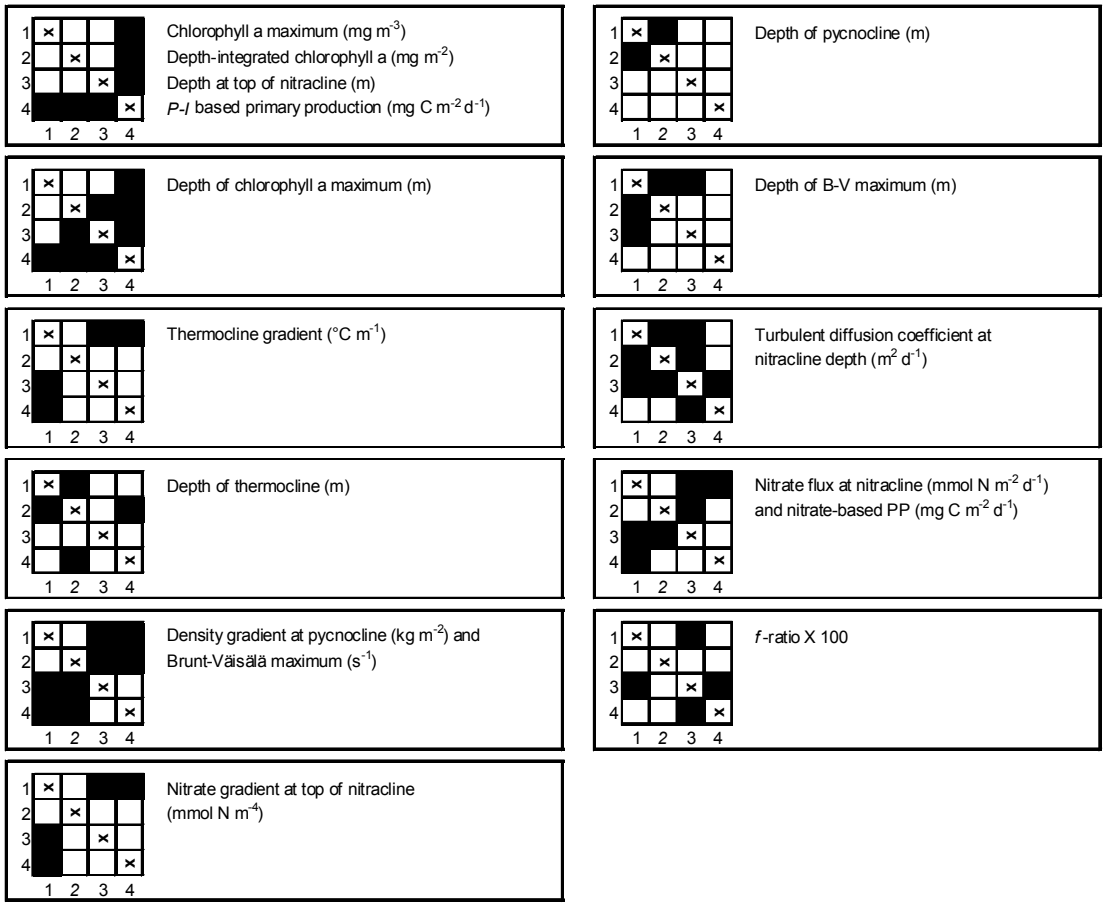

Figure 3.17. Significant differences of average values in the biogeochemical areas determined from an analysis of variance test. These results are based on Tukey honest significant difference test carried out in order to determine which areas are particularly different from each other. 1= Western Sargasso, 2= Centre Sargasso, 3= Eastern Atlantic, 4= Canary Current. Black squares indicate significant difference between two areas (95% confidence level).

taking place in the vertical, such as the horizontal processes derived from the coastal upwelling taking place near Africa. Thus, the diffusion model did not reflect the expected new production in the CC (≥ 60% of total production, according to Minas et al., 1986) that was found much lower (~15%) (Figure 16, d). On the contrary, the model diffusion successfully reproduced the expected new production in the rest of the section (21% of total production).

Typical depth-integrated chlorophyll *a* concentrations were around 24 mg m^{-2} in the open ocean. These estimates are consistent with those of Goericke and Welschmeyer (1998) in the Sargasso Sea (ES and CS) and Claustre and Marty (1995) in EA. Relatively high chlorophyll *a* values in some stations in the CS (~ 32 mg m^{-2}) were found (see Figure 3.6, above). This indicated the existence in the open ocean of relatively rich-chlorophyll patchy areas that might not be properly documented from satellite observations because of excessive smoothing (e. g. Longhurst et al., 1995; Sathyendranath et al., 1995). Such patches were not correlated with increasing nitrate fluxes suggesting factors other than nitrate as responsible for such the increasing of phytoplankton biomass. Fertilised waters in the Canary current promoted the increasing of chlorophyll *a* and primary production. Comparing the CC with the overall mean of the open ocean, the former site showed a depth-integrated chlorophyll *a* and primary production (31.6 mg Chl *a* m^{-2}; 488 mg C m^{-2} d^{-1}) significantly higher than the latter (23.9 mg Chl *a* m^{-2}; 24 mg C m^{-2} d^{-1})). The average depth of chlorophyll *a* maximum (DCM) was shallower in the CC (79 m depth) than in the open ocean (129 m depth). The DCM was also different between CS and EA, being deeper in the CS (141 m) than in EA (118 m). The deepening of chlorophyll is attributable to the lower turbulent diffusion observed in the former area (see Table 3.1) making the new production to be lower. Moreover, lower upward diffused nitrogen could be forcing the phytoplankton deepening in the water column, searching for nutrient-rich waters.

A common association of DCM with diffusive nitrogen fluxes across thermocline has been reported, particularly when thermocline coincides with the transition region between the nutrient-poor well-illuminated surface layers and the

darker, nutrient-rich deeper water layers as occurs at high latitudes (Holligan et al., 1984; Sharples et al., 2001). However, at lower latitudes with thermally stratified waters, DCM has been found more associated to the nutrient supply from the diffusive flux across the nitracline (Herbland and Voituriez, 1979; Cullen and Epply, 1981; Longhurst and Harrison, 1989; Varela et al., 1984; Helguen et al., 2002). In the present work, it is shown that DCM in the subtropical north Atlantic appears ~100 and ~40 m below the seasonal thermocline in open ocean and CC domains, respectively. Furthermore, DCM is highly correlated with the depth of maximum nitrate gradient (nitracline depth) (n = 85, r^2 = 0.69, P < 0.001) (Figure 3.18). On the other hand, no correlation is found between the depth of maximum vertical stability (Brunt-Väisälä frequency) and the depth of maximal chlorophyll *a* concentration, as observed in the NW Mediterranean Sea (Velásquez, 1997) and in the central Atlantic (Agustí and Duarte, 1999). The top depth of nitracline was following approximately the 26.0 isopycnal in the CS, EA and CC but independent of the density field in the ES area.

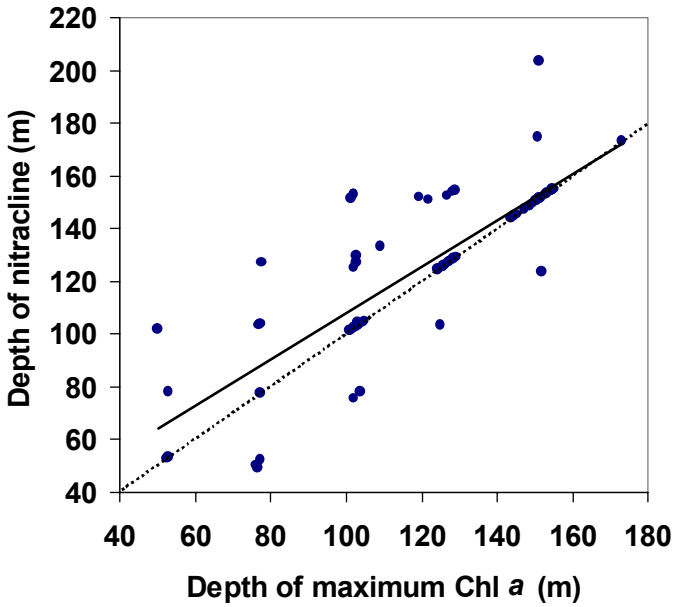

Figure 3.18. Relationship between the depth of chlorophyll *a* maximum (DMC) and the depth of the nitrate gradient maximum (DMN) (nitracline depth) with solid line indicating a lineal tend: DCM = 0.8775 (DNC) + 20.124 (n = 85; r^2 = 0.6893; p < 0.001). Dashed line represents 1:1 ratio.

In the open ocean domain, it is found that the vertical distribution of K_z was similar to that reported by Lande et al. (1989) in the central North Atlantic. They observed high diffusivity above the pycnocline followed by lower diffusivity (between 50 – 150 m depths), and slightly higher values at 300 m depth. K_z and nitrate flux increased eastward (except in CC). However, nitrate fluxes were found to be more dependent on the nitrate gradient (n = 86, r^2 = 0.79, $P < 0.001$) than to the diffusion term (n = 86, r^2 = 0.12, P = 0.001). The average upward diffused nitrate was estimated to be 0.53 mmol N m^{-2} d^{-1} (0.2 mol N m^{-2} $year^{-1}$). This represents a NP of 1.3 mol C m^2 yr^{-1}, near the expected new production of 1 mol C m^2 yr^{-1} (Williams and Follows, 1998). Previous estimates of nitrogen fluxes to the euphotic layer vary widely up to an order of magnitude, mainly depending on different range depths covered, locations and techniques. Lewis et al. (1986) estimated a lower value of nitrogen flux in the upper 200 m of the eastern Atlantic of about 0.14 mmol m^{-2} d^{-1} using direct measurements of turbulent diffusion and nitrate gradients. Jenkins (1988) estimated 0.6 ± 0.2 mol N m^{-2} y^{-1} (1.64 ± 0.55 mmol N m^{-2} d^{-1}) in the mixed layer using ^{3}He. Fasham et al. (1990) ecological model (FDM model) and McGillicudy and Robinson (1997) model yielded a nitrogen flux of 0.4 - 0.7 mol N m^{-2} yr^{-1} in the mixed layer of the Sargasso Sea being two to three times higher than our estimates. Hurtt and Armstrong (1996), after simplifying FDM model with reduced number of parameters, resulted in lower nitrogen flux estimates of 0.2 mol N m^{-2} yr^{-1} (0.55 mmol N m^{-2} yr^{-1}) matching our results. Estimates of upward diffused nitrogen to the euphotic zone in the present study can be assumed to represent the expected total new production. It is assumed equilibrium between the upward nitrogen flux to the euphotic zone and uptake rates of nitrate, as found in the central Atlantic (Planas et al., 1999).

It is widely believed that about 30% of the total production in the open ocean correspond to new production (Platt and Harrison 1985; Platt et al., 1989; McGillicuddy and Robinson, 1997; McGillicuddy and Robinson, 1997). In the present work, NP was 21% of total production (214 mg C m^{-2} d^{-1}) in the open ocean domain. This percentage matches with expected new production for the north Atlantic subtropical gyre (18%) (Planas et al., 1999). NP appeared increasing

eastward from 10% in WS, 24% in CS to 32% in the EA. In the CC, NP was estimated to be 15% of total production (488.4 mg C m^{-2} d^{-1}). This is quite below the expected estimates (64%) (Minas et al., 1986), thus suggesting that the upward turbulent diffusion is not responsible for fuelling the NP in this area. In the present work, observations of dissolved oxygen, nutrients and chlorophyll *a* vertical distributions (Figures 3.3, 3.4 and 3.5) suggested that horizontal transport processes (not studied here) mainly drive new production in the CC.

In summary, specific areas of the open ocean in the subtropical NA, showed unexpected patches of relatively high chlorophyll *a* concentrations. Nevertheless, these areas are not strongly altering the average for the entire subtropical zone. Some of such patches are linked to fertilisation processes related to subthermocline instabilities near Bahamas, but other patches located in the centre of the open ocean do not appear to respond to upward nitrogen fluxes from the deeper waters. The DCM was quite deeper than the thermocline and the nitrate concentrations around the thermocline depth were always below the detection limit. Therefore, the diffusive nitrate flow toward the well-illuminated water layers was estimated in the nitracline depth. The top depth of nitracline around 136 m west of 23°W was closely related to the 26.0 isopycnal in most of the section, except in the Western Sargasso where light shortage appears to control the nutrient uptake by phytoplankton at such depths, ignoring the isopycnal oscillations. The vertical diffusion model reasonably explained the expected new production in the open ocean (~21% of total primary production) but it could not explain new production in the Canary current area where nutrients appeared to respond to horizontal transport processes driven by coastal upwelling dynamics. New primary production appeared to be controlled by the diffusive nitrate fluxes taking place at the top of the nitracline depth, far below the nutrient depleted seasonal thermocline waters.

Chapter 4

A vertically resolved ecological model for plankton dynamic studies: “BLANES”

Abstract

A physical/ecological model is proposed to assess depth and time dependent vertical variability of plankton and nutrients in oligotrophic pelagic environments. Parameterisation of physical and biogeochemical processes was carried out in order to allow the model to assessing stocks and fluxes of nitrogen-based matter. The model proposed is called "Bio-adaptable Light And Nutrient dependent Ecosystem Simulator" (BLANES) representing the vertical dimension of the upper water layers of the open ocean from surface to 300 m depth. The model is vertically resolved, nitrogen-based, one-dimensional and turbulence driven. Time-variable irradiance and length of daylight are in accordance with latitude of selected stations. N-Nitrate, N-nitrite, N-ammonium, N-phytoplankton and N-zooplankton are the biogeochemical variables (state variables) in the model. Nitrite concentration is assumed to be dependent on the balance between phytoplankton exudation in the darkness and phytoplankton uptake in the light. Nitrite is affecting new production mainly fuelled by nitrate. Regenerated production takes place from ammnonium recycled in situ through zooplankton excretion. A physical and biogeochemical model description is presented with calibration/validation exercises of physical properties in the Catalan Sea, Algerian Sea and subtropical NA. The model successfully reproduces length of daylight and a clear-sky surface irradiance according to latitude. The mixed layer thickness is density dependent with turbulent diffusion values higher than 1E-4 m^2 s^{-1}. Maximum turbulent diffusion in the mixed layer is 14 cm^2 sec^{-1}, downward decreasing up to a minimum background value of 0.1 cm^2 sec^{-1} at 300 m depth. Photosynthesis is allowed to take place in the euphotic zone above 0.1% surface irradiance, being thinner than mixed layer in winter and thicker than that in summer. The model in the Catalan and Algerian seas reasonably reproduces temperature. Some overheating of surface waters is shown by the simulations in springtime in the Algerian Sea (~2 ºC). This is induced by a trend of the polynomial function imposed in the upper boundary to cause an early increase of surface temperature after wintertime.

4.1. Introduction

In the last three decades, important efforts have been conducted in order to model primary production in the upper ocean through numerical simulations of the structure and functioning of pelagic and benthic ecosystems. The coupling of the physical and biological environments, poorly developed in the beginnings (Denman and Platt, 1977; Steele, 1977; Kiefer and Kremer, 1981), has been lately greatly improved with the use of vertically resolved partial differential equations. Current models operate at several time scales ranging from hours to years. For example, Sharples et al. (2001) studied hourly events affecting primary production in the thermocline in a coastal area. Cruzado (1982), Varela et al. (1992, 1994) and Zakardjian and Prieur (1994), among others, have carried out ecological numerical studies at specific seasons of the year, mainly summer. The simulation of the planktonic system over the whole year and the even evaluation of intra-annual plankton variability has been gaining interest (v. gr. Evans and Parslow, 1985; Doney et al., 1996; Oguz et al., 1996; Levy et al., 1998; Sharples, 2001).

An important issue in modelling the pelagic domain is the vertical turbulent diffusion. This is the main mechanism responsible for transporting energy and matter in the ocean (Gargett, 1989; Gaspar et al., 1990). Turbulence, that promotes diffusion, causes mixing in the water column altering the upward and downward transport of dissolved and particulate matter. The diffusive transport is due to "molecular diffusion" and a more complex mechanism called "turbulent diffusion" the former being several orders of magnitude (10^3 to 10^5) smaller than the latter (Steele, 1977). Molecular diffusion is fluid-dependent (temperature, viscosity)and is present in both laminar and turbulent flows while turbulent diffusion is flow dependent and characterises the transport of heat and particles inherent to the pelagic communities structure and functioning (Gargett, 1989; Skogen et al., 1995; Estrada and Berdalet, 1997). Together with vertical turbulent diffusion, vertical advection (upwelling or sinking) accounts for the total transport of particles in the upper ocean.

The present study focuses on vertical turbulent diffusion and vertical advection promoting nutrient fluxes in the water column affecting the structure and functioning of phytoplankton and zooplankton communities.

Estimates of vertical transport of matter (organic and inorganic) in the upper waters of the ocean, strongly depend on the water structure (density field) that is widely variable making accurate quantification a difficult exercise (Kiefir and Kremer, 1981; Lewis et al., 1986). This makes the vertical mixing and stratification processes requiring parameterisations that simplify and provide realistic estimates of energy and matter flows (Gaspar et al., 1990). A reasonable parameterisation of the turbulent diffusion is given by Osborn (1980) (Equations 2.1 - 2.2) making turbulent diffusion to be inversely proportional to the Brunt-Väisälä Frequency (a measure of the water stability). In the proposed model, Osborn parameterisation of the turbulent diffusion is imposed, as it has been proven to work successfully in ecological simulating of upper waters during mixed and stratified conditions (e.g. Zakardjian and Prieur, 1994; Sharples et al., 2001; Bahamon and Cruzado, 2002). This parameterisation has been also validated in spring and summer conditions in NW Mediterranean and subtropical NA waters, as shown in Chapters 2 and 3, respectively.

Modelling of biological processes regarding primary production are often based on FDM model (Fasham et al., 1990) calibrated with oceanographic data from the Sargasso Sea. It is a single mixed-layer and nitrogen dependent model whose original version used a large set of variables and parameters that subsequently has been revised and improved. Sarmiento et al. (1993) coupled the FDM model to a hydrodynamic Princeton general circulation model (POM) finding, in general, not only a better fit of nitrate and ammonium dynamics but also inconsistencies in predicting the chlorophyll concentration as estimated by satellite data. Hurtt and Armstrong (1996) observed that the sinking rate of particulate organic nitrogen (PON) and the slope of photosynthesis-light curve were understimated in the FDM model. The application of POM-FDM in stations at latitudes over 30°N severely over-predicted the spring bloom and under-predicted the chlorophyll concentration

along the rest of the year. The fit of the POM-FDM model and its constraining power of data were also studied in depth by Evans (1999). More complex biogeochemical models like ERSEM, simulating biogeochemical seasonal cycles of carbon, nitrogen, phosphorous and silicon in the pelagic and benthic food webs of the North Sea have been built (Baretta et al., 1995; Varela et al., 1995). Coupled three-dimensional physical-biological models (v. gr. Skogen et al., 1995; Zavatarelli et al., 2000) have been developed with the same purpose.

In the present work, in order to evaluate stocks and fluxes of nitrogen in two oligotrophic ecosystems, a vertically resolved one-dimensional turbulence driven ecological model is proposed simulating the intra-annual variability of the ecological processes in the upper 300 m of the water column. N-Nitrate, N-nitrite, N-ammonium, N-phytoplankton and N-zooplankton are state variables of the model that was run for locations representing the conditions (temperature, salinity, and density) at hypothetical oceanographic stations in oligotrophic ecosystems. The model is called "Bio-adaptable Light And Nutrient dependent Ecosystem Simulator" (hereafter referred to as BLANES model) later used (Chapter 5) to explain part of the wide variability of the nitrogen standing stocks and fluxes in the upper ocean. The model is thought to assess the trophic structure and functioning of oligotrophic environments based on the nitrogen stocks flowing as nutrients or biological communities. In the previous cases described in Chapters 2 and 3 the role playing the density field in the vertical turbulent diffusion and its effect on primary production was evaluated. The BLANES model was built preserving that scheme of the density field affecting the upward transport of nutrients in both unstable waters (spring production in NW Mediterranean case study) and stratified waters (summer production in tropical NA case study). Phytoplankton primary producers were assumed to be dependent on light (at given latitudes), on nutrient availability and on zooplankton grazing pressure. The vertical turbulence scheme used in the model is calibrated and validated against field temperature measurements taken in the Catalan and Algerian Seas in the western Mediterranean.

4.2. Model description

Physical Framework

BLANES is a significantly improved version of the one-dimensional model described by Varela et al. (1992) originally thought to simulate the depth of chlorophyll maximum (DCM) during summer time. The current version, coupling physical and biogeochemical variables, simulates hypothetical oceanographic stations in selected areas of the open ocean reproducing the temporal evolution (hourly steps) of nitrogen available for primary producers including all its forms except the molecular nitrogen (N_2) in the upper water layers. The BLANES model covers the upper 300 m of the water column with temperature, salinity, density and irradiance as physical variables and nutrients (nitrate, nitrite and ammonium), phytoplankton and zooplankton nitrogen as biogeochemical variables. All variables are subject to advection and diffusion in the vertical direction maintaining the mass-conservation principle.

The relatively low variability of temperature (°C) and salinity (psu) at 300 m depth as deduced from field data, led us to fix values for these variables. Temporal evolution of temperature and salinity, imposed to the surface boundary were parameterised as sinusoidal functions, according to basic statistics (*mean* and *amplitude*) obtained from field data (Table 4.1):

$$B = mean + amplitude * sin\left(\frac{2\pi}{365 - phase}\right) \tag{4.1}$$

B representing temperature (°C) or salinity (psu) and *phase* depending on the form of the sinusoid.

Table 4.1 Basic statistics of temperature and salinity obtained from historical data, imposed as upper boundary and fixed at the bottom boundary in the BLANES model.

	Catalan Sea		Eastern subtropical NA	
Surface boundary	*Mean*	*Amplitude*	*Mean*	*Amplitude*
Temperature	17.9	±5.0	21.0	±3.0
Salinity	37.9	±0.3	37.0	±0.4
Bottom boundary	*Fixed value*		*Fixed value*	
Temperature	13.1		16.0	
Salinity	38.45		36.0	

Length of daylight (L1)

The latitude of the stations and the Julian day control the length of daylight in hours computed following Brock (1981):

$$L1 = 2W1 * \frac{180}{15\,\pi} \tag{4.2}$$

$$W1 = arccos\left\{-tan\left(L\right)\frac{\pi}{180} * tan\left(D1\right)\frac{\pi}{180}\right\} \tag{4.3}$$

$$D1 = 23.54\,sin\left[\frac{2\pi\left(284+N\right)}{365}\right] \tag{4.4}$$

where *W1* (in degrees) is the angle hour, *L* is latitude assumed as 40.25°N and 27.5°N for the CS and ESNA sites, respectively, *D1* is the declination of Earth i. e. the angular distance at solar noon between the sun and the Equator and *N* the number of days after 22nd December.

Photosynthetic available radiation (PAR)

Total surface incident irradiance was assumed to be dependent on Astronomy, this is, the height of the Sun's plane over the horizon (computed daily) and the height of the Sun over the horizon (computed hourly). Both functions were simulated by trigonometric functions (Equations 4.5, 4.6). A constant fraction of the total irradiance (0.45) was assumed to be PAR (Baker and Frouin, 1987). Exponential

extinction of PAR flowing through the water column depended on absorption and scattering by the water and on the self-shading effect by phytoplankton (Equation 4.7).

$$PAR(0) = P0 + P1\,sin\left(2\pi\,\frac{N}{365}\right) \tag{4.5}$$

$$PAR(0,t) = PAR(0)\left(1 + cos\left[2\pi\left\{\frac{t + L1 - 12}{L1}\right\}\right]\right) \tag{4.6}$$

$$PAR(i,t) = PAR(i-1,t)\,exp^{-\left(k_W + k_C * \left[PHY(i)\right] * D_z\right)} \tag{4.7}$$

P0 is the annual mean value of PAR in surface assumed to be 180 and 250 watt m^{-2} in the CS and ESNA sites respectively; *P1* is the amplitude of PAR here assumed as ±100 and ±160, respectively; *t* is the time step; *L1* is the length of daylight obtained from Equation 2; k_w is the coefficient of vertical light attenuation due to pure water only (assumed as 0.06 m^{-1}) and k_c is the constant for phytoplankton self-shading assumed as 0.03 m^2 (mmol N)$^{-1}$; *PHY(i)* is phytoplankton biomass at box *i* and D_Z is the grid vertical resolution (3 m).

Irradiance is an important factor to be assumed in ecological modelling, since it is crucial for the primary production processes, limiting them by deficit or excess as shown in the photosynthesis-irradiance model scheme in Figure 2.3. Figure 4.1 schematically represents irradiance and other physical processes forcing the BLANES model, as described below in the text. The figure schematises 100 boxes arranged in the vertical dimension, each 3 m thick.

Turbulent environment

Based on theoretical simulations, Zakardjian and Prieur (1998) concluded that vertical advection must be lower than 0.5 m d^{-1} in or near geostrophic fronts in the north-western Mediterranean to explain the vertical distribution of primary production, at least in summer time. Sensitivity tests of the BLANES model yielded a constant value of 0.05 m d^{-1} allowing a proper seasonal distribution of chlorophyll

a concentration in the water column. Higher velocities produced non-realistic values of all state variables close to the surface. In keeping continuity, we assumed that the upwelled flow to escape laterally from the upper box.

The vertical eddy diffusivity (K_z) is forced by the strength of stratification calculated from the density field according to Osborn (1980) formulation described in Chapter 2 (Equations 2.1, 2.2).

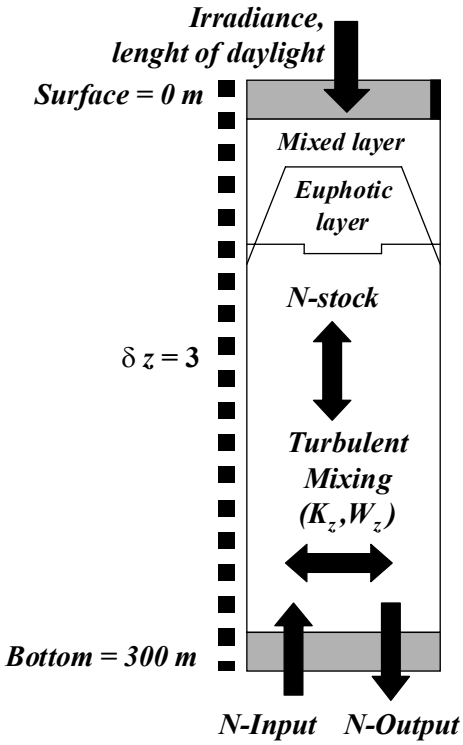

Figure 4.1. Diagram of the numerical grid used in the BLANES model. The mixed layer is thicker than the euphotic layer in autumn and winter but is thinner during spring and summer. Black block above to the right denotes lateral advection allowed compensating the upward advection.

The mixed-layer thickness can be defined according to selected parameters of the water column. Levy et al. (1998) assumed a mixed-layer thickness in western Mediterranean as that with turbulent diffusion higher than 10^{-5} m^2 s^{-1}. Hurtt and Armstrong (1996) considered a mixed layer using the 0.5° C temperature criteria in the Sargasso Sea. In the BLANES model, a sensitivity test allows to determine the appropriate lower limit of the mixed-layer. It was defined as the depth at which the density gradient in respect to the surface is 0.32 and 0.21 g kg^{-1} in the Catalan Sea

and ESNA cases, respectively. Nevertheless, when these gradients cross down the maximum lower limit in autumn and spring times (150 and 220 m in the Catalan Sea and ESNA, respectively), the density difference in respect to the surface was set up to 0.0003 g kg^{-1}. Thus, the mixed-layer depth controls the vertical distribution of K_Z allowing greater diffusion in the mixed layer (> 1E-4 m^2 s^{-1}) and lower values around stronger vertical density gradients. When the density of water in one box was greater than that just below it (plus a small δ value), overturning was applied to all state variables as follows:

$$If\ \rho_{i-1} > \rho_i + \delta\ then\ X(k,i) = \frac{X(k,i) + X(k,i-1)}{2}\ and\ X(k,i-1) = X(k,i) \tag{4.8}$$

where ρ_i is the density at box i, k represents any of the state variables and δ was a constant (δ = 0.00001).

Since overturning was not enough to explain the formation of the near surface phytoplankton bloom occurring in late winter and early spring, convection was necessary to be forced on all state variables along the entire mixed layer at the beginning of the year. Vertical convection simulations are of common use to determine appropriate values for model parameters unresolved by weak diffusivities (Large et al., 1994). In the present case, convection favoured both a faster upwelling of nutrients from deeper waters and the homogenisation of the state variables in the water column. In the model, convection was applied at the day tenth of the run along the entire mixed layer. The realistic character of this convection is supported in the Catalan Sea where convection affecting sometimes the entire water column is known to take place in January - February during deep water formation (Levy et al., 1998). In the Sargasso Sea (also in the subtropical North Atlantic), convection reaching 250 m depth has been reported at the end of February (Hurtt and Armstrong, 1996).

The biogeochemical model

The BLANES model was built to be applicable to any place of the open ocean where nitrogen is assumed to be limiting primary production. The model assesses nitrogen flowing throughout five compartments or state variables in the pelagic environment: Dissolved nitrate ($N\text{-}NO_2^-$), nitrite ($N\text{-}NO_3^-$) and ammonium ($N\text{-}NH_4^+$) are nutrients taken up by a phytoplankton community (N-Phytoplankton) in turn being grazed by a zooplankton community (N-Zooplankton). Zooplankton forces both recycling of ammonium, and non-recycling material as showed in the conceptual model in Figure 4.2.

The evolution equation used in the model for nitrate *(NO3)* is:

$$\frac{\partial NO3}{\partial t} = \frac{\partial}{\partial z}\left[K_z \frac{\partial NO3}{\partial z}\right] - w\frac{\partial NO3}{\partial z} - U_{NO3} * PHY \tag{4.9}$$

Uptake of nitrate by phytoplankton cells (U_{NO3}) is based on the Michaelis-Menten formulation:

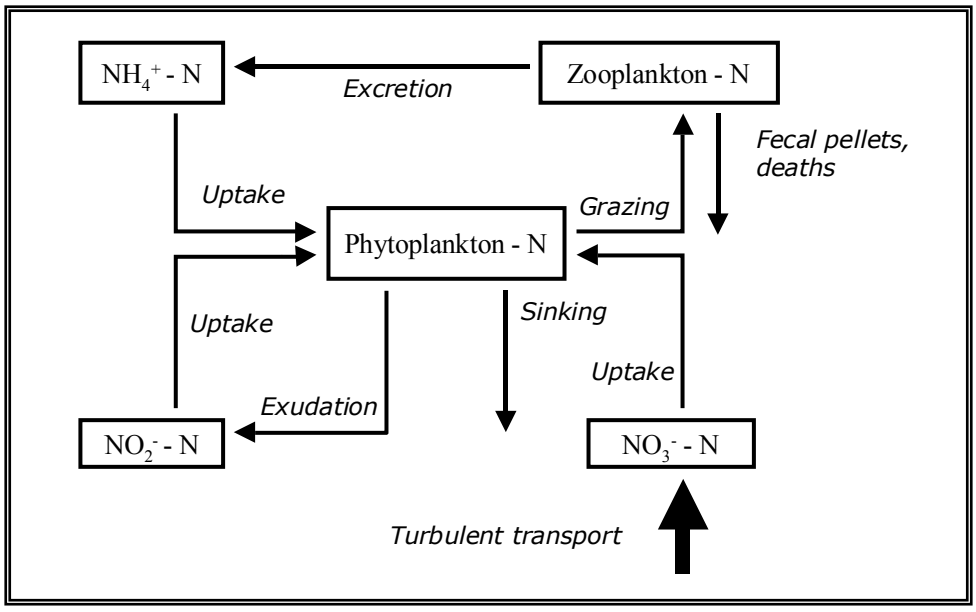

Figure 4.2. Conceptual model of the planktonic ecosystem based on the nitrogen fluxes.

$$U_{NO3} = V_{PHY} \frac{NO3}{K_{NO3} + NO3} e^{\Psi(NH4)} \tag{4.10}$$

V_{PHY} is phytoplankton maximum growth rate and K_{NO3} is the half-saturation constant for nitrate. The exponential function represents the suppression of nitrate uptake by ammonium ψ being the ammonium inhibition parameter for nitrate and nitrite uptake.

A fraction of the nitrate taken up during the light hours by phytoplankton is exuded in the dark as nitrite (PHY_{EXU}):

$$\text{If} \quad PAR(i,t) < PAR_{surface} * (0.1) \text{, then, } PHY_{EXU} = \gamma * U_{NO_3} * PHY \tag{4.11}$$

where i is the given box in the model and γ is the constant fraction of nitrite exudation by phytoplankton.

The evolution equation for nitrite *(NO2)* is

$$\frac{\partial NO2}{\partial t} = \frac{\partial}{\partial z}\left[K_z \frac{\partial NO2}{\partial z}\right] - w\frac{\partial NO2}{\partial z} + PHY_{EXU} - U_{NO2} * PHY \tag{4.12}$$

The uptake of nitrite (U_{NO2}) by phytoplankton is expressed similarly to that given for nitrate uptake:

$$U_{NO2} = V_{PHY} \frac{NO2}{K_{NO2} + NO2} e^{\Psi(NH4)} \tag{4.13}$$

The evolution equation for ammonium *(NH_4)* is

$$\frac{\partial NH4}{\partial t} = \frac{\partial}{\partial z}\left[K_z \frac{\partial NH4}{\partial z}\right] - w\frac{\partial NH4}{\partial z} + \in -U_{NH4} * PHY \tag{4.14}$$

where $\in$ is the fraction of nitrogen ingested by zooplankton that is excreted (see Equation 25).

The ammonium uptake (U_{NH4}) by phytoplankton cells is:

$$U_{NH4} = V_{PHY} \frac{NH4}{K_{NO4} + NH4} \tag{4.15}$$

Limitation of phytoplankton growth by PAR or by nutrients follows the Liebig's law of minimum. This means that the first resource to be depleted at a given time and depth in the water column (PAR/nutrients) stops the phytoplankton growth. Phytoplankton growth (nutrient uptake) limitation by light is formulated as described by Varela et al. (1992):

$$U_{PAR} = V_{PHY} \frac{PAR_{(z,t)}}{K_{PAR} + PAR_{(z,t)}} \tag{4.16}$$

K_{PAR} is the half-saturation constant of PAR (here assumed to be 20 watts m^{-2}). The proportion of each nutrient to be taken up (U) under light limitation when $U_{PAR} < U_{NO3} + U_{NO2} + U_{NH4}$, is computed as:

$$U = U_{PAR} * \frac{U_X}{\left(U_{NO3} + U_{NO2} + U_{NH4}\right)} \quad \text{for } U_X = \left(U_{NO_3} \; or \; U_{NO_2} \; or \; U_{NH_4}\right) \tag{4.17}$$

In order to avoid numerical errors in mass balance, no nutrient uptake by phytoplankton was assumed taking place at depths greater than 60 m below the box having 1% of surface PAR (lower limit of the euphotic layer). As a result, the maximum lower limit for phytoplankton uptake was 180 m in the CS and 280 m in the ESNA.

A chlorophyll-to-nitrogen ratio taken as 1 mg Chl (mmol N)$^{-1}$ (Marra et al., 1990) was used to compare field chlorophyll observations with N-phytoplankton model results. The evolution equation of N-phytoplankton is:

$$\frac{\partial PHY}{\partial t} = \frac{\partial}{\partial z}\left[K_z \frac{\partial PHY}{\partial z}\right] - \left(w + w_S\right)\frac{\partial PHY}{\partial z} + PHY\left(U_{NO3} + U_{NO2} + U_{NH4}\right) - PHY_{EXU} - G \tag{4.18}$$

where w_s is the settling velocity, and G is the phytoplankton grazed by zooplankton (see Equation 4.20).

The evolution equation of zooplankton (ZOO) is:

$$\frac{\partial ZOO}{\partial t} = \frac{\partial}{\partial z}\left[K_z \frac{\partial ZOO}{\partial z}\right] - w\frac{\partial ZOO}{\partial z} + \lambda * G - M - \in - \Omega \tag{4.19}$$

where λ is the zooplankton assimilation efficiency, G is grazing formulated as a Michaelis-Menten function (Equation 4.20), M represents the zooplankton mortality (Equation 4.21), $\in$ represents losses due to ammonium excretion by zooplankton (Equation 4.22) and Ω is the zooplankton faecal pellet production (Equation 4.23).

$$G = I_{max}[ZOO] * \left[\frac{PHY}{K_g + PHY}\right] \tag{4.20}$$

$$M = \mu * [ZOO]^2 \tag{4.21}$$

$$\in = G * (1 - \lambda) * 0.25 \tag{4.22}$$

$$\Omega = G * (1 - \lambda) * 0.75 \quad (4.23)$$

I_{max} is the maximum ingestion rate and K_g is the half-saturation constant for ingestion, μ is the zooplankton mortality rate multiplied, not by the classical closure linear term but by a quadratic function of the zooplankton biomass. This could be interpreted as either cannibalism within the zooplankton compartment or by another predator whose biomass is proportional to that of the zooplankton (Edwards and Yool, 2000). The sensitivity test of the BLANES model supported this parameterisation of zooplankton mortality since it yielded the best results for the zooplankton stocks. By using a similar parameterisation, Evans (1999) found similar effects on zooplankton with the FDM model.

The BLANES model runs from December 22nd to December 21st (assuming the year having 360 days). The rates of change were evaluated at 60 minutes time-step. A mass-conservation finite difference method was employed to compute advection and diffusion. Standard initial values of temperature, salinity, nitrate, nitrite, ammonium, chlorophyll and zooplankton concentrations along the upper 300 m depth were obtained after six years of simulation with arbitrary initial conditions and perpetual year driving forces. This length of time was necessary to make inter-annual variability smaller than 1% assuming a quasi steady state. The best fitting parameters and coefficients used in the above equations are summarised in Table 4.2.

Estimates of primary production and nitrogen fluxes

Primary production, the rate of inorganic carbon incorporated to the phytoplankton biomass, was estimated every time step based on the nitrogen flux. The Redfield C:N ratio of 6.625 was used to compute such a production. *New production* (Dugdale and Goering, 1967) was assumed as that originated by the uptake of nitrate flowing from the bottom boundary of the model domain. Uptake of nitrite was added to that of nitrate in order to estimate better the actual *new production*. The production derived from ammonium uptake was considered as *regenerated production*.

Table 4.2 Best fitting parameters and coefficients as deduced from the sensitivity test of the BLANES model used in the selected oligotrophic environments assuming similar ecological conditions.

Symbol	Value	Definition	Units
K_{NO3}	0.9	Half saturation constant for nitrate uptake	mmol N m^{-3}
K_{NO2}	0.8	Half saturation constant for nitrite uptake	mmol N m^{-3}
K_{NH4}	0.7	Half saturation constant for ammonium uptake	mmol N m^{-3}
ψ	1.5	Ammonium inhibition parameter for nitrate and nitrite uptake	mmol N m^{-3}
γ	0.025	Phytoplankton exudation fraction of nitrite	%
V_{PHY}	3.0	Phytoplankton maximum growth rate	d^{-1}
μ	0.1	Zooplankton mortality rate	d^{-1}
$\in$	80	Ammonium fraction of zooplankton excretion	%
Ω	20	Faecal pellets fraction of zooplankton excretion (detrital)	%
λ	30	Zooplankton assimilation efficiency	%
K_g	1.68	Zooplankton half saturation for ingestion	mmol N m^{-3}
I_{max}	1.2	Zooplankton maximum ingestion rate	d^{-1}

At 300 m depth, relatively low variability of nutrient concentrations is observed from historical database. At this boundary, vertical diffusion allows gains and losses of matter (depending on its concentration gradient) while advection produces gains or losses of matter depending on its concentration. Nitrate concentrations of 8 and 4 mmol m^{-3} were assumed to be constant at the lower boundary in the CS and ESNA sites respectively. The model allowed assessing the upward flux of nitrate from the water below the euphotic zone and the internal fluxes through the biogeochemical compartments. The flow of nitrogen was treated as a scalar magnitude (mmol N m^{-3} s^{-1}). In determining the total upward flux of nitrogen (μmol m^{-2} s^{-1}) at such depths the diffusive flux (K_z) was added to the advective flux term (w)

$$\text{nitrate flux} = wN + K_z\left(\frac{\partial N}{\partial z}\right) \tag{4.24}$$

4.3 Calibration/validation exercises of the physical framework

Calibration/Validation of irradiance, length of daylight, turbulence and mixed layer at different latitudes

Two selected hypothetical sites in open oligotrophic seas located at different latitudes were selected to calibrate and validate the light functioning, diffusion coefficient magnitudes and mixed layer depths. Those sites were located around 22.0°E, 28.0°N in the Catalan Sea, NW Mediterranean, and around 41.0°N, 2.0°E in the eastern subtropical North Atlantic. The selection of these locations was made on the basis of the relatively wide latitudinal separation (19° difference) and the availability of data to validate particularly the biogeochemical model results as shown in the next chapter. The equations describing length of daylight (4.2 to 4.4) yielded good simulations with the given parameters (Figure 4.3, left). Oscillation of PAR magnitudes as deduced from equations 4.5 - 4.6 where also successfully reproduced (Figure 4.3, right).

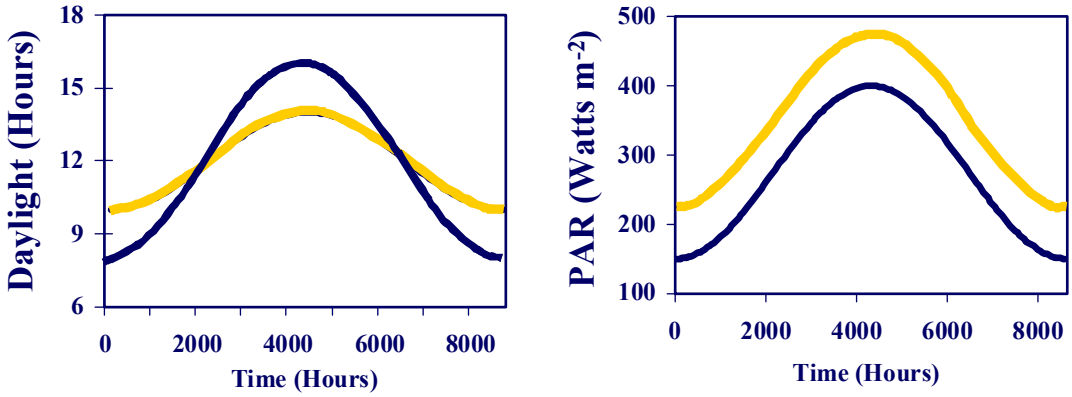

Figure 4.3. Time series of calculated PAR in surface and length of daylight in the Catalan Sea (yellow lines) and the eastern subtropical NA (blue lines).

Simulation results of the vertical turbulent diffusivity of the BLANES model are shown in Figure 4.4 with turbulent diffusion coefficient ranging from 0.1 to 14

cm^2 sec^{-1}. The use of the diffusivity parameterisation yielded values similar to previous estimates given by various authors. Lewis et al. (1988) determined a similar range of diffusivity (0.1-1.0 cm^2 sec^{-1}) explaining nitrogen fluxes in the eastern subtropical North Atlantic. Doney et al (1996) used a background diffusion of 0.1 cm^2 sec^{-1} in their modelling of a station close to Bermuda. Zakardjian and Prieur (1998) studied primary production in the Western Mediterranean using the Osborn (1980) parameterisation yielding a vertical distribution pattern of diffusion similar to our estimates, with the lowest diffusion in the main pycnocline of 0.5 cm^2 s^{-1}. Primary production in the Ligurian Sea was successfully modelled using a range of 0.0017 – 3 cm^2 sec^{-1} eddy diffusivities (Tusseau et al., 1995).

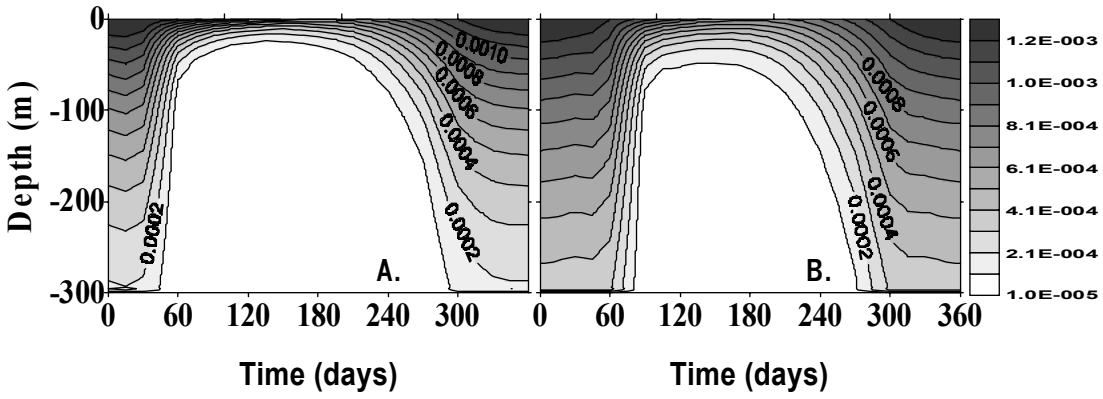

Figure 4.4. Time series of idealised vertical eddy diffusivity (K_Z in m^2 s^{-1}) in the Catalan Sea (A) and in the eastern subtropical NA (B).

The mixed-layer simulation was successfully reproduced in the eastern subtropical North Atlantic and in the Catalan Sea (Figure 4.5). Imposed density gradients allowed adequate thickness of the mixed-layer with mimimum and maximum values similar to those reported for the same areas, using turbulent diffusion criteria in western Mediterranean (Levy et al., 1998) and vertical temperature gradient criteria in the Sargasso Sea (Hurtt and Armstrong, 1996). Density dependent mixed-layer was shown to be useful in the selected environments with opposed salinity gradients (downward increasing in the Catalan Sea but downward decreasing in the ESNA case). This was an important issue in further comparison on both environments, since salinity gradients altered the vertical density

gradients and therefore, the turbulent diffusion (simulated temperature, salinity and density are shown in Chapter 5, Figure 5.2).

Simulations of the temperature, salinity and density fields are shown in the next chapter from an ecologically comparative point of view. Biogeochemical processes forced by the above physical framework are also explained in detail in Chapter 5. Nevertheless, before running the coupled physical and biogeochemical model, a modelling exercise of temperature was made with results compared with field observations in closer sites in the open western Mediterranean.

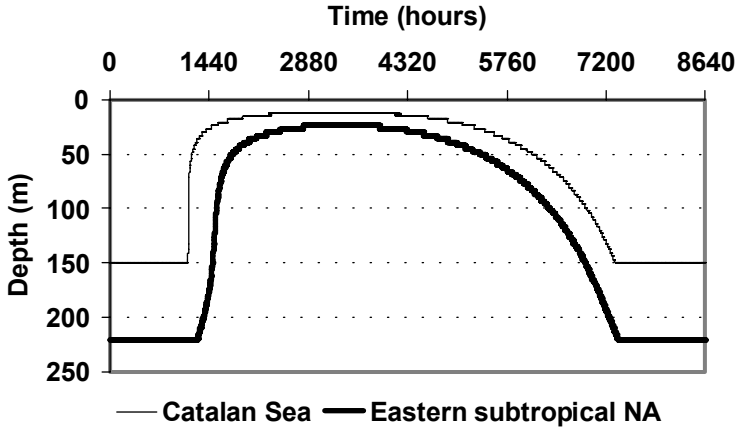

Figure 4.5. Idealised density-dependent mixing layer depths.

Calibration/Validation of temperature in upper waters of western Mediterranean seas

Two open ocean stations in the Catalan Sea and Algerian Sea were selected to calibrate and validate temperature. Initial profiles of temperature and salinity in the BLANES model were required to estimate the density field and consequently, the vertical turbulent diffusion that was affecting the temperature distribution. Temperature parameterisation of upper and lower boundaries was required to determine the internal heat fluxes. Using field data taken as repeated measurements in two sites in the selected stations, initial vertical profile and both upper and lower boundaries of temperature were calibrated and validated against field observations. Sites were selected from a hydrographic section carried out between Spain (Barcelona) and Algeria (Skikda) nine times visited from November 1999 to April

2000. One of the selected sites was located in the Algerian Sea, and the other was located in the Catalan Sea (Table 4.3). The temperature data were obtained from profiles carried out with expendable bathythermographs (XBT) launched from *Voluntary Observing Ships* (VOS) (as part of the EU-MFSPP project). Bathythermographs reached 360 m depth, but only data from the upper 300 m were used in this work. As initial conditions, a temperature profile from observations in cruise VOS 4 (see Table 4.2) and a salinity profile from historical database in the Catalan Sea (upper and lower boundaries are shown in Table 4.1) were assumed at the first Julian day. The evolution of surface and bottom temperatures was imposed as boundaries in the model. Temperature, nearly constant at 300 m depth around 13.1 °C was assumed to be fixed in the bottom boundary while surface temperature was assumed to be driven by a polynomial function as deduced from field data (Figure 4.6). Reference values for salinity in both sites were those used for the Catalan Sea as described in Table 4.1. Since density mostly depends on temperature (according to the Millero and Poisson, (1981) equation) no significant variations in density were expected to take place using this salinity standard reference for both environments.

Table 4.3. Location of selected sites visited from November 1999 to April 2000 to estimate the diffusion coefficient in the water column using BLANES. Sites were located in the Catalan Sea around 40.6° N, 2.8° E and in the Algerian Sea around 38.6° N, 5.1° E.

VOS cruise	Algerian Sea (Station number)	Catalan Sea (Station number)	Day of the year
2	21	6	306
3	13	35	333
4	21	4	343
5	21	4	13
6	23	6	30
7	21	6	41
8	21	7	73
9	13	29	103
10	23	7	119

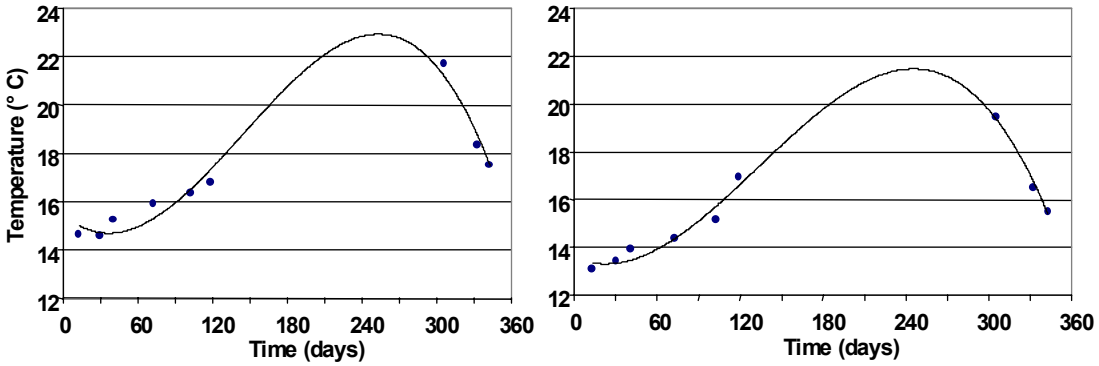

Figure 4.6. Surface temperature trend as deduced from *VOS* observations. On the left is shown the Algerian station located at 38.6 °N, 5.1 °E ($y= -2E-06x^3 + 0.0007x^2 - 0.0457x + 15.483$; $r^2=0.96$). On the right is shown the Catalan Sea station at 40.6 °N, 2.8 °E ($y= -1E-06x^3 + 0.0006x^2 – 0.0241x + 13.553$; $r^2=0.97$).

A five-year running time was necessary to make the inter-annual variability of the model simulations lower than 1%, assuming this variability as quasi-stationary. Monthly simulations of the year sixth were compared against field data. The model results were rather similar to field observations in the Catalan and Algerian seas as shown in Figures 4.7 and 4.8, respectively. In the Algerian Sea, overheating of surface layers took place (~2°C) in the simulation at the day 120 due to the shape of polynomial function that in this period tends to overestimate temperature (see Figure 4.6, left). The vertical diffusion parameterisation was assumed to be suitable under the given scheme. Thus, the mains forcing transporting heat and matter in the planktonic ecosystem was assumed to be ready to run the complete model, with integrated physical and biogeochemical modules. Calibration and validation of parameters, coefficients and processes regarding biology and geochemistry are shown in the Chapter 5. Their results will be used to make ecological distinction between oligotrophic ecosystems that basically works under similar forcings but showing different primary and secondary productions, as occurs with NW Mediterrean Sea and eastern subtropical north Atlantic areas.

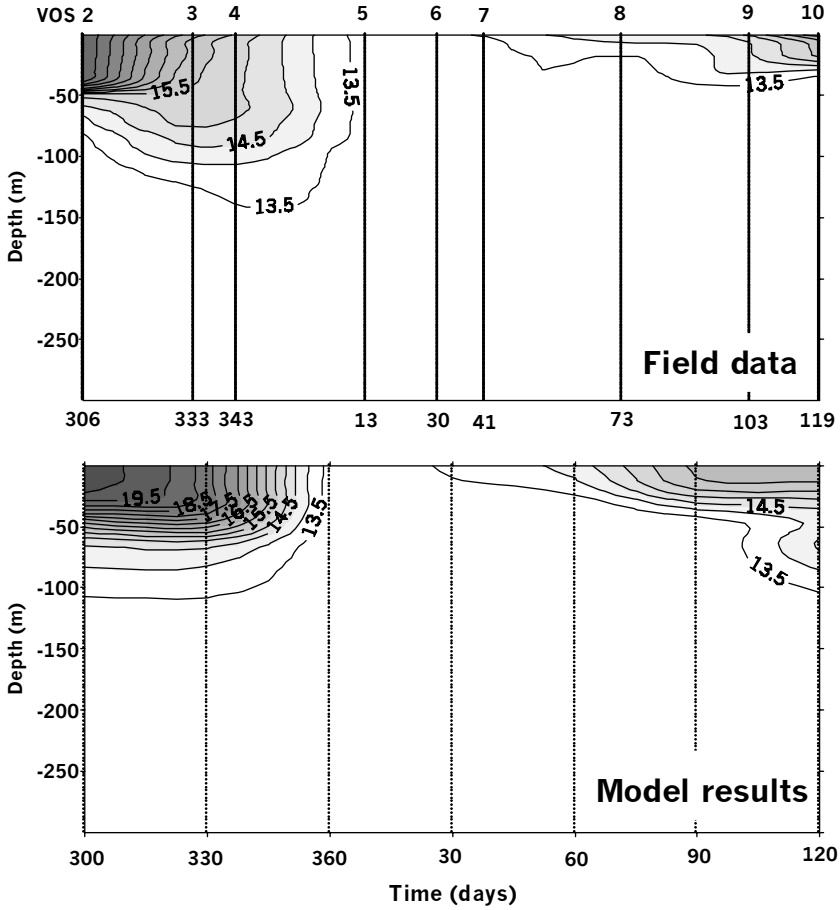

Figure 4.7. Comparison of field data (above) with model results (below) of depth and time evolution of temperature (°C) in the Catalan Sea with vertical lines indicating profiles from observations and model outputs, respectively.

4.4. Remarks and discussion

Key elements and processes of the pelagic ecosystem allowing assessment of phytoplankton primary production and zooplankton secondary production in waters of the upper ocean were selected and parameterised using the BLANES model. The model allows explaining vertical fluxes of nitrogen and new production in oligotrophic ecosystems, according to the water column structure. The model is also suitable to carry out ecological comparisons of environments subject to specific environmental conditions, particularly light and nutrients. The turbulent diffusion-advection scheme initially thought to be applied to stations located far away one from each other, was demonstrated to successfully work under density fields in

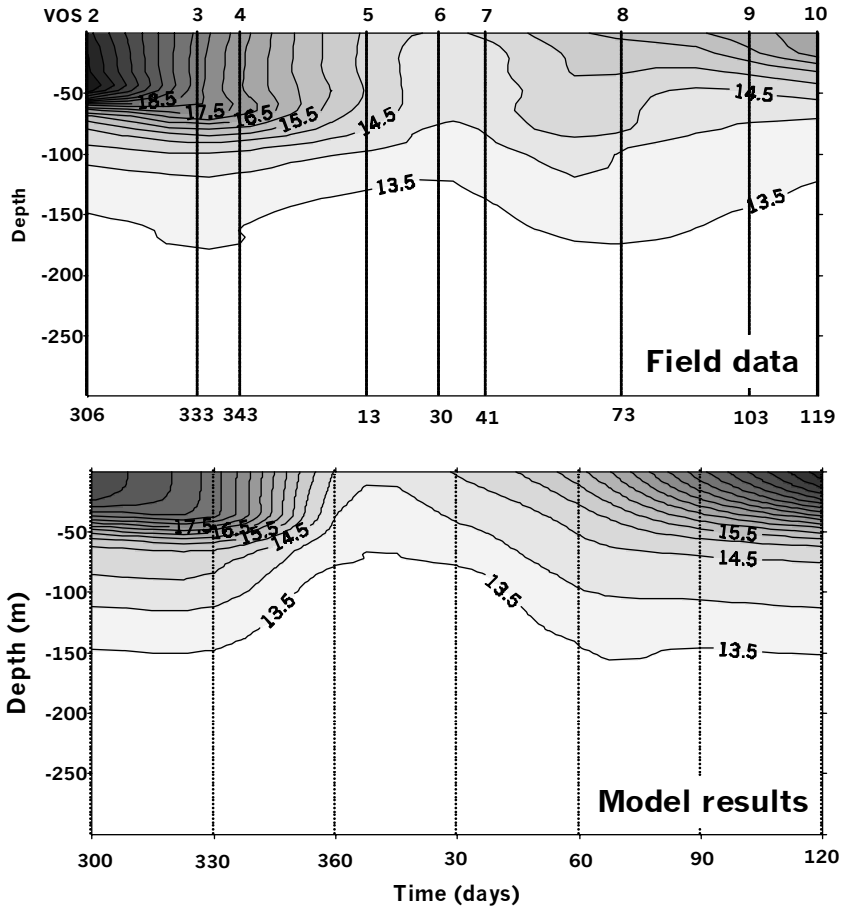

Figure 4.8. Comparison of field data (above) with model results (below) of depth and time evolution of temperature (°C) in the Algerian Sea with vertical lines indicating profiles from observations and model outputs, respectively.

relatively close hydrographic sites in western Mediterranean seas (Catalan and Algerian seas).

In the model, the different nitrogen species are assumed as state variables, allowing distinguishing the nitrogen cycling trough the given plankton communities. The model was built allowing the nitrogen to enter the system as nitrate. Part of the unassimilated nitrogen by phytoplankton can be converted to nitrite due to phytoplankton reduction in the dark. Nitrate and nitrite uptakes constitute the new production in the system. Then, phytoplankton is grazed by zooplankton that assimilates part of it, and excretes another portion as ammonium or faecal pellets

(regenerated production). Remineralisation by the way of bacteria (microbial loop) is assumed to be implicitly taking place below the euphotic zone in the bottom boundary of the model where nutrient-rich waters are supplying nitrogen to the system. In Chapter 5, the coupled physical and biogeochemical model is validated against field data from selected stations at latitudes far away among them, in order to observe the model functioning at different irradiance and daylights and also with different rates nutrient supply from deep waters.

Reasonable simulations of the time-variable irradiance and length of daylight in accordance with latitude of the selected stations were obtained. This physical framework is expected to force the micro-planktonic food webs of pelagic environments, assuming the food web as predictable from the phytoplankton and zooplankton communities with no distinction on the dominant populations at given periods of the year. It is assumed that the relatively vast taxonomic and functional complexity of a plankton community and diversity can be represented by a state variable (as whole community) with rapid adaptation of its populations to the environmental changes (McGrady-Steed et al., 1997). In general terms, BLANES model is not formulated with the aim of understanding of complex food webs as used in other models (e.g. ERSEM model, Baretta et al., 1995). Large projects carrying out studies with relatively high-level complexity in operational marine ecology are known to require large computational and human requirements that in practice obtain a limited use of results (Ebenhoh, 2000; Vichi, 2000). A new direction of ecological modelling is required toward more realistic and predictable biocheochemical processes changeable with current natural and human-driven environmental pressure (Doney, 1999).

The basic physics and biogeochemical structure of the model are thought to be widely flexible, making the model to be potentially applicable to various environmental problems. Flexibility of the model consists in allowing modifying the time evolution of surface irradiance and vertical structure of water (density) altering the turbulent diffusion scheme according to new changes. New state variables and more complex interactions into the euphotic zone or with the atmosphere are also

possible issues to be tackled in later studies. Potential applications of BLANES are described at the end of the next chapter, once the model functionality to assess different pelagic environments at different latitudes is proven, keeping similar ecological conditions. At the moment, BLANES allows the study of nitrogen stocks in given state variables and fluxes among them under variable conditions of surface heat and bottom nitrogen inputs. As a result of the model simulations, the variability of the upward nitrogen flux fuelling the primary production is expected to be a function of both the density field and the nitrate gradients. This allows comparative studies of pelagic environments under natural or human-induced pressures, being the main contribution of the model.

In brief, BLANES model reflects the current trend of modelling toward analysis of limited processes regarding marine biogeochemistry with comparison of matter fluxes. The comparative ecology framework, under which the BLANES has been developed, provides a useful highlighting of differences among involved physical, biological and chemical processes, making them easily identifiable for later practical purposes regarding environmental monitoring.

Chapter 5

Ecological comparison of the plankton functioning in oligotrophic ecosystems using BLANES: NW Mediterranean Sea and eastern subtropical North Atlantic

Abstract

In order to evaluate stocks and fluxes of nitrogen in oligotrophic ecosystems, numerical simulations with a one-dimensional turbulence driven ecological model (BLANES) are validated against field observations in NW Mediterranean Sea and eastern subtropical North Atlantic (ESNA) stations. The nitrate entering the euphotic zone through the lower boundary explained the low but continuous primary production in the two oligotrophic systems. Thickness of the mixed layer, gradient of nitrate, intensity of irradiance and grazing pressure of zooplankton on phytoplankton were found to be the main factors forcing the evolution of phytoplankton. The turbulence-dependent mixed-layer depth explained the summer thermohaline stratification in both ecosystems but could not explain the vertical mixing during wintertime. Convection at the beginning of the year was required to supply the nitrate needed for the formation of the late-winter phytoplankton blooms. The annual phytoplankton stocks were dependent on nitrate concentration at the lower boundary, doubling in the Catalan Sea the value of the ESNA. The phytoplankton maximum was deeper in the subtropical Atlantic than in the western Mediterranean, especially during summertime when the higher irradiance and daylight length made the euphotic layer thicker. In both locations zooplankton grazing was found to control the late winter phytoplankton bloom but reduced more than expected the subsurface phytoplankton concentration in summer. Phytoplanktonic dark nitrate reduction and exudation explained the nitrite maximum. Simulations of the nitrate entering below the euphotic zone was well explained from the density field and nitrate gradients with results in agreement with previous estimates of matter fluxes and yearly estimates of new phytoplankton primary production.

5.1 Introduction

Unlike in estuarine or wind-induced upwelling areas where most of primary production is based on external nitrate sources, oligotrophic oceanic environments are typically characterised by a high rate of ammonium-regeneration based primary production with low nitrate entering from adjacent ecosystems, mainly from deep waters (Dugdale and Goering, 1967). Such a new nitrogen supply at large mid-latitude open-ocean oligotrophic anticyclonic gyres is mainly depending on the diffusive-advective transport from the deep or lateral boundaries or even from atmospheric depositions (Duce et al., 1980; Lewis et al., 1986). The NW Mediterranean Sea, although with general cyclonic circulation giving rise to persistent thermohaline fronts, shows "new" primary production associated to the turbulent transport of nitrate from deeper waters as pointed out from several observational and numerical studies (Lohrenz et al., 1988; Salat, 1995; Zakardjian and Prieur, 1994; 1998, Estrada et al., 1999). The biological fixation of molecular nitrogen by planktonic cyanobacteria and benthic macroalgae (Gasol et al., 1997) and the deposition of airborne N-containing particles (Alarcon et al., 1990; Béthoux and Copin-Montégut, 1986) have been suggested as important nutrient sources for primary production in the NW Mediterranean.

In other areas of the ocean such as the Sargasso Sea, the inflow of nutrients brought to the surface has been mainly attributed to vertical diffusion from deeper waters (Menzel and Ryther, 1960; 1961; Denman and Gargett, 1983; McGuilligudy and Robinson, 1997). The role of the horizontal transport of nitrate across the intergyre boundaries by surface Ekman drift and the presence of geostrophic eddies have also been proposed as important mechanisms for nutrient supply (Williams and Follows, 1998). The atmospheric deposition of nutrients may also play an important role in sustaining primary production (Knap et al., 1986; Schutz et al., 1988). Such input could not significantly influence the subsurface chlorophyll maximum (Varela et al., 1994) affected mainly by deep nitrogen (Taguchi et al., 1988; Furuya, 1990).

In the eastern basin of the subtropical North Atlantic, the relationship between the primary production and physical processes like persistent or intermittent fronts (Owen, 1981) and biogeochemical processes (Marañon et al., 2000) have been little studied. Planas et al. (1999) attribute the control of primary production in the Central Atlantic to a balance between diffusive supply of nitrate and atmospheric deposition. Assessment of the nitrogen flux available for planktonic primary and secondary producers located in the upper water layers are important issues addressed through numerical modelling.

The estimates of nitrogen fluxes up to the euphotic zone vary widely according to the place of the ocean, field and numerical methods. The plankton communities structure are strongly interacting with such fluxes with a relatively vast taxonomic, functional complexity and diversity of plankton that nevertheless can be predictable from numerical simulations (McGrady-Steed et al., 1997; Serret et al., 2001). Fasham et al. (1990) and McGillicuddy and Robinson (1997) give values of nitrogen flux of waters in the Sargasso Sea from 0.40 to 0.72 mol m^{-2} $year^{-1}$, assuming phytoplankton and zooplankton as single state variables in the upper mixed layer. These values differ up to about an order of magnitude when compared with other estimates. In the Sargasso Sea, Doney et al. (1996) estimated the upward nitrogen flux at 300 m depth to be 0.06 mol N m^{-2} $year^{-1}$ similar to the value 0.072 mol N m^{-2} $year^{-1}$ calculated by Gruber and Sarmiento (1997). Bahamon et al. (2002) report an average nitrogen flux of 0.19 mol N m^{-2} $year^{-1}$ in subtropical NA including both eastern and western basins. In the Catalan Sea, the nitrogen entering the upper water layers fuelling the primary production has been estimated in the range between 0.26 to 0.64 mol N m^{-2} $year^{-1}$ (Tusseau et al., 1997; Levy et al., 1998).

In Chapters 2 and 3 the role played by the vertical structure of the upper water layers in the upward nitrate transport fuelling new phytoplankton production was analysed in both stratified (summer) and mixed (spring) conditions in oligotrophic ecosystems. Here, the same topic is addressed from numerical simulations along the year in stations located in open ocean areas in NW Mediterranean and subtropical North Atlantic, with cyclonic circulation inducing upwelling altering the nutrient and

plankton dynamics. An attempt is made to explain part of the relatively wide variability of the nitrogen fluxes estimates, based on vertical turbulent diffusion and advection variability in both areas. A comparative ecological study regarding primary production is made emphasising similarities and differences in biogeochemistry under similar physical forcings. The study is based on the diffusive-advective flux of nitrogen using the BLANES model, whose structure and function was described in the previous chapter. The trophic structure and functioning of these oligotrophic environments was based on nitrogen stocks flowing as nutrients or biological communities. The primary producers were assumed to be dependent on light, nutrient availability and grazing pressure. The stations selected were located at different latitudes, in the Catalan Sea (NW Mediterranean) and in the eastern boundary of the Subtropical North Atlantic.

The study areas

The structure and functioning of planktonic ecosystems in two places in open ocean areas were compared, one in the central Catalan Sea, NW Mediterranean (hereafter referred to as CS), and the other in the eastern subtropical North Atlantic Ocean (hereafter referred to as ESNA) (Figure 5.1). The field data used to validate the model results were obtained during various cruises carried out by staff from the Centro de Estudios Avanzados de Blanes (CEAB), Spain. Ninety-eight stations carried out in the Catalan Sea between 40-41°N, 1-3°E and twelve stations in the eastern subtropical North Atlantic between 20-24°E and 25-30°N were selected. The CS stations covered all seasons in the period 1985 – 1999 while the ESNA stations covered only winter 1991 and summer 1992 (Table 5.1). Preliminary analysis of field data allowed characterising the respective ecosystems with regard to nitrogen assumed to be both fuel and limit of biomass production (Dugdale, 1967; Berges and Falkowski, 1998). In absence of real-time series, existing historical data of temperature, salinity, chlorophyll *a*, nitrate and nitrite, were grouped by seasons and integrated at various depths in order to be compared with seasonally integrated results generated by the BLANES model.

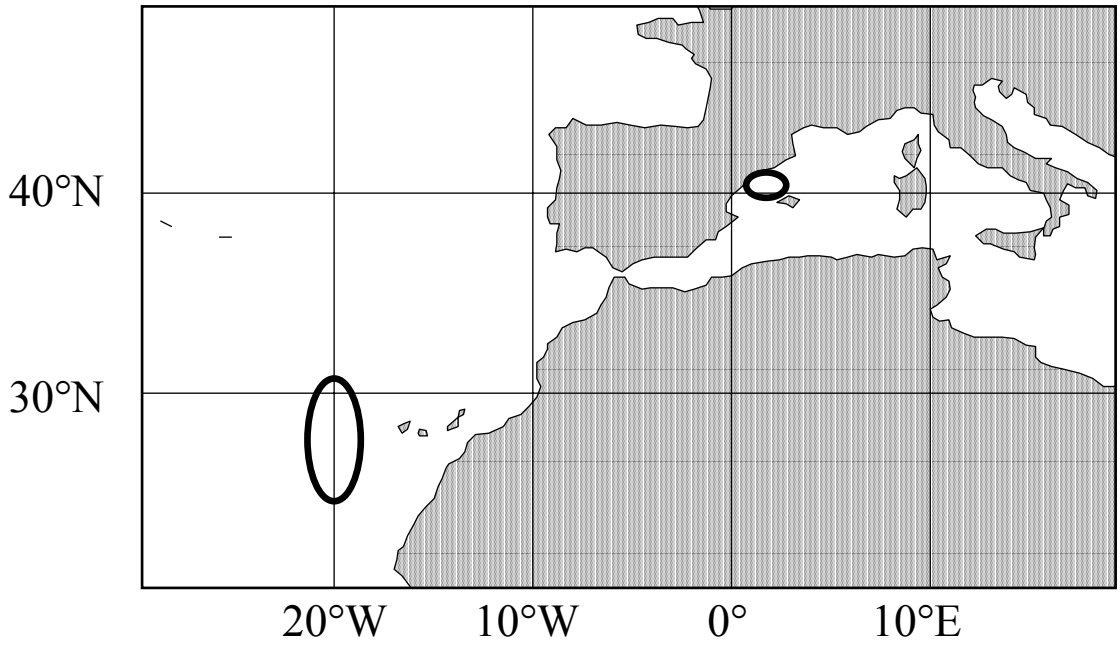

Figure 5.1. Location of sites represented by the model simulations. Vertical ovals mark the Catalan Sea; horizontal ovals indicate the eastern subtropical NA.

Table 5.1. Cruises from which data were obtained in the Catalan Sea and in the eastern subtropical North Atlantic.

Cruise	Year	Month	Number of stations
NW Mediterranean			
Caron	1985	Feb	5
Pelagolion III	1988	Feb	5
Fans II	1997	Feb	7
Cybele	1990	Apr	9
Yoyo I	1999	May	4
Mesoescala 95	1995	Jun	10
Fans III	1997	Jul	8
Tanit	1979	Aug	5
Pelagolion I	1986	Sep	8
Rhodiber 90	1991	Sep	9
Fans I	1996	Nov	9
Discovery 88	1988	Dec	7
Pelagolion II	1988	Dec	4
Tyro	1991	Dec	8
Eastern subtropical NA			
Challenger	1991	Feb	8
WOCE A5	1992	Aug	12

5.2. The physical environment

Simulations of temperature, salinity and density in depth and time in the upper water layers of both the CS and the ESNA are shown in Figure 5.2. Temperature showed the general seasonal trend in oligotrophic ecosystems (Figure 5.2, above). Typical temperature maxima in the surface were observed during summertime of 22.9 °C and 24 °C, in the CS and the ESNA stations, respectively. The minimum surface values in wintertime were 12.9 °C and 18 °C, respectively. The 15 °C isotherm in the CS was observed at approximately 80 m depth during spring and summer while in autumn it sank to about 120 m depth. This isotherm disappeared during wintertime due to the homogenisation forced in the mixed layer by the vertical convection which takes place at the beginning of the year thus making temperature 13.6 ± 0.6 °C along the entire water column. The 19° C isotherm in the ESNA was observed at ~100 m depth showing a similar temporal pattern of distribution than the 15°C isotherm described in the CS. The summer thermocline in the CS was found shallower and thinner (between ~30 and ~50 m depth) than in the ESNA (located between ~40 and ~90 m depth). The modelled vertical gradient of temperature above thermocline in the CS was twice the gradient in the ESNA station (0.09°C m^{-1} and 0.05°C m^{-1}, respectively). Just the opposite occurred below the thermocline, since the gradient in the former site was half of that observed in the latter (0.01°C m^{-1} and 0.02°C m^{-1}, respectively).

Salinity among simulated stations showed an inverse pattern of distribution in time and depth (Figure 5.2, middle). At surface, in the CS the lowest value was observed in summer (37.1) while the highest value appeared at the late autumn and winter times (37.9). Just the opposite occurred in the ESNA site, where the highest value was found in summer (37.3) while the minimum was found in late autumn and winter (36.6). In the vertical, salinity increases downward in the CS case while it decreases downward in the ESNA. A diffuse halocline was observed in the CS

between ~60 and ~80 m depth while in the ESNA station halocline is absent. The vertical gradients of salinity were relatively similar in both cases (0.002 and 0.003 in the CS and ESNA, respectively).

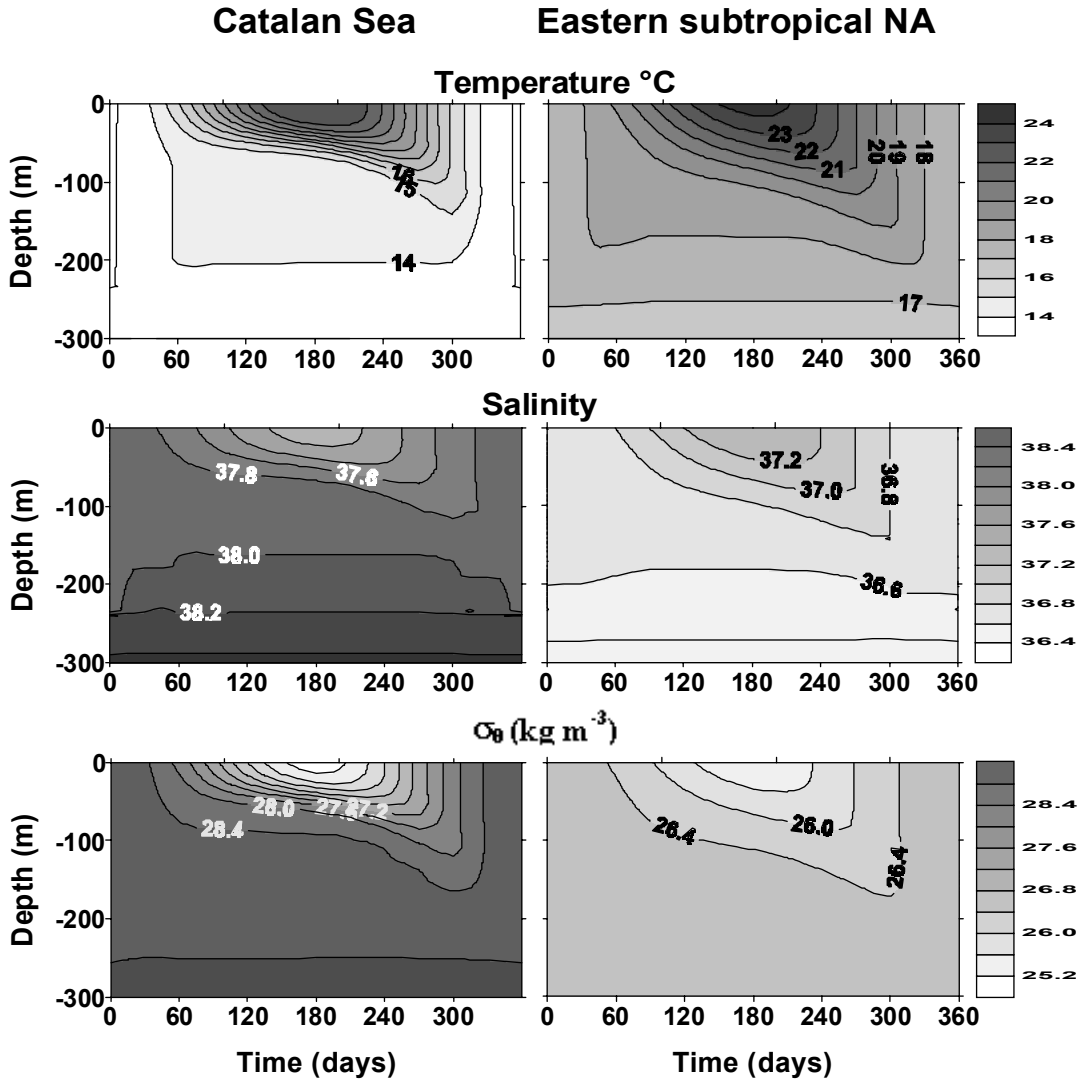

Figure 5.2. Simulated time series of temperature, salinity and density by the BLANES model.

In spite of the differing vertical distribution patterns of salinity, sigma theta kept mainly governed by temperature in both sites (Figure 5.2, down). A pycnocline parallel to thermocline was found in summertime in the CS between ~30 m and ~50 m depth, while in the ESNA case it was rather diffuse between ~30 and ~100 m

depth. Above the pycnocline, the gradients in the CS case were stronger, around 2.8 kg m^{-3} while in the latter, they were around 1.2 kg m^{-3}. Below the pycnocline, no strong variability was observed in the density gradient. Almost all year round, except in the early winter and late autumn, the density of the water layers above 100 m depth increased from 26.4 to 28.4 kg m^{-3} in the CS site while in ESNA, density decreased from around 24.8 to 26.4 kg m^{-3}.

The model temperature profiles seasonally averaged in the CS site fit well with field observations (Figure 5.3). The most important difference is found in autumn, when simulation underestimated temperature in about two degrees Celsius. Temperature observed, remains relatively homogeneous below ~100 m depth at all seasons while the model profiles tend to be more variable and in general, higher than observations. This suggests that eddy diffusion in the model is higher, but not significantly stronger than in reality below 100 m depth.

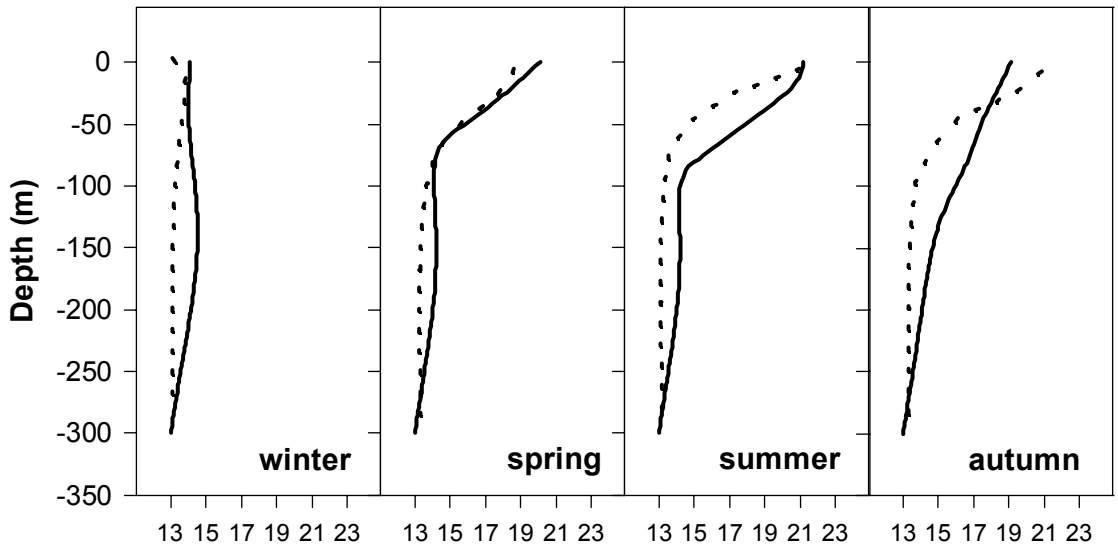

Figure 5.3. Comparison of seasonal mean values of simulated potential temperature (°C) (lines) with field observations (dots) in the Catalan Sea case study.

As occurs with temperature, the simulated vertical distribution of salinity by seasons in the CS shows relatively small differences with field observations (Figure 5.4). The summer halocline in the model simulations does not appear to be very

realistic, since in the field data, salinity shows only a small but constant downward gradient along the entire column (see Figure 5.2, middle left). We attributed this to the relatively high turbulent diffusion in the model, especially below 100 m depth. Salinity was particularly overestimated in autumn and winter in near 0.2 psu.

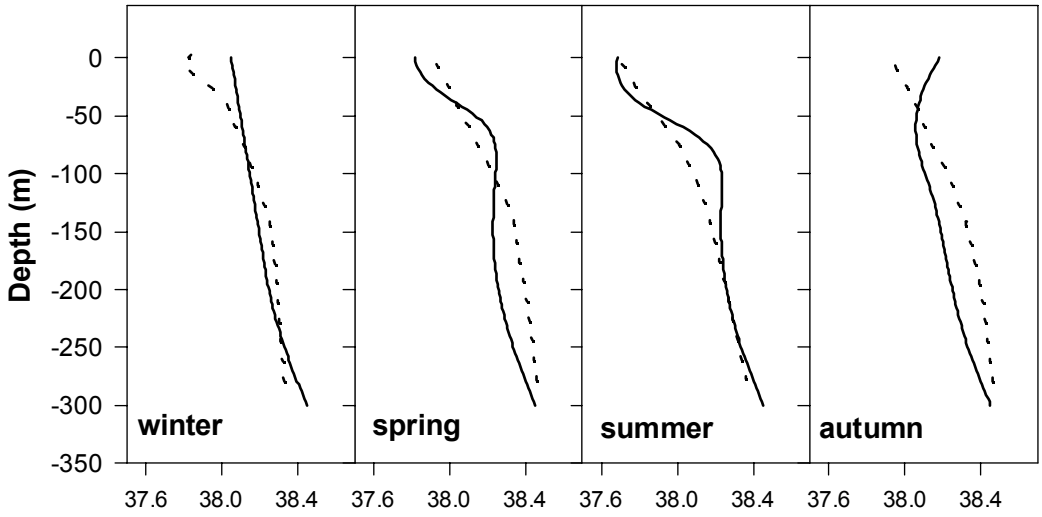

Figure 5.4. Comparison of seasonal mean values of simulated salinity (lines) with field observations (dots) in the Catalan Sea.

In the ESNA case, the BLANES model fits better than in the CS case the average temperature and salinity for winter and summer (Figure 5.5). The vertical distribution of turbulent diffusion appears realistic in this case, since modelled profiles of both temperature and salinity fit well field observations. This success in modelling could not be corroborated for the other seasons due to lack of field data.

5.3 Nutrients and plankton functioning

N-Nitrate and N-phytoplankton chlorophyll

The annual cycle of N-Nitrate (hereafter referred to as nitrate) modelled is shown in Figure 5.6. The typical situation of high nitrate depletion in surface waters

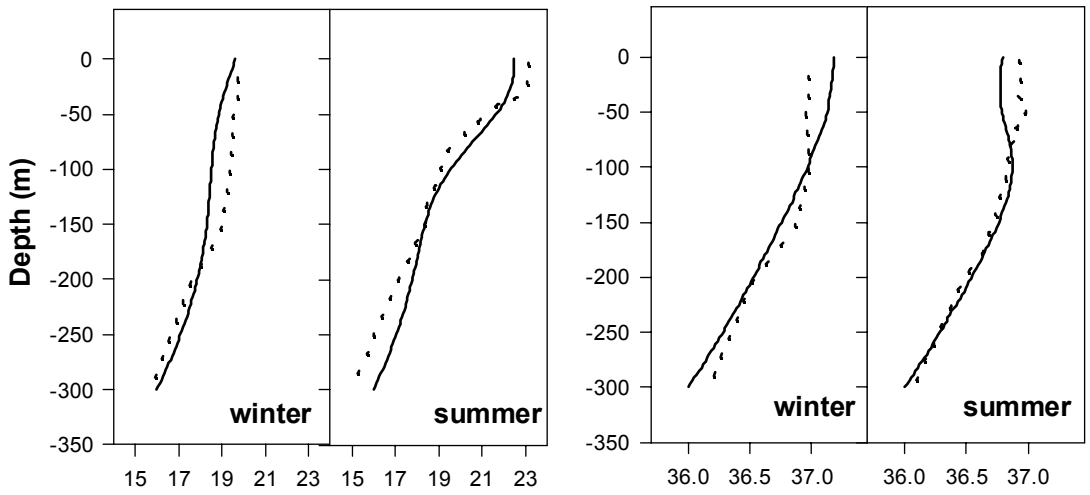

Figure 5.5. Comparison of mean values of simulated potential temperature (°C, left) and salinity (right) with field observations during winter and summer seasons, in the eastern subtropical NA. Continuous lines represent the simulations and dots are the field observations.

is common to the Catalan Sea and ESNA. In the early winter, the nitrate concentration is relatively high in surface due to the vertical convection applied to the mixed layer. This makes the values of nitrate at the beginning of the year around 1.5 mmol m^{-3} and 0.5 mmol m^{-3} in the CS and ESNA respectively. Upward flow of nitrate causes phytoplankton blooms to take place just near the surface at late winter, as described below. The blooming phytoplankton rapidly depletes nitrate in the surface layer that stays this way for the remaining of the year. Only in late autumn, a weak upwelling of nitrate from intermediate waters is observed going up to the subsurface as a consequence of the thickening of the mixed layer after summer stratification is over. Since nitrate concentration in the bottom boundary was twice as much in the CS than in ESNA, higher nitrate gradients below the thermocline were found there in the former case than in the latter (0.03 mmol m^{-3} and 0.02 mmol m^{-3}, respectively).

The thickness of nutrient-depleted surface water layer is higher in the ESNA site than in the CS. This is explained by phytoplankton activity covering a wider layer of water in the former case. In the CS, the 1.0 mmol m^{-3} nitrate isoline was

found around 80 m depth almost all year round except in early winter and late autumn, while in ESNA, it was found between 130-170 m depth over the whole year.

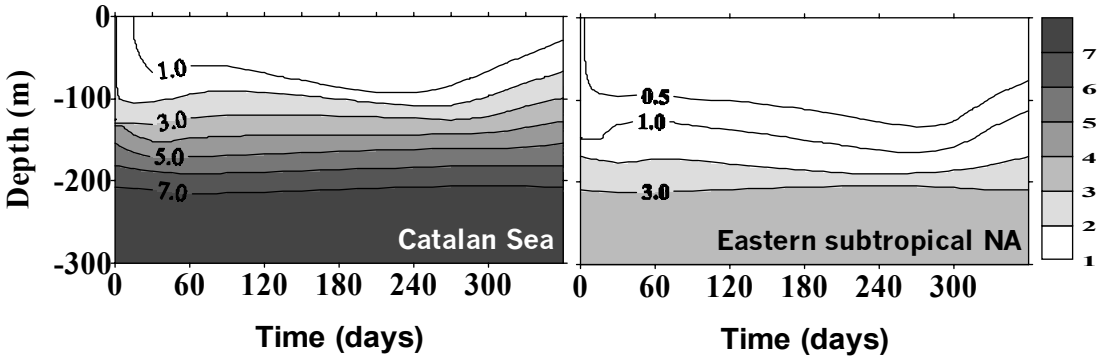

Figure 5.6. Simulated time series of nitrate in the selected oligotrophic environments (units in mmol m^{-3}).

The values of nitrate associated with the water layers below the thermocline were those corresponding to the isolines 1.0 mmol m^{-3} and 0.5 mmol m^{-3} in the CS and the ESNA simulations, respectively. The deeper the thermocline, the thicker the nitrate-depleted water layer. At ~210 m depth nitrate concentrations of 7.0 mmol m^{-3} and 3.0 mmol m^{-3} in the CS and ESNA respectively stay relatively homogeneous along the entire year. Since the phytoplankton did not show activity at this depth, it seems reasonable to consider this bottom boundary as a relatively constant fuelling of nitrate toward the upper layers. The comparison of the seasonal means of simulated nitrate with data observed in the field, show a high similarity for the CS (Figure 5.7). As occurred with temperature and salinity, the model appears to overestimate nitrate below 100 m depth except during autumn where a good match was found between model and field results.

In order to facilitate comparisons, hereafter we will refer to N-phytoplankton chlorophyll as chlorophyll *a* since phytoplankton to chlorophyll ratio was assumed to be 1 mg Chl (mmol N^{-3}). In the ESNA site, chlorophyll *a* was found about 40 m deeper than in the CS sites, looking for the nutrients that were scarcer in the upper layers. This was possible due to the high surface irradiance making the euphotic zone wider and allowing active phytoplankton to sink (Figure 5.8).

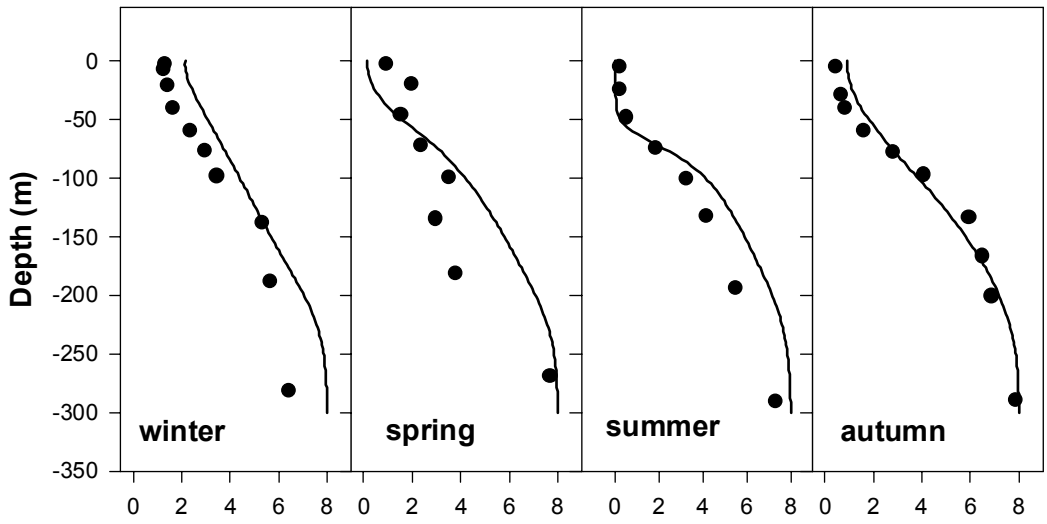

Figure 5.7. Comparison of seasonal mean values of modelled nitrate (dots) with field observations (lines) in the Catalan Sea (units in mmol m^{-3}).

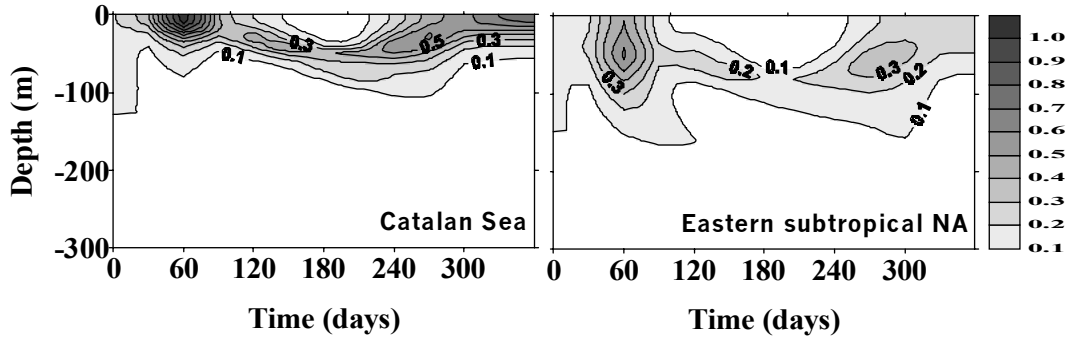

Figure 5.8. Simulated time series of phytoplankton chlorophyll in the selected oligotrophic environments (units in mmol m^{-3}).

The relatively low amount of nitrate available in the water column in the ESNA site in comparison with that in the CS, was considered as a limiting factor for the phytoplankton growth. In fact, in the former site chlorophyll *a* concentration was around half of that in ESNA. In late winter, a phytoplankton bloom appeared with a maximum around 0.6 mmol m^{-3} close to the surface in the Catalan Sea and 1.1 mmol m^{-3} at about 40 m depth in ESNA. These values contrasted with minimum found in summertime to be lower that 0.05 mmol m^{-3}. In both stations, surface chlorophyll increased in late summer and autumn forced by the weakening in daily irradiance and increasing in mixed layer depth that favoured at the same time, the increase of nitrate

concentrations in the upper layers. This second phytoplankton bloom never reached the maximum values observed in the late-winter/spring bloom. In the CS site, the maximum (1.1. mmol m^{-3}) was in the range of historical observations (Cruzado and Kelley, 1974; Estrada et al., 1999). In the ESNA site, chlorophyll *a* maximum (0.6 mmol m^{-3}) was half the maximum modelled by Doney et al. (1996) in the Sargasso Sea, in general agreement with observations from JGOFS Bermuda Atlantic Time-Series Site. Along the year, a persistent layer of water with chlorophyll concentration higher than 0.1 mmol m^{-3} was observed in both environments. In general, this layer was thicker and deeper in ESNA than in the Catalan Sea. The upper limit of the chlorophyll layer was found at surface during winter and early spring in the CS and solely in winter in ESNA. Then, the upper limit of this chlorophyll layer dropped down to a maximum of 50 and 75 m at the beginning of summer in the CS and ESNA cases, respectively. At the early spring, 0.1 mmol m^{-3} chlorophyll phytoplankton reaches the surface in both case studies. The lower limit of this chlorophyll layer was variable, having an average of 75 ± 25 m depth in the Catalan Sea, and 115 ± 40 m in ESNA.

Validation of simulated chlorophyll *a* in the Catalan Sea against field data is shown in Figure 5.9. At depths greater than ~60 m, the model underestimated by about 0.1 mmol m^{-3} the concentration of chlorophyll *a* during winter, spring and summer times. Such underestimate was in general, coincident with the overestimate observed in nitrate during these seasons. This suggests that the phytoplankton growing below 60 m depth in the model could be light-limited rather than by nitrate. In the CS simulation, the summer DCM was around 60 m depth, while the field data suggested an average maximum located at 75 m depth (Figure 5.9). Moreover in the model, N-phytoplankton rapidly diminished below the DCM, reaching the lowest value at about 100 m depth. On the contrary, the field data suggest a high phytoplankton activity below DCM that decreased linearly until about 140 m depth. DCM was found within the depth range given by other authors. Pedrós-Alió et al. (1999) and Estrada (1985) observed DCM in the NW Mediterranean at 40 – 80 m depth. DCM appeared associated more to the nitracline rather than the thermocline, as has been found in coastal zones (Holligan et al., 1984; Velasquez, 1997).

Irradiance in the DCM was about 0.5% that in surface in agreement with previous work carried out in the same area (Estrada, 1985; Morel et al., 1993; Varela et al., 1994).

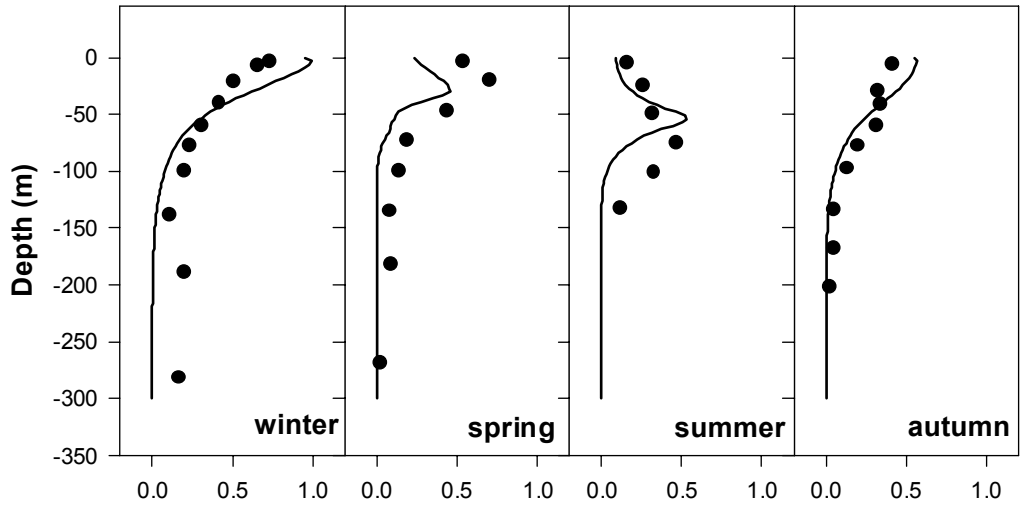

Figure 5.9. Comparison of seasonal mean values of simulated chlorophyll *a* (lines) with field data (dots) in the Catalan Sea case study (units in mmol m^{-3}).

Validation of nitrate and chlorophyll *a* during summer in ESNA is shown in Figure 5.10. A layer of nitrate-depleted surface waters appears reaching a bottom boundary of 90 m depth in the model, while in the field data it was 30 m deeper. The difference of the nitrate concentration between the model and field data over this 30 m layer, was less than 1 mmol m^{-3}, being higher in the model. This overestimating just coincides with underestimating of the chlorophyll *a* concentration at the same depth (Figure 5.10). As occurred in the CS, chlorophyll *a* observations beneath DCM where higher than the estimates given by the model, thus suggesting the phytoplankton growing in the model could be light limited rather than nitrate limited. The summer DCM in the Sargasso Sea, located at the same latitude, has been found by other authors around 120 m depth (Bricaud et al., 1992). Here, DCM was at nearly the same depth as deduced from field data, but the model spread such a maximum between 90 - 110 m depths. From both, the field data and the model results the DCM was found closer to the nitracline, being located at about 50 m and 90 m in the CS and ESNA, respectively.

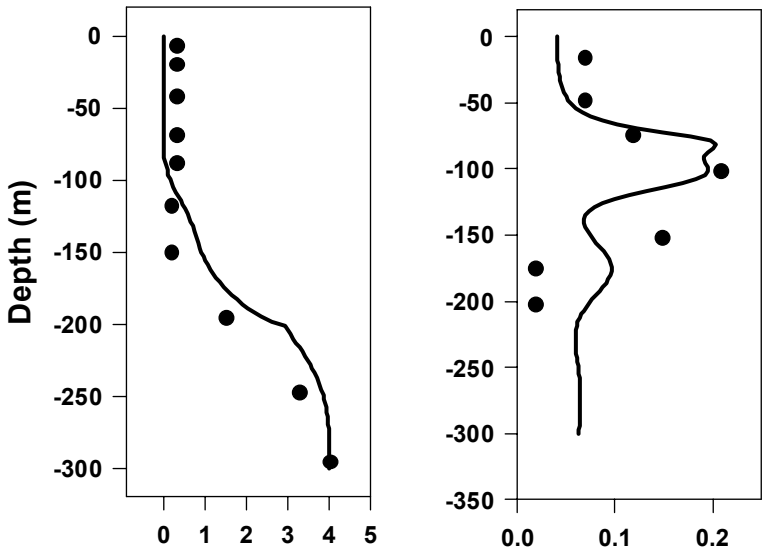

Figure 5.10. Comparison of mean values of simulated nitrate (left) and chlorophyll *a* (right) modelled with field observations during summer, in the eastern subtropical NA (units in mmol m^{-3}). Lines represent the model simulations and dots are the field observations.

N-Nitrite

As occurred with nitrate, nitrite was found highly depleted at the surface. A high rate of phytoplankton consumption of nitrate after the late winter bloom contributed to force such depletion (Figure 5.11). The nitrite maximum with concentrations higher that 0.1 mmol m^{-3} was generally found beneath the chlorophyll *a* layer. The average depth of such a maximum was 90 m and 140 m in the CS and ESNA, respectively. The maxima were observed in late summer (0.61 mmol m^{-3} and 0.4 mmol m^{-3}, respectively) after the weakening of the subsurface chlorophyll maximum and before it began raising upward in autumn. This nitrite maximum had a lag with regard to the formation of the DCM between 60 and 90 days in the CS and ESNA.

In the CS, simulated nitrite was validated with seasonal averages of field observations (Figure 5.12). A discrepancy was found during winter when nitrite was underestimated by about 0.1 mmol m^{-3} in the upper 50 meters. On the contrary, during summer, the average maximum was overestimated by about 0.1 mmol m^{-3}.

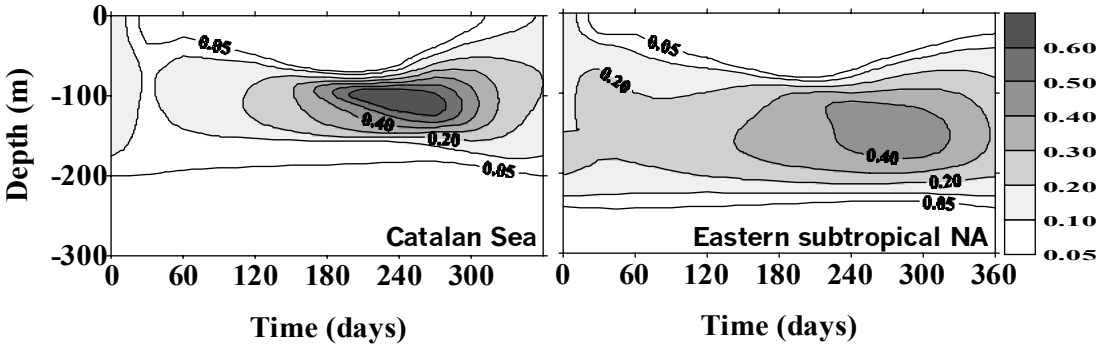

Figure 5.11. Simulated time series of nitrite in the selected oligotrophic environments (units in mmol m^{-3}).

The field data suggest that nitrite is accumulated in small amounts between 150 m and the bottom almost all year round, except in winter. Bacterial oxidation of organic matter not being considered in our model could explain this event. The uptake of nitrite was assumed to take place in the light hours in the euphotic layer while the

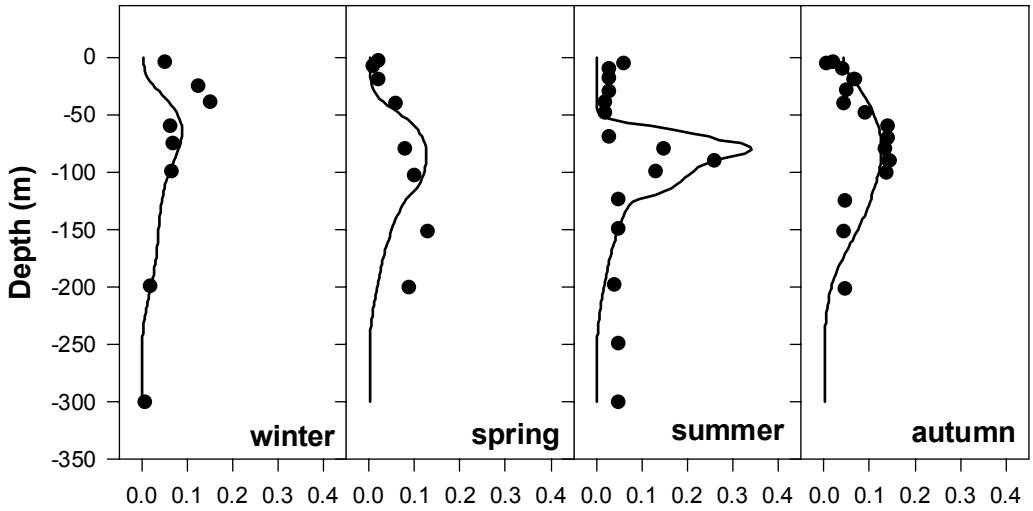

Figure 5.12. Comparison of seasonal mean values of simulated nitrite (lines) with field observations (dots) in the Catalan Sea case study.

nitrite exudation was assumed to take place at low radiation during the day and in the darkness at night. This made the layer beneath the chlorophyll maximum a good place for the nitrite exudation favoured by the phytoplankton self-shading in the DCM. In general, the model underestimated nitrite in the lower layers but this was consistent with the limited phytoplankton activity assumed at such depths.

Unfortunately, in the ESNA case, no validation was carried out for the simulated data since field observations were not available to be compared.

Current models rarely simulate the role of nitrite in the primary production. Vaccaro and Ryther (1960) early described the first nitrite maximum above 200 m depth in oligotrophic areas including the Mediterranean Sea. This nitrite was considered the result of both bacterial ammonium oxidation and nitrate reduction by phytoplankton at low light levels (Carlucci et al., 1970; Raimbault, 1986). Nevertheless, in our model we assumed the role of bacterial nitrification in the upper layer as numerically negligible (Eppley and Peterson, 1979). In such a way we found that the highest concentrations of nitrite were located below the DCM in close agreement with the field data and other related works reported for the Mediterranean Sea (Vaccaro and Ryther, 1960; Blasco, 1971).

N-zooplankton

Gains and losses of zooplankton were parameterised by equations that forced a less variable standing stock in time with respect to the phytoplankton standing stock (Figure 5.13). In general, a layer of maximum zooplankton density was observed following the phytoplankton maximum. This made that zooplankton showed two maxima, as for phytoplankton, localised close to the surface. One of the maxima occurred a month after the late winter phytoplankton bloom. The other maximum appeared during late autumn when phytoplankton was again increasing at the surface forced by a decrease in both the mixed layer and PAR. A considerable reduction of the zooplankton biomass in the surface and an increase in the bottom were features that appeared after the water column was homogenised in winter. In fact, the zooplankton concentration in the CS was highly depleted in January a feature that did not occur in ESNA. Nevertheless, in the former case, a layer with zooplankton biomass above 0.05 mmol m^{-3} was continuously kept around the year. Zooplankton was in agreement with the data reported for the same area by Alcaraz (1988) who estimated the N-zooplankton in summer time at about 0.06 - 0.08 mmol N m^{-3}. In the ESNA site, such a layer was not continuous but broken in late summer due to the relatively low phytoplankton availability that limited the sustainability of the

zooplankton standing stock. At the beginning of autumn when phytoplankton increased its biomass over 0.3 mmol m^{-3}, zooplankton concentration recovered as well, reaching concentrations above 0.05 mmol m^{-3}.

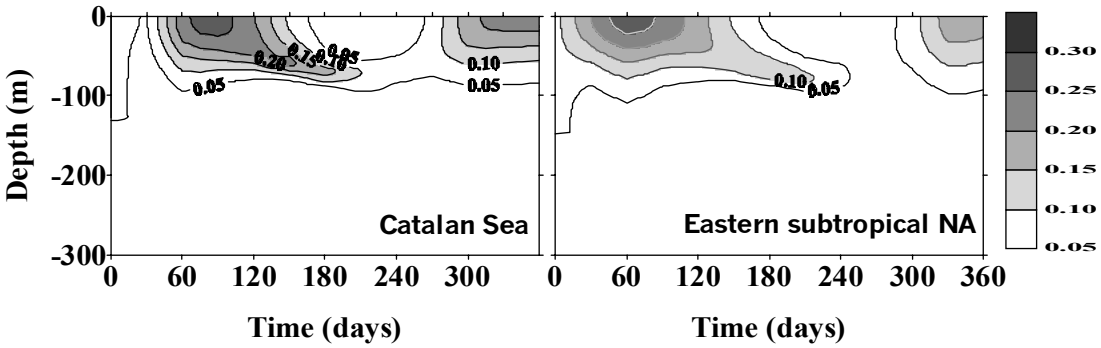

Figure 5.13. Simulated time series of simulated zooplankton in the selected oligotrophic environments (units in mmol m^{-3}).

The sensitivity test of the BLANES model allowed observing important changes in all the variables when the zooplankton maximum ingestion rate (I_{max}) was tested with values lower than the ones used in the model (1.2 d^{-1}). Zooplankton biomass exceeded a non-desirable zooplankton biomass (up to an order of magnitude) that produced a rapid reduction of the phytoplankton biomass. At the same time, this induced a high concentration of ammonia in the surface breaking the equilibrium in the nitrogen fluxes along the rest of compartments in the model. The best zooplankton mortality rate was 0.1 d^{-1}. With values lower than this the model became unstable while higher values forced a strong and unrealistic reduction of the zooplankton standing stock. Since a continuous layer of phytoplankton biomass was constantly found along the year in the CS simulation, the zooplankton grazing was understood as a factor not having a substantially limiting effect on the phytoplankton biomass unlike in the ESNA simulation. In both environments, the zooplankton grazing controlled the phytoplankton bloom in wintertime, but it made the phytoplankton biomass to be reduced up to ~0.5 mmol m^{-3} in the CS and ~0.2 mmol m^{-3} in the ESNA.

N-Ammonium

The ammonium distributions in the upper water layers in the CS and ESNA are shown in Figure 5.14. The Catalan Sea held the highest concentration of ammonium in summer at depths lower than the DCM, as the balance between the excretion by zooplankton and consumption by phytoplankton favoured the former process. In the NW Mediterranean, Estrada (1985) found an ammonium maximum reaching about 0.3 mmol m^{-3} around the DCM that is in the lower limit of our model results (0.3-0.4 mmol m^{-3}). Levy et al (1998) found a similar vertical distribution of the ammonium concentration modelled in the Ligurian Sea (NW Mediterranean). In our case, ammonium appeared depleted in surface waters during summer in both environments being nevertheless, longer in time in the ESNA since it persisted until mid-autumn. The zooplankton, source of ammonium, did not differ strongly between the simulated environments mainly due to the parameters used in both cases assumed to be equal. This made that in the ESNA station that zooplankton biomass could not be sustainable in late summer and the ammonium concentration was higher but more homogeneous in time.

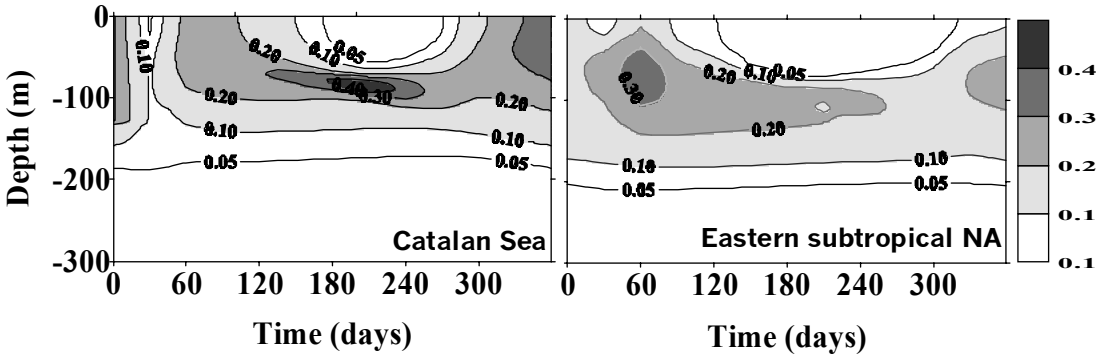

Figure 5.14. Simulated time series of ammonium in the selected oligotrophic environments (units in mmol m^{-3}).

Limitations of the current phytoplankton model scheme

It is known that the phytoplankton community rapidly changes its populations with time according to external changes of nutrients. This is that in an ecological niche of the dominant populations in one season is assumed to disappear with new environmental conditions for the next season, rapidly being occupied by new

populations appearing and rapidly adapting to the environmental changes. This factor suggested to be taken into account when making parameterisation of the model phytoplankton community were kept constant in the BLANES model, since phytoplankton parameters had the same value. Relatively good results were obtained since its seasonal averaged standing stock appeared in general, well represented. However, the population differentiation of the phytoplankton (and zooplankton) have been considered an important factor when an accurate balance of the primary production is desirable (Jochem and Zeitzschel, 1993; Morel et al., 1993; Armstrong, 1999).

The complexity of the phytoplankton populations has been widely studied in oligotrophic ecosystems. In the North Atlantic, the genus *Synechococcus* (0.7-1.2μm) and *Prochlorococcus* (0.6-0.8μm) have been suggested to be the most important contributors to the photosynthetic biomass during summer stratification (Li and Wood, 1988; Li et al., 1992; Olson et al., 1990). During wintertime, the role of the nutrient enrichment by vertical mixing appears to be more associated with the increase of the phytoplankton biomass (standing stock) rather than with increasing growth rates. Such a situation has been observed when phytoplankton growth is not severely limited by nutrient as suggested by the phytoplankton-zooplankton model by Goericke and Welschmeyer (1998). In the Sargasso Sea, phytoplankton forming the DCM has been observed to be well adapted to the local PAR conditions. There, as observed in the former case studied, phytoplankton increases the chlorophyll concentration instead of increasing the growth rate (Morel et al., 1993). In the same location, chlorophyll *a* in cyanobacteria and divinyl-chlorophyll *a* in prochlorophytes have been found to increase about five-fold while decreasing irradiance in depth (Morel et al., 1993). The carbon/Chl *a* ratio appears to be decreasing with increase in depth up to an order of magnitude (Goericke, 1998: Goericke and Welschmeyer, 1998). In the North Atlantic, prochlorophytes, cyanobacteria and flagellates have been found to be occupying specific places in the water column. In the subtropical North Atlantic, such groups represent between 27% and 43% of total chlorophyll biomass and dominate during spring and summer (Claustre and Marty, 1995). Their distribution in the water column, is stable prevailing cyanobacteria at surface,

prochlorophytes at intermediate waters and flagellates below the euphotic zone. Prochlorophytes and cyanobacteria are considered regulated by light (Urbach and Chisholm, 1998; Claustre and Marty, 1995) whereas flagellates living close to the nitracline are linked to nutrient availability and are responsible for new production. Growth rates vary as a function of depth from average values of 0.3 day^{-1} in the surface layer to <0.1 day^{-1} at 1.6 % light level. Diatoms are found in oligotrophic oceans at all times of the year but they rarely become the major component of the phytoplankton assemblage except during spring blooms and other brief periods of high productivity (Hulburt, 1990). Diatoms can contribute significantly to new production in the Sargasso Sea (Goldman, 1993) and could be responsible for 15-25% of the average annual productivity (Nelson and Brzezinski, 1997). Despite this complexity in the phytoplankton response to changes of the environment, we deduced from validation of the BLANES model that in general, the phytoplankton functioning can be studied as a whole community whose details can be summarised and reasonably represented in time and depth under the given controlled environment.

5.4 Primary production and nitrogen fluxes

Estimates of annual primary production by the BLANES model were compared with other estimates in the studied areas (Table 5.2), most of them derived from satellite viewing that give a general approaching of chlorophyll production in the surface ocean (Figure 5.15). The estimated annual primary production in the CS was 134.5 g C m^{-2}. Estimates of primary production derived from satellite information in the western Mediterranean range between approximately 150 g C m^{-2} $year^{-1}$ and 220 g C m^{-2} $year^{-1}$. Based on CZCS imagery, Morel and André (1991) calculated 94 g C m^{-2} $year^{-1}$ in the western Mediterranean, but further revision of such study gave higher values of 157.7 g C m^{-2} $year^{-1}$ (Antoine et al., 1995). From a photosynthesis-irradiance relationship model, taking into account a large set of chlorophyll and irradiance profiles and satellite images Sathyendranath et al. (1995), estimated for the

whole Mediterranean Sea a primary production of 218 g C m^{-2} $year^{-1}$. Platt et al. (1991) gave an average value of 180 g C m^{-2} $year^{-1}$ from their classification of marine areas by latitude, a value close to the estimation made by Tusseau et al. (1997) with a numerical model of the pelagic domain for the Ligurian Sea. Longhurst et al. (1995) estimated a primary production of 216 g C m^{-2} $year^{-1}$ using satellite information. Localised measurements of primary production have been made among other authors, by Lohrenz et al. (1988) who gave a value of 0.88 g C m^{-2} d^{-1} from ^{14}C in May, just on density fronts in the western Mediterranean. Estrada (1985) using the same approach estimated a range of values from 0.27 g C m^{-2} d^{-1} in the open Catalan Sea to 0.12 g C m^{-2} d^{-1} in coastal areas.

Table 5.2. Estimates of primary production (PP, g C m^{-2} $year^{-1}$) and *f*-ratios in the selected oligotrophic areas and comparison with other estimates from literature.

	Catalan Sea		Eastern Subtropical NA	
	PP	*f*-ratio	PP	*f*-ratio
NO_3-based estimates	51.7	0.38	16.5	0.26
(NO_3+NO_2)-based estimates	66.8	0.49	24.7	0.40
NH_4-based estimates	67.7	-	37.7	-
Total PP (based on NO_3+NO_2+NH_4)	134.5	-	62.4	-
Range of PP given by other authors	94-218¶	-	72-174¶¶	-

¶ Estrada (1985); Morel and Andre (1991); Tusseau et al (1997)

¶¶ Platt et al. (1991); Sathyendranath et al. (1995); Longhurst et al (1995)

The total estimate of primary production by the BLANES model in the ESNA site was 62.4 g C m^{-2} $year^{-1}$. This value lays in the low side of the estimates given by other authors for similar areas in the eastern basin of the Subtropical North Atlantic (Table 5.2). Platt and Harrison (1985) estimated an annual average primary production of 82 ± 22 g C m^{-2} $year^{-1}$ with a new production estimate (25±7 g C m^{-2} $year^{-1}$) similar to our estimate based on both nitrate and nitrite (24.7 g C m^{-2} $year^{-1}$).

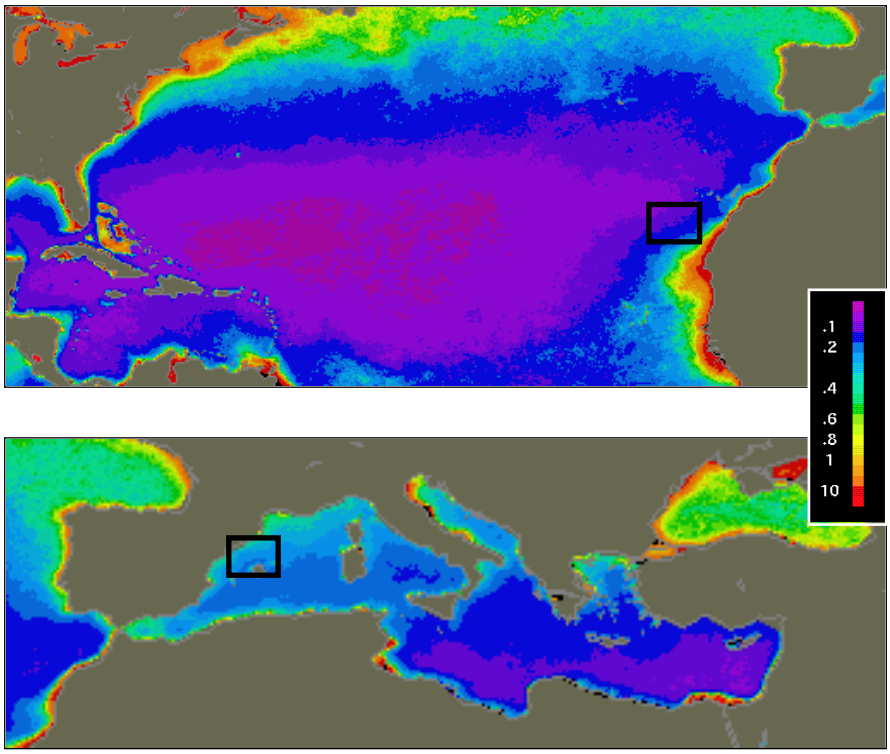

Figure 5.15. General view of marine environments with stations used to calibrate the BLANES model. Pictures are the composite results of all Nimbus-7 Coastal Zone Color Scanner chlorophyll *a* (mg m^{-3}) data acquired between November 1978 and June 1986. Approximate stations location are indicated in black squares in the subtropical North Atlantic (up) and Mediterranean Sea (down (Provided by NASA/GSFC).

The underestimating of the annual production deduced from the model, may be attributed to low regenerated production that in the model represents 60% of the whole production (*f*-ratio = 0.4, see discussion below). Comparison of our model results with field estimates for this site faced the same difficulty as for the CS site. The latitudinal variation of the productivity has been widely studied and recently corroborated along the north Atlantic by Marañon et al. (2000). The selected area, the eastern boundary of the subtropical North Atlantic gyre, corresponds to a specific biogeochemical province as described by Sathyendranath et al. (1995) (see discussion in Chapter 4). One of the features in this province is its primary production around 122-124 g C m^{-2} $year^{-1}$ (Longhurst et al., 1995). Field measurements of primary production in this area in May and October (Marañon et

al., 2000) yielded values in the range 0.1 - 0.3 g C m^{-2} d^{-1} within the daily average obtained in our simulations (0.18 g C m^{-2}).

The nitrate entering the model domain from the lower boundary and the nitrite produced by phytoplankton are assumed to fuel *new production*. The sum of both values made the model to overestimates new production when compared to other estimates for oligotrophic ecosystems. In this study, however, the *new production* based on nitrate only was in good agreement with other estimates, as described below. In the Catalan Sea, the nitrate-based *new production* accounted for 39% of the whole production (134.5 g C m^{-2} $year^{-1}$), very similar to the estimates (35%) given for the Ligurian Sea by similar models (Tusseau et al., 1997), though this area showed higher values of production. In the ESNA case, nitrate-based *new production* contributed to 26% of the whole production (61.9 g C m^{-2} $year^{-1}$). The new production here estimated (16 g C m^{-2} $year^{-1}$) is rather similar to that expected for North Atlantic (around 12 – 24 g C m^{-2} $year^{-1}$) but the expected fraction of new production is just the double, (Campbell and Aarup, 1992); Williams and Follows, 1998). This address us to suggest that the model simulation of the upward nitrogen flux is functional for both simulated areas of the open ocean, but the total primary production is here underestimated.

The vertically integrated annual nitrate + nitrite based *new production* versus total production (*f*-ratio) was 0.49 in the CS and 0.40 in ESNA (see Table 5.2). In both cases, the typical *f*-ratio expected to occur in oligotrophic ecosystems (~0.2), was observed only during summer (0.25 and 0.21, respectively). This value increased up to 0.88 in winter in the CS while in ESNA it reached 0.82. In the Sargasso Sea, Platt and Harrison (1985), using field measurements, estimated a value between 0.9 in winter and 0.1 in late spring. Tusseau et al. (1997) estimated in the NW Mediterranean by numerical simulations a value similar to that given for the Sargasso Sea. The role of nitrite in estimating the new primary production was found significant since it represented 22% and 35% of the *new production* in the CS and ESNA sites, respectively. The vertical distribution of the *f*-ratio in our simulations is shown in Figure 5.16. Maximum recycling occurred just in and above the continuous

deep chlorophyll maximum layer, where nitrate and nitrite concentrations were very low. Below this layer, where the nitrite production and nitrate consumption were relatively high with respect to the rest of the water column, a low production was observed corresponding to *new production* (*f*-ratio of 0.75 - 0.85 in both stations). In other studies the *f*-ratio studied has been assumed to be dependent on the size structure of the phytoplankton community (Tremblay et al., 1997). The *f*-ratios observed in our simulations, however, were consistent with estimates given by Platt and Harrison (1985) for oligotrophic nitrogen-limited systems.

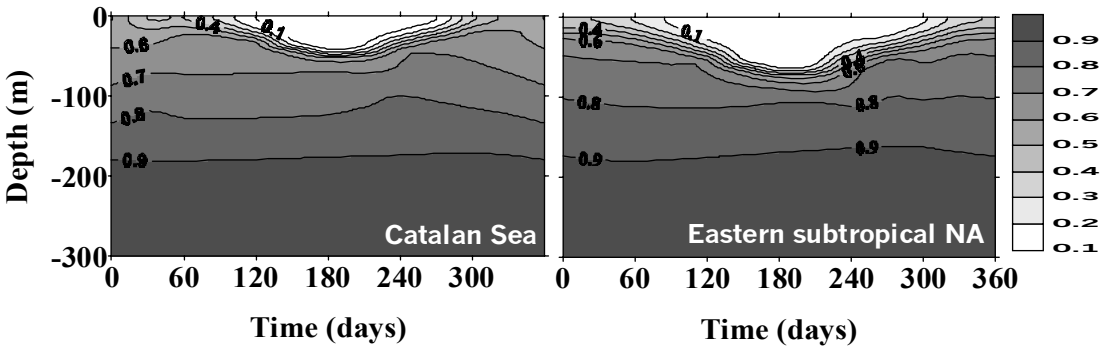

Figure 5.16. Time evolution of *f*-ratio in the vertical dimension. *f*-ratio was assumed as the ratio between the phytoplankton uptake of nitrate plus the nitrite uptake (new production) with respect to the whole nutrients uptake (total production) in the ecosystem.

At the range of 290 - 300 m depths, the diffusive-advective transfer of nitrogen into the model domain was 0.38 mmol N m^{-2} d^{-1} and 0.19 mmol N m^{-2} d^{-1} in the CS and ESNA, respectively. Just twice as great a transfer rate was found in the former with respect of the latter, a combination of similar background diffusivity and vertical advection existing at such depth but with a concentration of nitrate in the CS twice as high as that in the ESNA. The nitrogen transfer increases upwards with the increase of the vertical nitrate gradient. Following this trend, at 190-200 m depths, the nitrogen gained by the system, higher than that transferred at the bottom boundary, was similar in both cases (0.44 and 0.32 mmol N m^{-2} d^{-1} in the CS and ESNA, respectively). At 190 - 200 m depth ranges, the diffusive flux of nitrate was higher in ESNA (0.20 mmol m^{-2} d^{-1}) than in the CS (0.14 mmol m^{-2} d^{-1}) due to a higher gradient induced by phytoplankton activity at greater depths. Below the euphotic layers (~120-130 and ~150-150 m in the CS and ESNA cases, respectively),

the total flux of nitrogen increased up to 1.78 and 0.61 mmol m^{-2} d^{-1} (equivalent to 0.64 and 0.22 mol N m^{-2} $year^{-1}$), respectively. The advective fluxes in both cases decreased upward with the nitrate concentration. A summary of the nitrogen fluxes below the mixed layer depth is shown in Table 5.3.

Table 5.3. Estimates of nitrogen fluxes at several depths below the euphotic layer. Simulated areas are Catalan Sea (CS) and eastern subtropical North Atlantic (ESNA).

Area	Depth (m)	Advective fluxes (μmol m^{-2} d^{-1})	Diffusive fluxes (μmol m^{-2} d^{-1})	Total fluxes (μmol m^{-2} d^{-1})	(mol m^{-2} y^{-1})
CS	120 - 130	144	1632	1776	0.64
	190 - 200	298	140	438	0.16
	290 - 300	380	5	385	0.14
ESNA	150 - 160	24	582	606	0.22
	190 - 200	120	197	317	0.11
	290 - 300	187	5	192	0.07

The nitrate entering below the euphotic layer in the CS (0.64 mol N m^{-2} $year^{-1}$) matched quite well the estimated exported production of 0.7 mol N m^{-2} $year^{-1}$ from the upper layer in the Ligurian Sea (Tusseau et al., 1997). Levy et al. (1998) calculated a vertical flux of nitrogen at 100 m depth in the Ligurian Sea of 0.26 mol N m^{-2} $year^{-1}$. This value reflects a relatively low activity of phytoplankton at such specific depth forced by a lower nitrate gradient if compared with that estimated in the Catalan Sea. The flux at 100 m depth in the Ligurian Sea is comparable with that found in the Catalan Sea in the range of 170 -180 m depth.

The simulated nitrogen flux in ESNA is within the range given for the western basin of the subtropical NA gyre. Doney et al. (1996), at a station close to Bermuda, gave an annual estimate of upward nutrient flux across the 300 m depth surface of 0.06 mol N m^{-2} closely matching our estimates at the same depth in the ESNA site (0.07 mol N m^{-2} $year^{-1}$). The nitrogen flux estimated by Gruber and Sarmiento (1997) in the Sargasso Sea (0.072 mol N m^{-2} $year^{-1}$) was also coincident whit our estimate suggesting similarities in the amount of nitrogen required to sustain the low but continuous primary production. The nitrate flux estimated by the BLANES model at

the base of the euphotic layer (0.606 mmol m^{-2} d^{-1}) was somewhat lower than the value given by Lewis et al. (1986) for the same area (0.807 mmol m^{-2} d^{-1}). Nevertheless, our estimate differs from field measurements by Jenkins (1988) who computed a flux of 0.6±0.2 mol N m^{-2} $year^{-1}$ (our estimate was 0.22 mol N m^{-2} $year^{-1}$) by using ^{3}He as a diffusion tracer along the thermocline. McGillicudy and Robinson (1997), using a coupled physical-biological model, estimated the upward flux of nitrogen in the Sargasso Sea in 0.5 mol N m^{-2} $year^{-1}$. This estimate is close to that estimated by Fasham et al. (1990) using numerical simulation of the planktonic domain in the Sargasso Sea (0.56 ± 0.16 mol N m^{-2} $year^{-1}$). Later, a simplified version of the Fasham et al's model with a reduced number of parameters, resulted in lower estimates of the nitrogen flux of 0.2 mol N m^{-2} $year^{-1}$ (Hurtt and Armstrong, 1996) matching our model results. The model results are also close to those given by Bahamon et al. (2002) (0.19 mol N m^{-2} $year^{-1}$) in the whole subtropical north Atlantic for summer. We consider crucial the horizon at wich nitrogen flux is computed. From the BLANES model simulations it is deduced that nitracline is about 90 m below thermocline. We estimated fluxes below the euphotic layer, that are below nitracline where the nitrate gradient exceeds those in thermocline but diffusion is much lower than in the upper layer what results in a reduction of the nitrogen flux.

The material exported downward from the euphotic zone in both simulated stations was compensated with the upward nitrate flow. The averaged daily budget of the planktonic activity, i.e. the nitrogen fluxes among the various compartments of the model integrated over the year and averaged daily, was also calculated and shown in Figure 5.17. Total nitrogen taken up by phytoplankton in the CS case was about twice that in the ESNA case (4.67 mmol N m^{-2} d^{-1} and 2.15 mmol N m^{-2} d^{-1}, respectively), thus explaining the higher biomass found in the former. About 83% of phytoplankton were ingested by zooplankton in both cases, similar to the estimated by Tusseau et al. (1997) in the simulation of the Ligurian Sea. The role of zooplankton in exporting material was a little higher in ESNA than in the CS (77% and 62% of the phytoplankton ingested, respectively). In both sites, the rate of production of both ammonium by zooplankton and nitrite by phytoplankton were only slightly higher than the rate of uptake by phytoplankton.

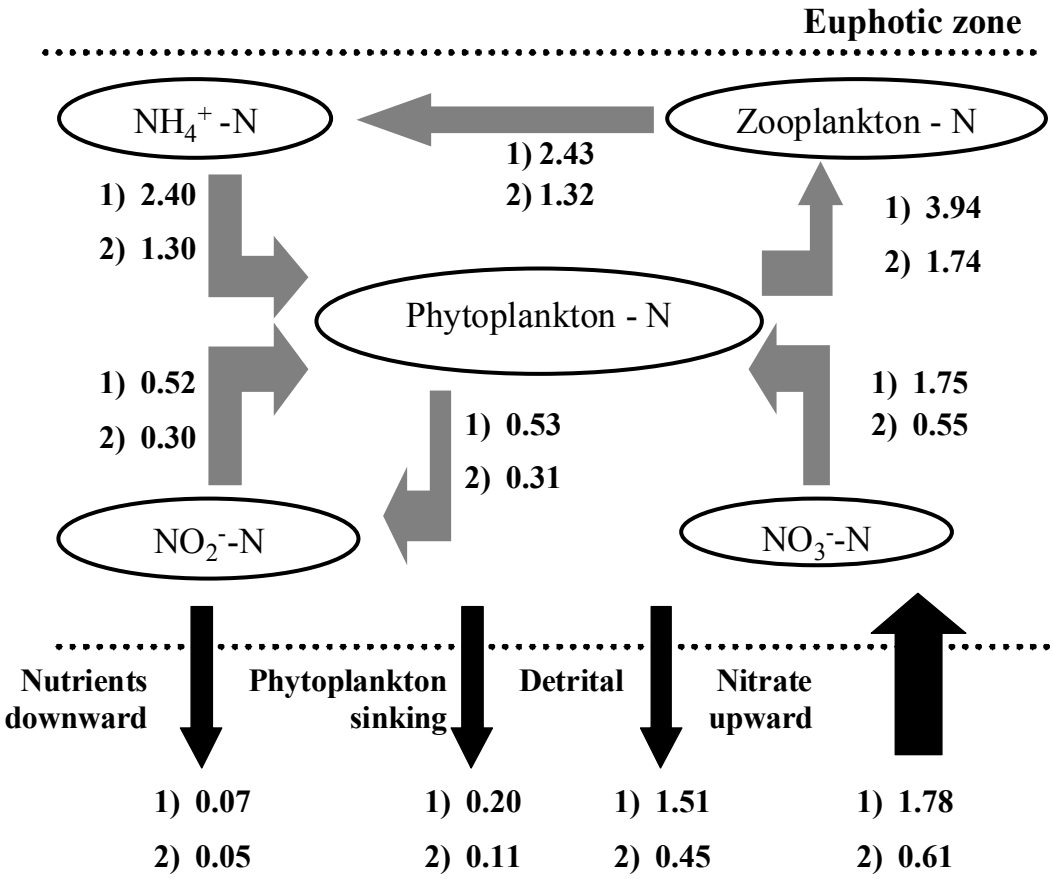

Figure 5.17. Assessments of mean flux of nitrogen (mol N m^{-2} d^{-1}) among the state variables in the euphotic zone of the Catalan Sea (1) and the eastern subtropical NA (2).

Simulated pelagic domains showed annual nitrogen stocks in the euphotic layer of the water column as shown in Figure 5.18. It is deduced that the phytoplankton biomass is mainly controlled by the amount of nitrogen in the waters below the euphotic zone. In subtropical NA, with about a half of nitrogen below the euphotic zone than that in NW Mediterranean, the phytoplankton stock is smaller as well but not at the same proportion, but higher. An explanation for this is given by a higher displacement of the ammonium and nitrite stocks to the phytoplankton stock in subtropical NA. This left out the role of zooplankton stock in this unbalance since the zooplankton grazing biomass was proportional to the nitrate in the bottom. An interesting balance (2:1) between the summa of phytoplankton, ammonium and nitrite stocks (159 and 78 mmol N m^{-2} in the Catalan Sea and subtropical NA,

respectively) is found proportionally in agreement with nitrate at the bottom boundaries (8 and 4 mmol N, respectively). Nitrogen stocks were always higher in the CS than in ESNA: zooplankton and nitrite were about twice higher in the former place while phytoplankton, ammonium and nitrate were about 2/3 higher in the former. Nitrate represented 80% of the whole nitrogen stock in the CS and 70% in the ESNA, thus evidencing factors other than nitrate in limiting the uptake processes, such as light limitation and grazing pressure.

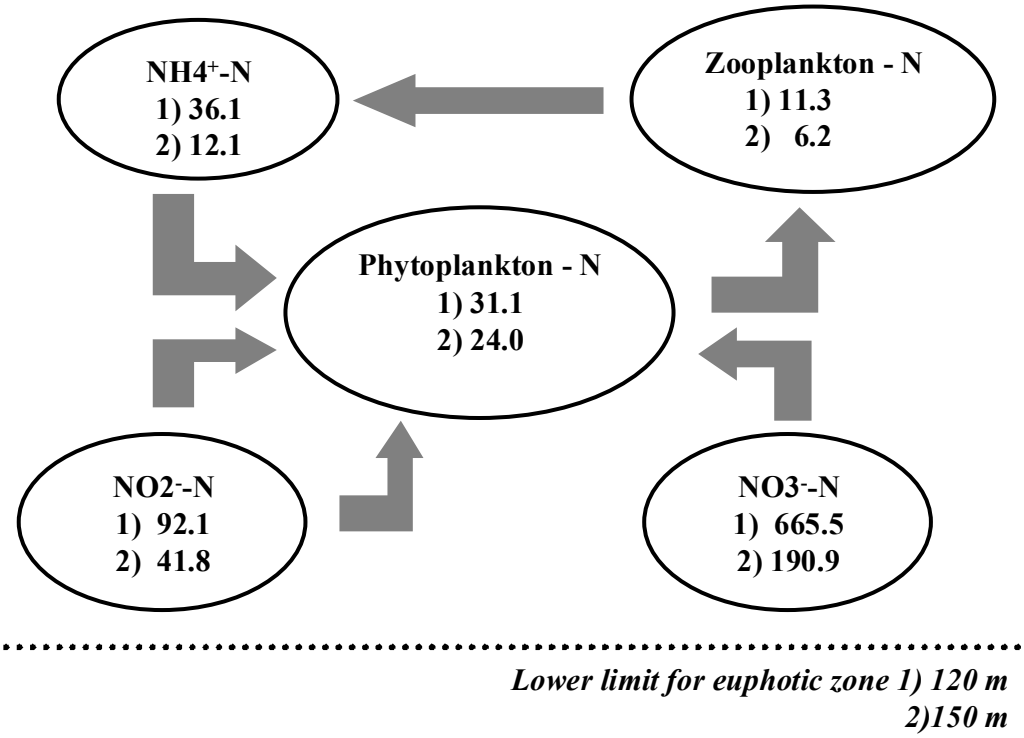

Figure 5.18. Annual means of the nitrogen stock (mmol N m^{-2}) in the euphotic zone of the Catalan Sea (1) and the eastern subtropical NA (2).

5.4 Remarks and discussion

The simulations of the plankton functioning at two oligotrophic marine environments with similar physical and biogeochemical properties and different latitudinal positions were in general, close to time and depth observations. The

variables better assessed in the model were chlorophyll *a*, nitrate and nitrite. Fuelling of the system by nitrate from the bottom boundary explained the relatively low but continuous primary production both in the Catalan Sea and in the eastern boundary of the subtropical North Atlantic. The latitudinal positions of the oceanographic sites studied, affected the surface radiation and length of the daylight what was decisive as limiting factor for the phytoplankton growing along the water column. In general, the amount of irradiance appears to mainly control the chlorophyll maximum depth while the amount of nitrate at the bottom boundary is mainly controlling the phytoplankton biomass. The phytoplankton maximum was deeper in subtropical NA than in western Mediterranean, especially during summertime when the higher irradiance and daylight length made the euphotic layer thicker. In both locations zooplankton grazing controlled the late winter phytoplankton bloom but reduced more than expected the subsurface phytoplankton concentration in summer.

The formation of the deep chlorophyll *a* maximum (DCM) (N-phytoplankton maximum) as typical for summer time in stratified oceans, was coincident with nutrient depletion of surface waters, with the thinnest mixed layer and with the highest daily surface irradiance and the highest daylight length. DCM was estimated to be at ~60 and ~90 m depth in the CS and ESNA, respectively more linked to nutricline depth variation than that of thermocline. The hypothesis that phytoplankton exudation in the dark explains the nitrite maximum was shown to be acceptable.

To simulate the late winter bloom, the homogenisation of the mixed layer at the beginning of the year (convection) was required supplying enough nutrients to the surface layers what produced a double effect on N-phytoplankton. At the beginning, homogenisation favoured a reduction of N-phytoplankton concentration in surface layers and, two months later, induced an N-phytoplankton bloom based on the new nutrients supplied to the surface waters from below. In consequence, the new/total primary production ratio was strongly affected by the water column mixing that favoured first the new production but later enhanced the recycled production.

Thickness of the mixed layer, nitrate gradients, intensity of irradiance and grazing pressure of zooplankton on phytoplankton were the main factors forcing the phytoplankton evolution. Higher phytoplankton production rates in winter were the result of fertilisation in the upper waters induced by a thick mixed layer reaching waters below the euphotic zone promoting the deeper nutrients to go up to the surface. Unlike what happened in the Catalan Sea, ESNA required winter convection forcing to increase enough the nutrients in surface thus allowing a proper simulation of the late-winter phytoplankton bloom. Higher surface irradiance at subtropical stations was expected to contribute to the increased production of phytoplankton biomass in nutrient-limited waters. Nevertheless, this was restricted particularly in winter and spring, by the reduced nitrogen concentrations reaching the surface as a result of a weak convection preventing the surface waters to be fertilised as occurred in the NW Mediterranean.

Estimates of turbulent diffusion from density explained the upward-downward nitrogen flux in the oligotrophic ecosystems. Upward advection of matter was compensated by losses due to sinking of phytoplankton and zooplankton death and excretions. The upward fluxes of nitrate below the euphotic zone were 0.64 and 0.22 mol N m^{-2} $year^{-1}$ in the Catalan Sea and ESNA stations respectively in agreement with previous estimates carried out by field measurements and other model simulations.

Since the plankton functioning in both ecosystems was modelled to have a yearly input of inorganic material from below the euphotic layer compensated with downward losses of material, both ecosystems in NW Mediterranean and eastern subtropical North Atlantic are assumed to be near the metabolic balance. This means that along the year, the systems neither export nor import carbon from adjacent environments. In Chapter 3, current conflicting conclusions about the trophic state of the open sea ecosystems were pointed out, also tackled by Nixon (1985) in coastal areas. While net heterotrophy, with microbial respiration exceeding photosynthesis is attributed to oligotrophic open-ocean ecosystems by some studies (del Giorgio and Cimbleris, 1997; Duarte and Agustí, 1998), a net metabolic balance is deduced from

other studies (Williams, 1998; Serret et al., 2001). The approximation given here agrees with the later assumption pointing out that oligotrophic systems are near the net metabolic balance, as deduced from the flux balance of matter below the euphotic zone. Under the current structure of the BLANES model, the matter balance was desirable not only for ecological, but for numerical purposes in order to avoid any inter-annual trend inducing the "collapse" (negative tend) or "saturation" (positive tend) of the plankton system. Inter-annual variability is nevertheless, possible to evaluate under strict comparison with time series field observations or data assimilation while the model runs.

The ecological applications of BLANES are widely diverse. Physical, biological and chemical components of BLANES are modular, allowing a relatively easy adaptability to specific environmental problems regarding plankton. Some potential applications to environmental problems with few modifications of the basic model are outlined:

Oxygen solubility. A next step toward the plankton functioning understanding is thought to be oriented toward estimating the plankton metabolism by means of the inclusion of dissolved oxygen as a state variable in the model. This also would allow setting the basis to other pathways of new production estimates based on the apparent oxygen utilisation and the oxygen utilisation rates. In Chapter 2, dissolved oxygen was shown to be closely linked to the biomass production (photosynthesis) and consumption (oxidation, respiration) allowing to give estimates of the carbon balance (autotrophy or heterotrophy) of the plankton communities. Oxygen solubility linked to phytoplankton production and microplankton consumption would also help to study mechanistic processes regarding the role of the mixed layer in storing the organic matter surplus during spring and early summer periods.

Phytoplankton blooms. Dissolved oxygen diminishing in open and coastal water are often linked to episodic phytoplankton biomass excesses, well known as phytoplankton blooms that generate high rates of organic matter respiration. This also affects negatively cultures of fishes, shrimps and bivalves, among others,

altering the tissues smelling. Low critical oxygen concentrations prevent an adequate metabolism of aerobic organism even could be dead. The simulation of phytoplankton blooms due to upwelling processes is closely linked to the advection scheme of BLANES. Moreover, the basic structure of BLANES also allows imposing other lateral nitrogen inputs at desirable depths. This could allow evaluating the role-played by other nitrogen sources besides the nutrient-rich deep waters in the phytoplankton blooming.

Optics and photosynthesis. It is known that downwelling (and upwelling) of solar spectral irradiance modifies the phytoplankton structure, which selectively adapts the physiology to particular irradiance conditions at specific depths. This is crucial to understand biogeochemical cycles in the upper ocean as a function of phytoplankton activity. This has strong feedback applicability on modelling photosynthesis for remote sensing of primary production. This would also allow, for instance, estimating potential effects of selective spectral irradiances (e.g. UV-A, UV-B) on primary production.

Other state variables in the plankton domain. The current BLANES version allows that various new state variables can be added. This will require new calibration and validation of the given parameters, with specific responses to the new forcing. Thus, bacteria, phytoplankton and zooplankton groups selected by sizes of taxa can be added. Limitations of processing time must be considered when new variables and parameters are added, since those could prevent a rapid visual checking throughout the window made for that purpose. Addition of other nutrients as state variables, like phosphorous, silicate and iron could contribute to understand the plankton functioning even at high latitudes with high nutrient and low chlorophyll systems.

Toward a long term, high quality, integrated data assimilation system. Data assimilation is a very recent research area in oceanography requiring strong support of ecosystem modelling. Data assimilation is called to provide robust assimilation methods for combined observations from a suite of instruments, such as surface and

subsurface floats equipped with sensors, fixed networks of data collections platforms and ship-borne experiments with satellite measurements. Adequate initialisation techniques of models concentrated in these issues would serve to develop strategic ocean models for predictions. Increase of space resolution particularly in coastal areas, and nesting of regional biogeochemical models (like BLANES) into more complex hydrodynamic models allowing to observe the ocean in all their complexity and variability, is an essential challenge of data assimilation systems. Complementing the statement pointed out at the beginning of this dissertation, acquired data are crucial not only to the scientific community, but also to operational agencies such as weather services and fisheries agencies, and to decision-makers throughout society. Actually, BLANES is intended to be part of MFSTEP, European project oriented toward exploring and improving tools for ocean and coastal model forecasting.

Chapter 6

Conclusions

6. CONCLUSIONS

The marine phytoplankton response to different external forcings with emphasis on vertical nitrogen fluxes at different latitudes was successfully assessed. Based on chlorophyll concentrations, estimates of phytoplankton production were obtained and evaluated with regard to expected new production derived from upward flowing nitrogen to the euphotic zone from deeper waters. In addition to field observations and historical data set analysis, a light and nutrient (nitrogen) dependent ecological model was proposed and calibrated against different oligotrophic environments in western Mediterranean and subtropical North Atlantic. Numerical simulations, even with intrinsic limitations due to parameterisation and simplifications of the complex plankton ecology, provided suitable answers to the questions raised regarding the functioning of plankton.

A transient metabolic imbalance (heterotrophy) in a narrow-shelf area of the NW Mediterranean Sea in late spring appears linked to organic and inorganic matter accumulation in the mixed layer. Plankton carbon consumption exceeding phytoplankton carbon production (heterotrophy) appears to be linked to a transient organic and inorganic matter excess probably accumulated in the mixed layer as a consequence of negligible downward sinking of the matter produced in late winter phytoplankton blooming. Net community production, decreasing with increasing daily-integrated irradiance, suggested a light-saturated phytoplankton community with irradiance favouring the community respiration over the phytoplankton production. Turbulent diffusion parameterisation into and below the mixed layer was successfully validated in a transitional period from homogeneous to thermally stratified water column.

Parameterisation of vertical turbulent diffusion from density is functional for modelling ecological processes in upper waters of the ocean. The Osborn turbulent diffusion model was successfully applied to estimate the yearly nitrogen transport up to and into the upper water layers. Low-density gradients in winter induced high diffusion homogenising all the variables in the water column, fertilising the upper

water layers. High-density gradients in summertime favoured low rates of diffusion around the nutrient impoverished thermocline, but diffusion slightly increased down to water layers below the euphotic zone with nutrient rich waters favouring the fuelling of new production. This gross scheme allowed estimating the yearly upward flow of new nitrate entering the euphotic zone, which was compensated with sinking of particulate material. The diffusion model is not applicable to areas of the ocean with horizontal fluxes of nutrients controlling new production as occurs off the Canary current.

Diffusion of nitrate at the nitracline depth located ~ 100 m below the seasonal thermocline drives summer new production in subtropical north Atlantic. It is commonly generalised that new production and chlorophyll maximum are controlled by diffusion across the maximum thermal gradient in the water column (thermocline). This assumption is thought to be restricted to certain areas of the ocean with thermocline nearly coincident with the maximum nitrate gradient (nitracline) in the upper water layers. Observations in the oligotrophic subtropical North Atlantic showed that during summer, the seasonal thermocline is located in nutrient-depleted water layers while chlorophyll maxima are located below and therefore can not control new production. It was found that the upward nitrate flux regulating new phytoplankton biomass is dependent on the density gradients and mainly on the nitrate gradients at the top of nitracline, the latter located around 100 m below the seasonal thermocline.

Nitrogen-limitation of phytoplankton biomass production is more evident in the subtropics than in the temperate ocean. Model simulations allowed assessing the phytoplankton biomass as a function of nutrients (nitrogen) and latitude. Nevertheless, the water-column integrated phytoplankton biomass was mainly controlled by the amount of nitrogen entering the euphotic zone. In subtropical NA, with about half of the nitrogen concentration at 300 m depth than in NW Mediterranean, the phytoplankton stock was also smaller, somewhat more than a half that found in the latter case. An explanation for this is given by the ammonium and nitrite stocks prevailing over the phytoplankton stock in subtropical NA that does not

take place in the NW Mediterranean. This is attributed to a higher ammonium excretion and nitrite exudation in the NW Mediterranean that cannot be compensated by the phytoplankton uptake rates.

Latitudinal variability of plankton scenarios implies a different yearly solar heating of the upper waters altering both phytoplankton photosynthesis and mixing processes in the water column, with the latter process dominating the control of the phytoplankton biomass. Different heating (induced by different irradiances) of surface waters at different latitudes altered both the phytoplankton response (primary production) to the light available and the water column structure (density). The new production to total primary production ratio was higher in winter and lower in summer in both temperate (NW Mediterranean) and subtropical latitudes (subtropical NA). Higher production rates in winter were the result of the upper waters fertilising induced by a thick mixed layer reaching waters below the euphotic zone and promoting the deeper nutrients to go up to the surface. Higher surface irradiance at subtropical station favouring a thicker winter mixed layer than at the temperate station, did not increase enough the phytoplankton biomass and production due to the relatively low nutrient concentrations in the deeper waters. This prevented that surface waters in the subtropical station were as much nutrient enriched as occurred in the temperate station with a thinner mixed layer but with higher nutrient concentrations at deep waters.

Light and nutrient availability explain the depth of chlorophyll maxima whose concentrations are regulated by grazers. Unlike thick winter mixed layer bringing up nutrients to the surface from deep waters, thin mixed layer during summertime reduces possibilities to fertilise the surface. In summer, nutrients are scarce in surface waters, particularly by the phytoplankton consuming during the late-winter bloom. Since the phytoplankton growth rates overpasses the zooplankton grazing rates during winter, the phytoplankton bloom is formed at the end of the season. However, grazing gains importance with time as zooplankton gains biomass whereas phytoplankton is nutrient-limited in the upper water layers, thus making the phytoplankton maxima was lower. In the subtropical station, higher light availability

in the water column made the phytoplankton biomass to be deeper searching for nutrients. The balance of light availability and nutrient concentration controlled the chlorophyll maximum depth, but the zooplankton grazing prevented this maximum to reach greater concentrations.

A common trend of phytoplankton in both subtropical and temperate zones formed two surface phytoplankton blooms along the year. Two phytoplankton maxima were observed to take place in the early spring and autumn. The former was the result of the thick mixed layer bringing up nutrients to the surface, as described above. The latter bloom was found to be accompanied by increasing of the mixed layer thickness after summer due to the cooling of surface waters promoting overturning of upper water layers and the decrease of light available at relatively great depths preventing the phytoplankton growth. This second phytoplankton maximum was favoured also by the reduction of the zooplankton grazing that in summer decreases its biomass as a consequence of the phytoplankton shortage. The lagged grazing pressure of zooplankton on phytoplankton allowed the formation of the second phytoplankton blooms.

The intra-annual variability of the phytoplankton primary production under the current BLANES structure excludes eventual yearly trends of production in upper water layers. The yearly carbon budget in the upper waters of the open ocean remains under discussion. In this work, yearly input of inorganic material from below the euphotic layer was compensated with downward losses of material. Under this scheme, NW Mediterranean and eastern subtropical North Atlantic ecosystems were nearly balanced in absence of other external nitrogen sources, such as atmospheric depositions and horizontal inputs from nutrient-rich neighbouring boundaries. The matter balance was desirable not only for ecological but for numerical purposes, in order to avoid any inter-annual trend that could “collaps” (negative trend) or “saturate” (positive trend) the systems.

The nitrite maximum in upper water layers is explained by the phytoplankton exudation in the dark. One particular feature of the upper water column is the presence of a nitrite maximum. Several hypotheses explaining this maximum have been given based on field experiments on specific phytoplankton and bacteria populations, but little importance has been given to the role played by nitrite exudation by the phytoplankton community in the dark. The model estimates agree with previous field observations providing evidence that under scarce or null irradiance, phytoplankton exudates relatively high nitrite concentrations below the phytoplankton maximum.

Mixed layer variability, available light and nitrogen, and zooplankton grazing are key elements for modelling plankton dynamics in oligotrophic ecosystems. The numerical ecological simulations provided evidence that complex ecological interactions in the water column can be parameterised and quantified at different places in the ocean keeping similar basic structures of pelagic ecosystems. The diffusion-advection schemes of the water column did not explain by themselves the dynamics (time and depth variability) of the ecosystems. Seasonal patterns of plankton communities were forced by the interaction among the turbulence-advection scheme, light and nutrient availability and grazing pressure.

BLANES is applicable to any place of the ocean subject to a similar ecological framework. Selected key elements and processes of the pelagic ecosystem in the upper water layers of the open ocean reasonably reproduced the given environments at different latitudes using similar biogeochemical structure and functioning. This suggests that the model, after an adequate tuning, can be applicable to other places in the ocean subject to similar ecological forcings.

Bibliography

Bibliography

Agawin, N.S.R., Duarte, C.M., Agustí, S., 2000. Nutrient and temperature control of the contribution of picoplankton to phytoplankton biomass and production. *Limnology and Oceanography* 45, 591-600.

Agusti, S., Duarte,C., 1999. Phytoplankton chlorophyll a distribution and water column stability in the central Atlantic. *Oceanologica Acta* 22, 193-203.

Alarcon, M., Cruzado, A., Alonso, S., 1990. Atmospheric Long-range Transport of Pollutants to the Northwestern Mediterranean. *Rapports Commission internationale Exploration Mer Mediterranee* 32(1), 189.

Alcaraz, M., 1988. Summer zooplankton metabolism and its relation to primary production in the Western Mediterranean. *Oceanologica Acta SP*, 185 -191.

Aminot, A., 1983. Dosage de l´oxygène dissous. In: Aminot, A., Chaussepied, M. (Eds), *Manuel des analyses chimiques en milieu marin. Centre National pour l´exploitation des océans*. CNEXO, Paris, 395.

Anderson, L.A., Sarmiento, J.L., 1995. Global Ocean phosphate and oxygen simulations. *Global Biogeochemical Cycles* 9, 621-636.

Antoine, D., Morel, A., André, J.-M., 1995. Algal pigment distribution and primary production in the Eastern Mediterranean as derived from coastal zone color scanner observations. *Journal of Geophysical Research* 100: 16193 - 16209.

Arhan, M., Mercier, H., Bourlès, B., Gouriou, Y., 1998. Hydrographic sections across the Atlantic at 7°30N and 4°30S. *Deep-Sea Research I* 45, 829-872.

Armstrong, R.A., 1999. Stable model structures for representing biogeochemical diversity and size spectra in plankton communities. *Journal of Plankton Research* 21(3), 445 - 464.

Baker, K.S., Frouin, R., 1987. Relation between photosynthetically available radiation and total insulation at the ocean surface under clear skies. *Limnology and Oceanography* 32, 1370-1377.

Bahamón, N., Cruzado, A. 2002. Modelling nitrogen fluxes in oligotrophic environments: NW Mediterranean and NE Atlantic. *Ecological Modelling* (*submitted*)

Bahamón, N., Velasquez, Z., Cruzado, A. J., 2002. Phytoplankton primary production and nitrogen fluxes in stratified subtropical north Atlantic waters. *Deep-Sea Research* (*submitted*).

Baretta, J.W., Ebenhöh, W., Ruardij, P., 1995. The European regional seas ecosystem model, a complex marine ecosystem model. *Netherlands Journal of Sea Research* 33(3/4), 233-246.

Berges, J.A., Falkowski, P.G., 1998. Physiological stress and cell death in marine phytoplankton: Induction of proteases in response to nitrogen or light limitation. *Limnology and Oceanography* 43(1), 129-135.

Béthoux, J-P., Copin-Montégut, G., 1986. Biological fixation of atmospheric nitrogen in the Mediterranean Sea. *Limnology and Oceanography* 31(6), 1353-1358.

Béthoux, J-P., Copin-Montégut, G., 1988. Phosphorus and nitrogen in the Mediterranean Sea: specifities and forecasting. *Oceanologica Acta* 9(sp), 75-78.

Bissett, W.P., Meyers, M.B., Walsh, J.J., Muller-Karger, F.E., 1994. The effects of temporal variability of mixed layer depth on primary productivity around Bermuda. *Journal of Geophysical Research* 99(4), 7539-7553.

Blasco, D., 1971*a*. Acumulación de nitritos en determinados niveles marinos por acción del fitoplancton. *Ph. D. Thesis*, Universidad de Barcelona.

Blasco, D., 1971*b*. Composición y distribución del fitoplancton en la región del afloramiento de las costas peruanas. *Investigaciones Pesqueras* 35(1), 61-112.

Blight, S.P., Bentley,T.L., Lefevre, D., Robinson, C., Rodrigues, R., Rowlands, J., Williams, P.J.leB., 1995. Phasing of autrophic and heterotrophic plankton metabolism in a temperate coastal ecosystem. *Marine Ecology Progress Series* 128, 61-75.

Bricaud, A. Morel, A., Tailliez, D., 1992. Mesures optiques. In: J. Neveux (Ed), Les maximums profonds de chl a en mer des Sargasses. Données physiques, chimiques et biologiques. *Campagne Chlomax. Campagnes Océanographiques Françaises No. 17.* CNRS-Groupe de Recherche P4, Banyuls-sur-Mer, France, pp. 39-47

Brock, T.D., 1981. Calculating solar radiation for ecological studies. *Ecological Modelling* 14, 1-19.

Calbet, A., Alcaraz, M., Saiz, E., Estrada, M., Trepat, I., 1996. Planktonic herbivorous food webs in the Catalan Sea (NW Mediterranean): temporal variability and comparison of indices of phyto-zooplankton coupling based on state variables and rate processes. *Journal of Plankton Research* 18(12), 2329-2347.

Campbell, J W., Aarup, T., 1992. New production in the North Atlantic derived from seasonal patterns of surface chlorophyll. *Deep-Sea Research* 39, 1669-1694.

Carlucci, A.F., Hartwig, E.O., Bowes, P.M., 1970. Biological production of nitrite in seawater. *Marine Biology* 7, 161-166.

Carpenter, J. H. 1965. The accuracy of the Winkler method for dissolved oxygen analysis. *Limnology and Oceanography* 10, 135-140.

Carril, A.F., Menéndez, C.G., Nuñez, M.N., 1997. Climate change scenarios over the South American Region: An intercomparison of coupled general atmosphere-ocean circulation models. *International Journal of Climatology* 17, 1613-1633.

Claustre, H., Marty, J-C. 1995. Specific phytoplankton biomasses and their relation to primary production in the tropical North Atlantic. *Deep-Sea Research I* 42(8), 1475-1493.

Craig, H., Hayward, T., 1987. Oxygen supersaturation in the ocean: biological versus physical contributions. *Science* 235, 199-202.

Cruzado, A., Kelley, J.C., 1974. Continuous measurements of nutrient concentrations and phytoplankton density in the surface water of the western Mediterranean Sea, winter 1970. *Thalassia Jugoslavica* 9(1/2), 19-24.

Cruzado, A., 1982. Simulation model of primary production in coastal upwelling off Western Sahara. *Rapports et Proces verbaux. Reunion Commission internationale Exploration Mer Mediterranee* 180, 228-233.

Cruzado, A., Velásquez, Z., Pérez, M.C., Bahamón, N., Grimaldo, N.S., Ridolfi, F. 2002*a*. Nutrient fluxes from the Ebro River and subsequent across-shelf dispersion. *Continental Shelf Research*, 22 (2), 349-360

Cruzado, A., Velásquez, Z., Bahamón, N., Grimaldo, N.S., Puigdefabregas, J., Provost, C., 2002*b*. Sub-mesoscale and time variability in the Blanes Canyon , NW Mediterranean Sea., (*in prep*.)

Culberson, C.H. 1991. Dissolved oxygen. *Protocol "WOCE". WHP Operations and methods. Technical Report*. College of Marine Sciences. U. de Delaware. Newark, Delaware. U.S.A.

Cullen, J.J., Epply, R.W., 1981. Chlorophyll maximum layers of the southern California Bight and possible mechanisms of their formation and maintenance. *Oceanologica Acta* 4, 23-32.

Del Giorgio, P.A., Cimbleris, A., 1997. Respiration rates of bacteria exceed phytoplankton production in unproductive systems. *Nature* 385, 148-151.

Denman, K.L., Gargett, A.E., 1983. Time ansspace scales of vertical mixing and advection of phytoplankton in the upper ocean. *Limnology and Oceanography* 28: 801-815.

Denman, K.L., Platt, T., 1977. Biological prediction in the sea. In: E.B. Kraus (Ed), *Modelling and prediction of the upper layers of the ocean*, Pergamon, Oxford, pp. 251-262.

Doney, S.C., Glover, D.M., Najjar, R.G., 1996. A new coupled, one-dimensional biological-physical model for the upper Ocean: applications to the JGOFS Bermuda Atlantic Time-Series Study (BATS) site. *Deep-Sea Research II*, 43: 591-624.

Doney, S.C., 1999. Major challenges confronting marine biogeochemical modeling. *Global Biogeochemical Cycles* 13 (3), 705-714.

Duarte, C.M., Agustí, S., 1998. The CO_2 balance of unproductive aquatic ecosystems. *Science* 281, 234-236.

Duarte, C.M., Agustí, S., del Giorgio, P.A., Cole, J.J., 1999. Regional carbon imbalances in the oceans. Response. *Science* 284, 1735b.

Duce, R.A., Unni, C.K., Ray, B.J., Prospero, J.M., Merrill, J.T., 1980. Long-range atmospheric transport of soil dust from Asia to the tropical North Pacific: temporal variability. *Science* 209: 1522-1524.

Dugdale, R.C., Goering, J.J., 1967. Uptake of new and regenerated forms of nitrogen in primary productivity. *Limnology and Oceanography* 12: 196-206.

Dugdale, R.C., 1967. Nutrient limitation in the sea: dynamics, identification and significance. *Limnology and Oceanography,* 12: 685-695.

Ebenhoh, W., 2000. Critical analysis of the status quo in marine ecosystem modelling. *Biological Observations in Operational Oceanography*. EuroGOOS Publication No. 15, Eurogoos Office, Southampton.

Edwards, A.M., A. Yool, 2000. Role of higher predation in plankton population models. *Journal of Plankton Research* 22 (6): 1085-1112

Eppley, R.W., Peterson, B.J., 1979. Particulate organic matter flux and planktonic new production in the deep ocean. *Nature* 282, 677-680.

Estrada, M., 1985. Primary production at the deep chlorophyll maximum in the western Mediterranean. In: Gibbs, P.E. (Ed), *Proceeding of the 19th European Marine Biology Symposium*. Cambridge University Press, 109-121.

Estrada, M., Berdalet, E., 1997. Phytoplankton in a turbulent world. *Scientia Marina*. 61(Sup. 1), 125-140.

Estrada, M., Margalef, R., 1988. Supply of nutrients to the Mediterranean photic zone across a persistent front. *Oceanologica Acta* 9, 133-142.

Estrada, M., 1996. Primary production in the northwestern Mediterranean. *Scientia Marina* 60, 55-64.

Estrada, M., Margalef, R. 1988. Supply of nutrients to the Mediterranean photic zone acros a persistent front. *Oceanologica. Acta* 9, 133-142.

Estrada, M., Varela, R.A., Salat, J., Cruzado A., Arias, E., 1999. Spatio-temporal variability of the winter phytoplankton distribution across the Catalan and North Balearic fronts (NW Mediterranean). *Journal of Plankton Research* 21(1), 1-20.

Evans, G.T., Parslow, J.S., 1985. A model of annual plankton cycles. *Biological Oceanography* 3, 327-347.

Evans, G.T., 1999. The role of local models and data sets in the Joint Global Ocean Flux Study. *Deep-Sea Research I* 46, 1369-1389.

Falkowski, P.G., Barber, R.T., Smetacek, V., 1998. Biogeochemical controls and feedbacks of ocean primary production. *Science* 281, 200-206.

Fasham, M.R. Ducklow, H.W., McKelvie, S.M., 1990. A nitrogen-based model of plankton dynamics in the oceanic mixed layer. *Journal of Marine Research* 48(3), 591-639.

Flynn, K.J., Flynn, K., 1998. Release of nitrite by marine dinoflagellates: Development of a mathematical simulation. *Marine Biology* 130(3), 455-470.

Fowler, S.W., Small, L.F.., La Rosa, J., 1991. Biological considerations in the measurement of dissolved free amino acids in seawater and implications for chemical and microbiological studies. *Marine Ecology Progress Series* 25, 13-21.

Furuya, K., 1990. Subsurface chlorophyll maximum in the tropical and subtropical western Pacific Ocean: vertical profiles of phytoplankton biomass and its relationship with chlorophyll a and particulate organic carbon. *Marine Biology* 107, 529-539.

Garcia, H. E., Gordon, L. I., 1992. Oxygen solubility in seawater: Better fitting equations. *Limnology and Oceanography* 37, 1307-1312.

Garcia, H., Cruzado, A., Gordon, L., Escanez, J., 1998. Decadal-scale chemical variability in the subtropical North Atlantic deduced from nutrient and oxygen data. *Journal of Geophysical Research* 103, 2817-2830.

Gargett, A.E., 1989. Ocean turbulence. *Annual Reviews of Fluids Mechanic* 12, 419-451.

Garver, S.A., Siegel, D.A., 1994. Variability in near-surface particulate absorption spectra: What can a satellite ocean color imager see? *Limnology and Oceanography* 39, 1349-1367.

Gasol, J.M., del Giorgio, P.A., Duarte, C.M., 1997. Biomass distribution in marine planktonic communities. *Limnology and Oceanography* 42(6), 1353-1363.

Gaspar, P., Grégoris, Y., Lefevre, J-M., 1990. A simple eddy kinetic energy model for simulations of the oceanic vertical mixing: test at station Papa and long-term upper ocean study site. *Journal of Geophysical Research* 95(C9), 16179-16193.

Goericke, R., Welschmeyer, N.A., 1998. Response of Sargasso Sea phytoplankton, growth rates and primary production to seasonally varying physical forcing. *Journal of Plankton Research* 20(12), 2223-2249.

Goericke, R., 1998. Response of phytoplankton community structure and taxon-specific growth rates to seasonally varying physical forcing in the Sargasso Sea off Bermuda. *Limnology and Oceanography* 43(5), 921-935.

Goericke, R., Welschmeyer, N.A., 1998. Response of Sargasso Sea phytoplankton, growth rates and primary production to seasonally varying physical forcing. *Journal of Plankton Research* 20, 2223-2249.

Goldman, J.C., 1993. Potential role of large oceanic diatoms in new primary production. *Deep-Sea Research 40*, 159-168.

Granata, T., Vidondo, B., Duarte, C.M., Satta, M.P., Garcia, M., 1999. Hydrodynamics and particle transport associated with a submarine canyon off Blanes (Spain) NW Mediterranean Sea. *Continental Shelf Research* 19, 1249-1263.

Gruber, N., Sarmiento, J.L., 1997. Global patterns of marine nitrogen fixation and denitrificacion. *Global Biogeochemical Cycles* 11, 235-266.

Handoh, I.C., Bigg, G.R., 2001. Use of a reduced-gravity model to evaluate present and past primary productivity in the tropical open ocean. *Limnology and Oceanography* 46(7), 1632-1641.

Hasle, G.R., 1978. Using the inverted Microscope. In: Phytoplankton manual. Ed: Sournia, A., UNESCO, United Kingdom, 337.

Hasle, G.R., Syvertsen, E., 1997. Marine diatoms. In: Tomas,C. R., editor. *Identifying marine phytoplankton*. Academic Press, USA, 858.

Helguen, S.L., LeCorre, P., Madec, C., Morin, P., 2002. New and regenerated production in the Almeria-Oran front area, eastern Alboran Sea. *Deep-Sea Research* I 49, 83-99.

Herbland, A., Voituriez, B., 1979. Hydrological structure analysis for estimating the primary production in the tropical Atlantic Ocean. *Journal of Marine Research* 37, 87-101.

Herman, A.W., Platt, T. 1986. Primary production profiles in the ocean: estimation from chlorophyll/light model. *Oceanologica Acta* 9(1), 31-40.

Hoch, M.P., Kirchman, D.L., 1993. Seasonal and interannnual variability in bacterial production and biomass in a temperate estuary. *Marine Ecology Progress Series* 98, 283-295.

Holligan, P.M. Harris, R.P. Newell, R.C. Harbour, D.S. Head, R.N. Linley, E.A.S. Lucas, M.I. Tranter, P.R.G., Weekley, C.M., 1984. Vertical distribution and partitioning of organic carbon in mixed, frontal and stratified waters of the English Channel. *Marine Ecology Progress Series* 14, 111-127.

Hulburt, E.M., 1990. Description of phytoplankton and nutrients in spring in the western North Atlantic. *Journal of Plankton Research* 12, 1-28.

Hurtt, G.H. Armstrong, R.A., 1996. A pelagic ecosystem model calibrated with BATS data. *Deep-Sea Research II* 43(2-3), 653-683.

Jamart, B.M., Winter, D.F., Banse, K., Anderson, G.C., Lam, R.K., 1977. A theoretical study of phytoplankton growth and nutrient distribution in the Pacific Ocean off the northwestern U.S coast. *Deep-Sea Research* 24, 753-773.

Jacques, N., Oriol, L., 1992. Distribution des chlorophylles et des pheopigments. In: J. Neveux (Editor), Les maximums profonds de Chl *a* en Mer des Sargasses. Données physiques, chimiques et biologiques. *Campagne Chlomax. Campagnes Océanographiques Françaises No. 17* CNRS-Groupe de Recherche P4, Banyuls-sur-Mer, France, 82-98

Jamart, B.M., Winter, D.F., Banse, K., Anderson, G.C., Lam, R.K., 1977. A theoretical study of phytoplankton growth and nutrient distribution in the Pacific Ocean off the northwestern U.S coast. *Deep-Sea Research* 24, 753-773.

Jeffrey, S.W., Humphrey, G.F., 1975. New spectrophotometric equations for determining chlorophylls a,b,c1 and c2 in higher plants, algae and natural phytoplankton. *Biochemisch Physiologie Pflanzen* 167, 191-194.

Jeffrey, S.W., Welschmeyer, N.A., 1997. Spectrophotometric and fluorometric equations in common use in oceanography. In: Jeffrey, S.W., Mantoura, R.F.C., Wright, S.W. (Eds), *Phytoplankton pigments in oceanography*. UNESCO, France, 661.

Jenkins, W., 1988. Nitrate flux into the euphotic zone near Bermuda. *Nature* 331, 521-523.

Jenkins, W.J., Wallace, D.W.R., 1992. Tracer based inferences of new primary production in the sea. In: Falkowski, P.G., Woodhead, A.D. (Eds), *Primary productivity and biogeochemical cycles in the sea*. Plenum Press, New York, 550.

Jochem, F.J. Zeitzschel, B., 1993. Productivity regime and phytoplankton size structure in the tropical and subtropical North Atlantic in spring 1989. *Deep-Sea Research II* 40(1-2), 495-519.

Kawase, M., Sarmiento, J.L., 1985. Nutrients in the Atlantic thermocline. *Journal of Geophysical Research* 90, 8961-8979.

Kiefer, D.A., Olson, R.J., Holm-Hansen, O., 1976. Another look at the nitrite and chlorophyll maxima in the central North Pacific. *Deep-Sea Research* 23, 1199-1208.

Kiefer, D.A., Kremer, J.N., 1981. Origins of vertical patterns of phytoplankton and nutrients in the temperate open ocean: A stratigraphic hypothesis. *Deep-Sea Research* 28, 1087-1105.

Knap, A. Jickells, T. Pszenny, A., Galloway, J., 1986. Significance of atmospheric-derived fixed nitrogen on productivity of the Sargasso Sea. *Nature* 320, 158-160.

Kyewalyanga, M.N., Platt, T., Sathyendranath, S., Lutz, V., Stuart, V., 1998. Seasonal variations in physiological parameters of phytoplankton across the North Atlantic. *Journal of Plankton Research* 20(1), 17-42.

Lande, R., Li, W.K.W., Horne, E.P.W., Wood, A.M., 1989. Phytoplankton growth rates estimated from depths profiles of cell concentration and turbulent diffusion. *Deep-Sea Research* 36, 1141-1159.

Large, W.G,, McWilliams, J.C., Doney, S.C., 1994. Ocean vertical mixing: a review and a model with a nonlocal boundary layer parameterization. *Reviews of Geophysics* 32, 4.

Levy, M. Memery, L., Andre, J-H., 1998. Simulation of primary production and export fluxes in the northwestern Mediterranean Sea. *Journal of Marine Research* 56(1), 197-238.

Lewis, M.R., Harrison, W.G., Oakey, N.S., Hebert, D., Platt, T., 1986. Vertical nitrate fluxes in the oligotrophic ocean. *Science* 234, 870-873.

Lewis, M.R., Harrison, W.G., Oakey, N.S., Hebert, D., Platt, T., 1986. Vertical nitrate fluxes in the oligotrophic ocean. *Science* 234, 870-873.

Li, W.K.W., Wood, M., 1988. Vertical distribution of North Atlantic ultraphytoplankton: Analysis by flow cytometry and epifluorescence microscopy. *Deep-Sea Research* 35, 1615-1638.

Li, W.K.W. Dickie, P.M. Irwin, B.D., Wood, A.M., 1992. Biomass of bacteria, cyanobacteria, prochlorophytes and photoynthetic eukaryotes in the Sargasso Sea. *Deep-Sea Research* 39(3-4), 501-519.

Lohrenz, S.E. Wiesenburg, D.A. DePalma, I.P. Johnson, K.S., Gustafson, D.E., 1988. Interrelationships among primary production, chlorophyll, and environmental conditions in frontal regions of the western Mediterranean Sea. *Deep-Sea Research* 35(5), 793-810.

Lohrenz, S.E., Knauer, G.A., Asper, V.L., Tuel, M., Michaels, A.F., Knap, A.H., 1992. Seasonal variability in primary production and particle flux in the northwestern Sargasso Sea: U.S. JGOFS Bermuda Atlantic Time-series Study. *Deep-Sea Research* 39, 1373-1391.

Longhurst, R.A., Harrison, G.W., 1989. The biological pump: profiles of plankton production and consumption in the upper ocean. *Progress in Oceanography* 22, 47-123.

Longhurst, A., Sathyendranath, S., Platt, T., Caverhill, C., 1995. An estimate of global primary production in the ocean from satellite radiometer data. *Journal of Plankton Research* 17, 1245-1271.

Malone, T.C, Pike, Sh.E., Conley, D.J., 1993. Transient variations in phytoplankton productivity at the JGOFS Bermuda time series station. *Deep-Sea Research* I 40, 903-924.

Marañón, E., Holligan, P.M., Varela, M., Mouriño, B., Bale, A.J., 2000. Basin-scale variability of phytoplankton biomass, production and growth in the Atlantic Ocean. *Deep-Sea Research I* 47, 825-857.

Marra, J., Bidigare, R.R., Dickey, T.D., 1990. Nutrients and mixing, chlorophyll and phytoplankton growth. *Deep-Sea Research* 37(1), 127-143.

Masó, M., Sabatés, A., Olivar, M.P., 1998. Short-term physical and biological variability in the shelf-slope region of the NW mediterranean during the spring transition period. *Continental Shelf Research* 18, 661-675.

Mayer, D.A., Molinari, R.L., Festa, J.F., 1998. The mean and annual cycle of upper layer temperature fields in relation to Sverdrup dynamics within the gyres of the Atlantic Ocean. *Journal of Geophysical Research* 103, 18545-18566.

McGillicuddy, D.J., Robinson, A.R., 1997. Eddy-induced nutrient supply and new production in the Sargasso Sea. *Deep-Sea Research I* 8, 1427-1450.

McGrady-Steed, J., Harris, P.M., Morin, P.J., 1997. Biodiversity regulates ecosystem predictability. *Nature* 390, 162-165.

Mellor, G.L., Yamada, T., 1982. Development of a turbulence closure model for geophysical fluid problems. *Reviews of Geophysics and Space Physics* 20(4), 851-875.

Menzel, D.W., Ryther, J.H., 1960. The annual cycle of primary production in the Sargasso Sea off Bermuda. *Deep-Sea Research* 6, 351-367.

Menzel, D.W., Ryther, J.H., 1961. Annual variation in primary production of the Sargasso Sea off Bermuda. *Deep-Sea Research* 7, 282-288.

Menzel, D.W., Hulburt, E.M., Ryther, J.H., 1963. The effect of enriching Sargasso sea water on the production and species composition of the phytoplankton. *Deep-Sea Research* 10, 209-220.

Millard, R.C., Owens, W.B., Fofonoff, N.P., 1990. On the calculation of the Brunt-Väisälä frequency. *Deep-Sea Research* 37, 167-181.

Millero, F.J. Poisson, A., 1981. International one-atmosphere equation of state of sea water. *Deep-Sea Research* 28A(6), 625-629.

Minas, H.J., Minas, M., Packard, T.T., 1986. Productivity in upwelling areas deduced from hydrographic and chemical fields. *Limnology and Oceanography* 31, 1182-1206.

Miquel, J., Fowler, S., La Rosa, J., 1994. Dynamic of the downward flux of particles and carbon in the open northwestern Mediterranean Sea. *Deep-Sea Research* I 41, 243-261.

Moloney, C.L., Field, J.G., 1991. The size-based dynamics of plankton food webs. I. A simulation model of carbon and nitrogen flows. *Journal of Plankton Research* 13, 1003-1038.

Morel, A., Ahn, Y-W., Partensky, F., Vaulot, D. and Claustre, H., 1993. *Prochlorococcus* and *Synechococcus*: a comparative study of their size, pigmentation and related optical properties. *Journal of Marine Research* 51, 617-649.

Morel, A.,, André, J.-M., 1991. Pigment distribution and primary production in the western Mediterranean, as derived and modeled from coastal zone color scanner observations. *Journal of Geophysical Research* 96, 12685-12698.

Morel, A., Antoine, D., Babin, M., Dandonneau, Y., 1996. Measured and modeled primary production in the northeast Atlantic (EUMELI JGOFS program): the impact of natural variations in photosynthetic parameters on model predictive skill. *Deep-Sea Research I* 43(8), 1273-1304.

Mura, M.P., Agusti, S., Cebrián, J., Satta, M.P., 1996. Seasonal variability of phytoplankton biomass and community composition in Blanes Bay (1992-1992). Publ. Espec. Inst. Esp. Oceanogr. 22, 23-29.

Nelson, D.M., Brzezinski, M.A., 1997. Diatom growth and productivity in an oligotrophic midocean gyre: A 3-yr record from the Sargasso Sea near Bermuda. *Limnology and Oceanography* 42(3), 473-486.

Nixon, S.W., 1995. Coastal marine eutrophication: a definition, social causes, and future concerns. *Ophelia* 41, 199-219.

Oguz, T. Ducklow, H. Malanotte-Rizzoli, P. Tugrul, S. Nezlin, N.P., Unluata, U., 1996. Simulation of annual plankton productivity cycle in the Black Sea by a one-dimensional physical-biological model. *Journal of Geophysical Research* 101(C7), 16585-16599

Oguz, T., Ducklow, H.W., Malanotte-Rizzoli, P., Murray, J.W., Shushkina, E.A., Vedernikov, V.I., Unluata, U., 1999. A physical-biochemical model of plankton productivity and nitrogen cycling in the Black Sea. *Deep-Sea Research* I 46, 597-636.

Olson, R.J., 1981. Differential photoinhibition of marine nitrifying bacteria: a possible mechanism for the formation of the primary nitrite maximum. *Journal of Marine Research* 39(2), 227-238.

Olson, R.J. Chisholm, S.W. Zettler, E.R. Altabet, M.A., Dusenberry, J.A., 1990. Spatial and temporal distribution of phrochlorophyte picoplankton in the North Atlantic Ocean. *Deep-Sea Research* 37, 1033-1051.

Osborn, T.R., 1980. Estimates of the local rate of vertical diffusion from dissipation measurements. *Journal of Physical Oceanography* 10, 83-89.

Owen, R.W., 1981. Fronts and eddies in the sea: Mechanisms, interactions and biological effects. In: A.R. Longhurst (Ed), *Analysis of Marine Ecosystems*, Academic Press, London, pp. 197-233.

Parrilla, G., Lavín, A., Bryden, H., García, M., Millard, R., 1994. Rising temperatures in the subtropical North Atlantic Ocean over the past 35 years. *Nature* 369, 48-51.

Pedrós-Alió, C., Calderón-Paz, J-I., Guixa-Boixereu, N., Estrada, M., Gasol, J.M., 1999. Bacterioplankton and phytoplankton biomass and production during summer stratification in the northwastern Mediterranean Sea. *Deep-Sea Research I* 46, 985-1019.

Planas, D., Agustí, S., Duarte, C., Granata, T., 1999. Nitrate uptake and diffusive nitrate supply in the Central Atlantic. *Limnology and Oceanography* 44(1), 116-126.

Platt, T., Harrison, W.G., 1985. Biogenic fluxes of carbon and oxygen in the ocean. *Nature* 318, 55-58.

Platt, T., Harrison, W.G., Lewis, M.R., Li, W.K.W., Sathyendranath, S., Smith, R.E., Vezina, A.F., 1989. Biological production of the oceans: The case for a consensus. *Marine Ecology Progress Series* 52, 77-88.

Platt, T., Caverhill, C., Sathyendranath, S., 1991. Basin-scale estimates of oceanic primary production by remote sensing: The North Atlantic. *Journal of Geophysical Research* 96, 15147-15159.

Platt, T., Harrison, W.G., 1985. Biogenic fluxes of carbon and oxygen in the ocean. *Nature* 318, 55-58.

Raimbault, P., 1986. Effect of temperature on nitrite excretion by three marine diatoms during nitrate uptake. *Marine Biology* 92, 149-155.

Rastetter, E.B., 1996. Validating models of ecosystem response to global change. How can we best assess models of long-term global change? *BioScience* 46(3), 190-198.

Riley, G.A., Stommel, H., Bumpus, D.F., 1942. The relationship of the vertical turbulence and spring diatom flowering. *Journal of Marine Research* 5, 67-87.

Romero, O.E., Lange, C.B., Swap, R., Wefer, G., 1999. Eolian-transported freshwater diatoms and phytoliths across the equatorial Atlantic record: Temporal changes in Saharan dust transport patterns. *Journal of Geophysical Research* 104, 3211-3222.

Salat, J., 1995. The interaction between the Catalan and Balearic currents in the southern Catalan Sea. *Oceanologica Acta* 18(2), 227-234.

Sarmiento, J.L., 1993. Ocean carbon cycle. *Chemistry & Environment*, pp. 30-43.

Sarmiento, J.L. Slater, R.D. Fasham, M.R.J. Ducklow, H.W. Toggweiler, J.R., Evans, G.T., 1993. A seasonal three-dimensional ecosystem model of nitrogen cycling in the North Atlantic euphotic zone. *Global Biogeochemical Cycles* 7, 417-450.

Sathyendranath, S. Longhurst, A. Caverhill, C.M., Platt, T., 1995. Regionally and seasonally differentiated primary production in the North Atlantic. *Deep-Sea Research I* 42(10): 1773-1802.

Satta, M.P., Agusti, S., Mura, M.P., Vaqué, D., Duarte, C.M., 1996. Microplankton respiration and net community metabolism in a bay on the NW Mediterranean coast. *Aquatic Microbial Ecology* 10, 165-172.

Sciandra, A., Amara, R., 1994. Effects of nitrogen limitation on growth and nitrite excretion rates of the dinoflagellate *Prorocentrum minimum*. *Marine Ecology Progress Series* 105(3), 301-309.

Schmitz, W.J., McCartney, M.S., 1993. On the North Atlantic Circulation. *Reviews of Geophysics* 31, 29-49.

Schott, F., Visbeck, M., Send,U; Fisher,J; Stramma,L; Desaubies,Y (1996): Observations of deep convection in the Gulf of Lions, Northern Mediterranean, during the winter of 1991/1992. *Journal of Physical Oceanography* 26, 505-524.

Schutz, L.W., Prospero, J.M., Buat-Menard, P., Carvalho, R.A.C., Cruzado, A., Harriss, R., Heidam, N.Z., Jaenicke, R., 1988. The long-range transport of mineral aerosols: Group report. In: A.H. Knap (Ed), *The Long-Range Atmospheric Transport of Natural and Contaminant Substances*, NATO ASI Series. Series C: Mathematical and Physical Sciences - Vol 297, Kluwer Academic Publ., Dordrecht, pp. 197-230.

Selmer, J-S. Ferrier-Pages, C. Cellario, C., Rassoulzadegan, F., 1993. New and regenerated production in relation to the microbial loop in the NW Mediterranean Sea. *Marine Ecology Progress Series* 100, 71-83.

Serret, P., Fernández, E., Sostres, J.A., Anadón, R., 1999. Seasonal compensation of microbial production and respiration in a temperate sea. *Marine Ecology Progress Series* 187, 43-57.

Serret, P., Robinson, C., Fernández, E., Teira, E., Tilstone, G., 2001. Latitudinal variation of the balance between plankton photosynthesis and respiration in the eastern Atlantic Ocean. *Limnology and Oceanography* 46(7), 1642-1652.

Sharada, M.K., Yajnik, K.S., 2000. Comparison of simulations of a marine ecosystem model with CZCS data in the North Indian Ocean. *Inverse Methods in Global Biogeochemical Cycles*. Geophysical Monograph 114. Bangalore, India.

Sharples, J., 1999. Investigating the seasonal vertical structure of phytoplankton in shelf seas. *Marine Models* 1, 3-38.

Sharples, J., Moore, C.M., Rippeth, T.P., Holligan, P.M., Hydes, D.J., Fisher, N.R., Simpson, J.H., 2001. Phytoplankton distribution and survival in the thermocline. *Limnology and Oceanography* 46(3), 486-496.

Skogen, M.D. Svendsen, E. Berntsen, J. Aksnes, D., Ulvestad, K.B., 1995. Modelling the primary production in the North Sea using a coupled three-dimensional physical-chemical-biological ocean model. *Estuarine, Coastal and Shelf Science* 41, 545-565.

Smayda, T.J., 2001. Biogeographycal studies of marine phytoplankton. *Oikos* 9, 158-191.

Sournia, A., 1986. Atlas du phytoplancton marin. Centre National de la Recherche Scientifique, Paris. 219 pp.

Steele, J., 1977. Ecological modelling of the upper layers. In: E.B. Kraus (Ed), *Modelling and prediction of the upper layers of the ocean*, Pergamon Press, Oxford, U.K., pp. 243-250.

Steidinger, K.A., Tangen, K., 1997. Dinoflagellates. In: Tomas, C.R. *Identifying marine phytoplankton*. Academic Press, USA, 858.

Sournia, A., 1990. *Atlas du phytoplancton marin*.Vol. 1. Edition du Centre National de la Recherche Scientifique, Paris, 261.

Taguchi, S., DiTullio, G.R., Laws, E.A., 1988. Physiological characteristics and production of mixed layer and chlorophyll maximum phytoplankton in the Caribbean Sea and western Atlantic Ocean. *Deep-Sea Research* 35(8), 1363-1377

Tremblay, J-E. Klein, B. Legendre, L. Rivkin, R.B., Therriault, J-C., 1997. Estimation of f-ratios in oceans based on phytoplankton size structure. *Limnology and Oceanography* 42(3), 595-601.

Tusseau, M.H. Lancelot, C. Martin, J.M., Tassin, B., 1997. 1-D coupled physical-biological model of the northwestern Mediterranean Sea. *Deep-Sea Research II*, 44(3-4), 851-880.

Urbach, E., Chisholm, S.W., 1998. Genetic diversity in *Prochlorococcus* populations flow cytometrically sorted from the Sargasso Sea and Gulf Stream. *Limnology and Oceanography* 43(7), 1615-1630.

Vaccaro, R.F., Ryther, J.H., 1960. Marine phytoplankton and the distribution of nitrite in the sea. *Journal du Conseil Permanent International de Exploration de la Mer* 25, 260-271.

Varela, R. Cruzado, A. Tintoré, J., García, E., 1992. Modelling the deep-chlorophyll maximum: A coupled physical-biological approach. *Journal of Marine Research* 50, 441-463.

Varela, R.A., Cruzado, A., Tintore, J., 1994. A simulation analysis of various biological and physical factors influencing the deep-chlorophyll maximum structure in oligotrophic areas. *Journal of Marine Systems* 5, 1-15

Varela, R.A. Cruzado, A., Gabaldón, J.E., 1995. Modelling primary production in the North Sea using the European Regional Seas Ecosystem Model. Netherlands *Journal of Sea Research* 33(3/4), 337-361.

Velásquez, Z., 1997. Fitoplancton en el Mediterráneo Noroccidental. *Ph.D. Thesis*, Universitat Politècnica de Catalunya, Barcelona. 271 p.

Vichi, M., 2000. The influence of high frequency surface forcing on productiviy in the euphotic layer. *Biological Observations in Operational Oceanography*. EuroGOOS Publication No. 15, Eurogoos Office, Southampton.

Waser, N.A.D, Harrison, P.J., Nielsen, B., Calvert, S.E., Turpin, D.H., 1998. Nitrogen isotope fractionation during the uptake and assimilation of nitrate, nitrite, ammonium, and urea by a marine diatom. *Limnology and Oceanography* 43(2), 215-224.

Whitledge, T.E., Malloy, S.C., Patton, C.J., Wirick, C.D., 1981. Automated nutrient analyses in seawater. *Brookhaven National Laboratory*. U.S. Dept. of Energy and Environment, Upton, N.Y.

Williams, P.J. leB., 1993. On the definition of plankton production terms. *ICES marine Science Symposium* 197, 9-19.

Williams, P.J. leB., 1998. The balance of plankton respiration and photosynthesis in the open oceans. *Nature* 394, 55-57.

Williams, P.J. leB., Jenkinson, N.W., 1982. A transportable microprocessor-controlled precise Winkler titration suitable for field station and shipboard use. *Limnology and Oceanography* 27(3), 576-584.

Williams, P.J. leB., Robinson, C., 1991. Analysis of oxygen-based productivity measurements through phase I of the EROS 2000 Programme. *Water Pollution Research Reports* 28, 151-162.

Williams, R.G., Follows, M.J., 1998. The Ekman transfer of nutrients and maintenance of new production over the North Atlantic. *Deep-Sea Research I* 45, 461-489.

Williams, P.J. le B., Bowers, D.G., 1999. Regional carbon imbalances in the oceans. *Nature* 284, 1735b.

WMO-UNEP, 2001. Climate change 2001: Synthesis Report of the Intergovernmental Panel on Climate Change (IPCC). Third Assessment Report. Summary for policymakers, as approved by the XVIII Session of the IPCC at Wembly, United Kingdom, 24 to 29th September 2001. 76 p.

WOCE, 1991. WOCE Operations Manual. Volume 3: The observational programme. Section 3.1: *WOCE Hydrographic program*. Part 3.1.3. *WHP Operations and Methods*, 68/91, WPH Office Report WHP 91-1, Woods Hole, Mass

Zakardjian, B., Prieur, L., 1994. A numerical study of primary production related to vertical turbulent diffusion with special reference to vertical motions of the phytoplankton cells in nutrients and light fields. *Journal of Marine Systems* 5, 267-295.

Zakardjian, B., Prieur, L., 1998. Biological and chemical signs of upward motions in permanent geostrophic fronts of the Western Mediterranean. *Journal of Geophysical Research* 103(C12), 27849-27866.

Zavatarelli, M., Baretta, J.W., Baretta-Bekker, J.G., Pinardi, N., 2000. The dynamics of the Adriatic Sea ecosystem. An idealized model study. *Deep-Sea Research I* 47, 937-970.